ABSTRACT

Title of Thesis: Understanding Urban Stormwater Denitrification in
                                        Bioretention Internal Water Storage Zones

                                        Sara J. Igielski, Masters of Science, 2016

Thesis Directed By: Allen P. Davis
                                        Department of Civil and Environmental Engineering

Free-draining bioretention systems commonly demonstrate poor nitrate removal. In this study, column tests verified the necessity of a permanently saturated zone to target nitrate removal via denitrification. Experiments determined a first-order denitrification rate constant of 0.0011 min^{-1} specific to Willow Oak woodchip media. A 2.6-day retention time reduced 3.0 mg-N/L to below 0.05 mg-N/L. During simulated storm events, hydraulic retention time may be used as a predictive measurement of nitrate fate and removal. A minimum 4.0 hour retention time was necessary for in-storm denitrification defined by a minimum 20% nitrate removal. Additional environmental parameters, e.g., pH, temperature, oxidation-reduction potential, and dissolved oxygen, affect denitrification rate and response, but macroscale measurements may not be an accurate depiction of denitrifying biofilm conditions. A simple model was developed to predict annual bioretention nitrate performance. Novel bioretention design should incorporate bowl storage and large subsurface denitrifying zones to maximize treatment volume and contact time.

UNDERSTANIDNG URBAN STORMWATER DENITRIFICATION IN BIORETENTION
INTNERNAL WATER STORAGE ZONES

by:
Sara J. Igielski

Thesis submitted to the Faculty of the Graduate School of the
University of Maryland, College Park in partial fulfillment
of the requirements of the degree of
Masters of Science
2016

Advisory Committee:
Professor Allen P. Davis, Chair
Assistant Professor Birthe Kjellerup
Assistant Professor Stephane Yarwood

Table of Contents

List of Tables

List of Figures

Chapter 1 Introduction

1.1.   Background

Nitrogen (N) is an essential nutrient for all living organisms. The Haber Bosch

process, an artificial nitrogen fixation process, converts atmospheric nitrogen (N_2) to

ammonia (NH_3) using a metal catalysis under high temperatures and pressures.

Industrialized ammonia production not only provided multiple new pathways of

bioavailable N into the environment, e.g., commercialized fertilizer, food production, and

fossil-fuel combustion, but also permanently affected the biogeochemical cycling of N

(Gruber and Galloway 2008; Collins et al. 2010). Predicted increased population trends,

demand for food, agricultural practices, energy use, and rapid urbanization, are only some

of the contributors to elevated anthropogenic nitrogen fluxes, and consequently,

environmental harm.

First and foremost, the exploitation and augmentation of N has accelerated the

global carbon cycle. In particular increased atmospheric CO_2 levels are often associated

with global warming (Gruber and Galloway 2008). Secondly, excess N has led to

eutrophication and associated water-quality problems (Collins et al. 2010; Payne et al.

2014). Global socioeconomic shifts encouraged by land use development and widespread

urbanization have only intensified the environmental risks of excess N.

Urban stormwater plays a crucial role in N management. It is a major source of N

input, and the pathway of stormwater in the environment dictates the extent of N

biotransformation, movement, and fate within a landscape. Reduction of N loading in

urban stormwater is one approach that must be employed in order to protect and restore

threatened ecosystems (Collins et al. 2010; Davis et al. 2010). Nature-based stormwater

control measures (SCMs) have been studied and developed to address the hydrologic and water quality concerns, including N management (Davis et al. 2010, 2012b).

One specific technology of interest is bioretention, an infiltration-based SCM, to intercept and temporarily store stormwater before discharging to receiving surface water bodies. Effective design shall integrate fundamental principles of hydrologic flow and physical, chemical and/or biologically-mediated unit processes (Davis et al. 2009, 2010; Hunt et al. 2012). Hydrologic goals emphasize design(s) to mitigate peak flow and/or reduce total volume, as the bioretention cell outflow shall mirror predevelopment surface water hydrology (Hunt et al. 2012).

Simultaneously, a design can target specific unit processes to improve effluent water quality. One approach is via the reduction of outflow volume (Hunt et al. 2006; Li and Davis 2009; Hunt et al. 2012). Other opportunities include but are not limited to sedimentation, infiltration/filtration, adsorption, biotransformation, and bio-uptake (Davis et al. 2010). Bioretention cells have demonstrated effective removal of suspended solids, heavy metals, phosphorus, oil and grease, and fecal coliform (Davis et al. 2001, 2006, 2009; Hunt et al. 2006; Sun and Davis 2007; Hatt et al. 2009; Li and Davis 2009). However, bioretention has not shown the same level of success with respect to N management. This can be attributed to the dynamic biogeochemical complexity of the N cycle (Isobe and Ohte 2014), and the biotransformation processes, i.e., ammonification and nitrification, that tend to favor the production of nitrate. Table 1-1 outlines N speciation present in urban stormwater and annual bioretention performance with respect to each species. Results highlight the effectiveness of particulate removal, i.e., organic N, due to sedimentation and filtration (Li and Davis 2014), whereas N transformations tend

2

to convert bioavailable N to nitrate (Figure 1-1; Table 1-1). Nitrate production and

leaching has been demonstrated in numerous laboratory and field-scale studies (Davis et

al. 2001; Hsieh and Davis 2005; Hunt et al. 2006, 2008; Hatt et al. 2009; Li and Davis

2014). Furthermore, conventional bioretention design is characterized as free-draining.

Infiltrated water is captured with a lateral, perforated drain present in a gravel layer

beneath the filter media (Brown and Hunt 2011) and/or allowed to percolate the

underlying in-situ soil. The filter media, as shown in Figure 1-1 , was predominantly

aerobic, so, ammonification followed by nitrification favored the production of nitrate;

the nitrified stormwater was then discharged via the underdrain or infiltrated to

underlying soil. When taking into account the two pathways (exported by underdrain or

leached to underlying soil), then, the total nitrogen (TN) removal is only 10% (Table

1-1).

Table 1-1 Summary of Annual N-Speciation Mass Pollutant Loadings from a Conventional Free-Draining Bioretention Cell in College Park, MD. Data originally presented in Li and Davis (2014).

	Speciation	Annual Mass In (kg/ha/yr)	Annual Export (kg/ha/yr)	Annual Leach (kg/ha/yr)
Particulate	*Organic N*	8.0	1.3	0
Dissolved	*Organic N*	2.2	3.3	2.1
	Ammonium	1.3	0.15	0.09
	Nitrate	2.4	3.5	2.2
	Nitrite	0.14	0.01	
Sum	*Total Nitrogen*	14.0	8.2	4.39
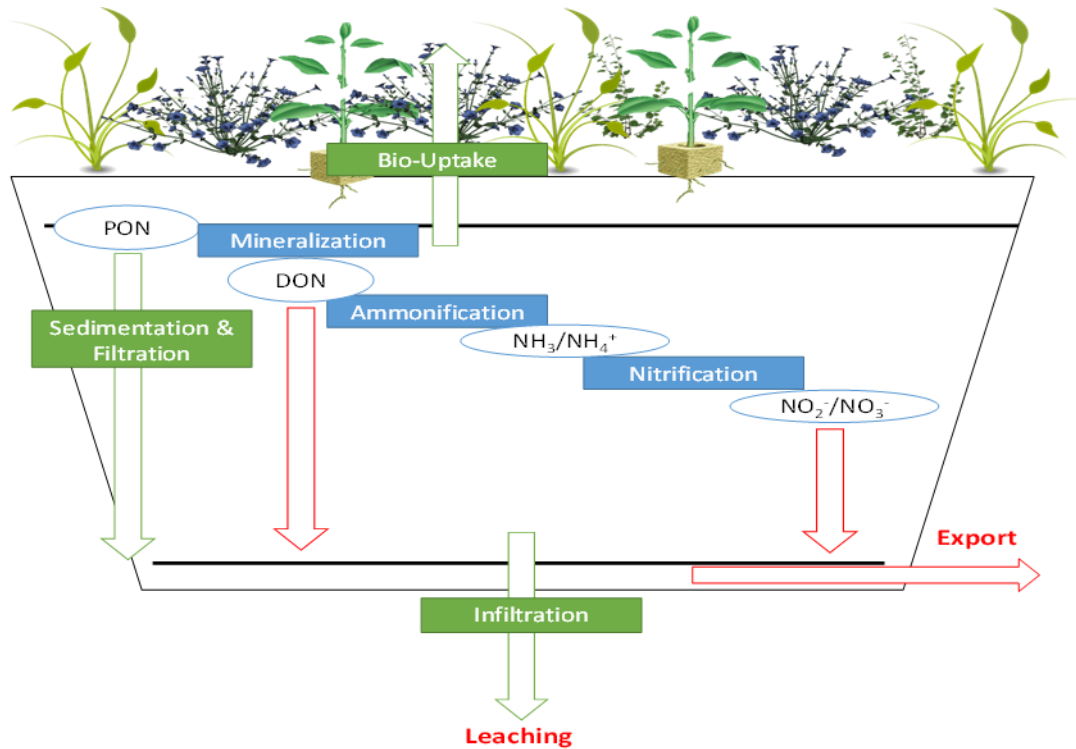
Figure 1-1 Fate of N in conventional bioretention cell where the production of nitrate is favored during and between storm events due to the presence of aerobic conditions. Leaching of nitrate and poor overall TN removal is observed. Figure is modified from Li and Davis (2014).

Thus, a modified bioretention design is necessary to specifically target nitrate removal via denitrification if TN removal is to be significantly improved (Li and Davis 2014). Denitrification is a facultative respiratory pathway where the oxidation state of nitrogen is reduced from +5 (nitrate) to 0 (dinitrogen gas) through a series of 4 reductive steps as catalyzed by microbial produced enzymes (Jones et al. 2008; Isobe and Ohte 2014) (Figure 1-2).

The ability to denitrify is ubiquitous in the environment. Denitrifying microorganisms are not restricted to a particular phylogenetic classification (Jones et al. 2008; Morgan-Sagastume et al. 2008; Warneke et al. 2011b; Saarenheimo et al. 2015). Rather, since these are facultative microbes, oxygen is preferred over nitrate as the

terminal electron acceptor (Robertson and Kuenen 1990). It is the responsibility of the

designer to create favorable conditions that will require denitrifiers to utilize this

respiratory pathway for survival. In order for the reduction of nitrogen to be

thermodynamically favorable, anoxic conditions and an external carbon source must be

present. The general stoichiometric equation for denitrification using a simple

carbohydrate (CH_2O) as the electron donor is shown below:

$$5CH_2O + 4NO_3^- + 4H^+ \rightarrow 2N_2 + 5CO_2 + 7H_2O \qquad\qquad \text{1-1}$$
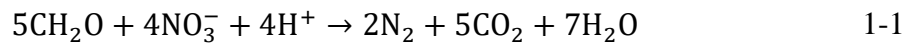
The complete denitrification reaction is designated as the release of the benign

form of nitrogen, dinitrogen gas (N_2), into the atmosphere. However, if denitrification is

not complete, i.e., the final reductive step is not achieved since all denitrifiers do not

contain the *nosZ* gene (Jones et al. 2008; Robertson and Kuenen 1990), then the process

will release nitrous oxide (N_2O), a greenhouse gas (Figure 1-2).
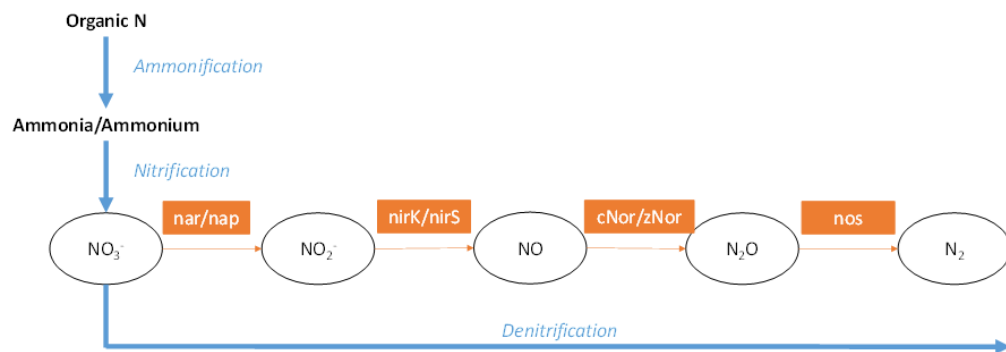
Figure 1-2. Overview of the production of nitrate and the reductive steps involved in complete denitrification with the respective enzymes responsible for each reductive step (orange).

Previous research has demonstrated that bioretention can create anoxic conditions

by creating a continuously saturated zone and providing an electron donor such as

organic carbon (Kim et al. 2003; Lynn et al. 2015a; Peterson et al. 2015). Such

environmental conditions can be stimulated by the incorporation of an internal water

storage zone (IWSZ) at the bottom layer of a bioretention cell; this can be achieved via

the substitution of a traditional underdrain with an upturned elbow configured drainage

pipe (Kim et al. 2003; Brown and Hunt 2011; Hunt et al. 2012; Lynn et al. 2015a; b;

Peterson et al. 2015) (Figure 1-3). Ideally, the reengineered bioretention design will

maintain an upper aerobic zone for nitrate production. The IWSZ layer below is designed

to temporarily store and remove nitrate via denitrification prior to stormwater export

(Figure 1-3).
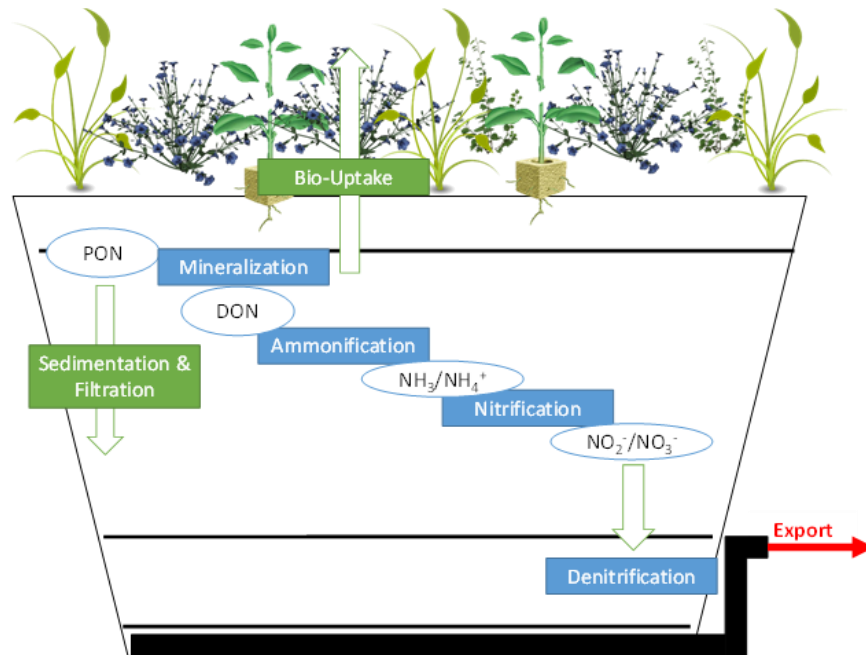
Figure 1-3. Modification of a traditional bioretention cell to include an upturned elbow-configured drainage pipe as to create an IWSZ and promote biological denitrification and improve TN removal.

The media composition and characteristics of the IWSZ, including the selected

carbon source is of critical concern to promote biological denitrification (Kim et al.

2003). Woodchips have often been regarded as an optimal carbon source because they are cost-effective, exhibit stable decomposition, and leach minimal organic matter when subject to continuously saturated conditions (Kim et al. 2003; Lynn et al. 2015a; b; Peterson et al. 2015). The selected carbon source will influence the rate of nitrate removal and the associated diversity and abundance of the present denitrifiers and entire microbial community (Warneke et al. 2011b).

Other environmental parameters will also affect nitrate behavior, e.g., influent nitrate concentrations, wetting/drying cycles, organic N leaching, temperature, dissolved oxygen, pH, aerobic/anoxic conditions, and contact time (Kim et al. 2003; Brown and Hunt 2011; Warneke et al. 2011a; b; Schmidt and Clark 2013; Hoover et al. 2015; Lynn et al. 2015b; Peterson et al. 2015; Subramaniam et al. 2016). In particular, Brown and Hunt (2011) and Li and Davis (2014) acknowledged the significant contribution of runoff volume reduction in order to meet total nitrogen (TN) removal goals but did not successfully target denitrification by not providing an external carbon source or creating anoxic conditions, respectively. Brown and Hunt (2011) and Lynn et al. (2015b) reported low nitrate removal due to insufficient hydraulic residence time, e.g., less than three hours, within the IWSZ. Furthermore, Subramaniam et al. (2016) only reported 0-15% nitrate removal during a laboratory scale storm event with a conventionally draining stormwater biofilter, whereas between events, nitrate removal was high. With this in mind, the optimization of denitrification, and total N removal, within the context of urban stormwater management will be investigated.

1.2. Research Objectives

The goal of this research is to enhance the total nitrogen removal by targeting denitrification in the IWSZ of a modified bioretention cell. In order to evaluate performance and denitrification efficiency, the following objectives are proposed:

1. Previous research, e.g., Lynn et al. (2015a; b) and Peterson et al. (2015), have established the presence of denitrifying microorganisms in a permanently saturated sublayer of bioretention to specifically target nitrate removal. Following precedent of previous work, a series of tests will aim to identify specific environmental conditions that are responsible for biofilm development and maturation, whereby the denitrifying microbes are believed to inhabit. This is verified through the subsequent analysis of effluent nitrate, modification of internal environmental conditions, and metagenomic sequencing of all bacterial genomes present in the woodchips after one-year of operation.

2. Evaluate denitrification kinetics with respect to reaction order and an associated rate constant. Previous literature reports are compared and analyzed with respect to influent nitrate concentration, media components and composition, supplemented carbon substrate, and context of design, i.e., agricultural management, wastewater treatment, urban stormwater management, etc. Previous work in the bioethanol industry have identified specific pretreatment methods in order to target physical lignin removal from woodchips (Wang et al. 2008, 2010; Jeong et al. 2010; Chaudhary et al. 2012; Singh et al. 2015). Pretreatment methods are adopted to delignify the woodchips and expose cellulose to an accelerated enzymatic degradation rate. It is hypothesized that an environment

that provides more bioavailable carbon for denitrifying microbes will respond an increased denitrification kinetic rate.

3. Biofilms, or micro-niche environments, are responsible for the inhabitance and metabolic activities of microorganisms, including denitrifiers (Costerton et al. 1995). It is believed that the bulk-liquid movement, including nitrogen fate, within the system is affected by system geometry, fluid flow rate, and media characteristics, e.g., size, composition, and hydraulic conductivity. If nitrate is unable to move from the bulk-liquid to the biofilm via diffusion, then denitrification cannot occur. It is necessary to identify the contribution of each mass transport mechanism– advection, dispersion, and diffusion – as to predict nitrate movement and potential removal within the system.

4. Re-engineered bioretention design shall be centered upon an identified hydraulic retention time (HRT). An increased HRT should correlate with an increased nitrate removal. Identifying the relationship between HRT and diffusion dominated mass transport is necessary to determine if in-storm denitrification will occur, and how kinetics and transport will limit the nitrate removal.

5. Application of HRT and nitrate removal shall allow for field-scale annual nitrate removal prediction patterns. A simple model is developed to characterize IWSZ performance with respect to annual nitrate removal that can be applied to any climate and rainfall/runoff response. To verify a model specific to the Maryland climate, storms are translated for laboratory simulation and IWSZ nitrate removal is quantified.

6. HRT-based bioretention design prompts TMDL regulatory compliance with respect to TN. Since a larger HRT is expected to coincide with increased nitrate removal, then design should focus on reduced infiltration rate and increased storage volume. Such parameters are of interest because there is not a one size fits all approach to meet the HRT design criteria. Flexibility and creativity shall exist in the modified bioretention cell - pretreatment mechanisms, bioretention surface storage, upper media layer(s) characteristics, and inclusion of an IWSZ – as to collectively target TN removal.

Chapter 2 Methodology

2.1. Laboratory Design

2.1.1. Column Design

Two separate columns were designed in this experiment, however, the media preparatory methods were identical. Mixed media was prepared as described in *Control* <u>Media</u>. Both columns were completely wrapped in aluminum foil to prevent light penetration into the column.
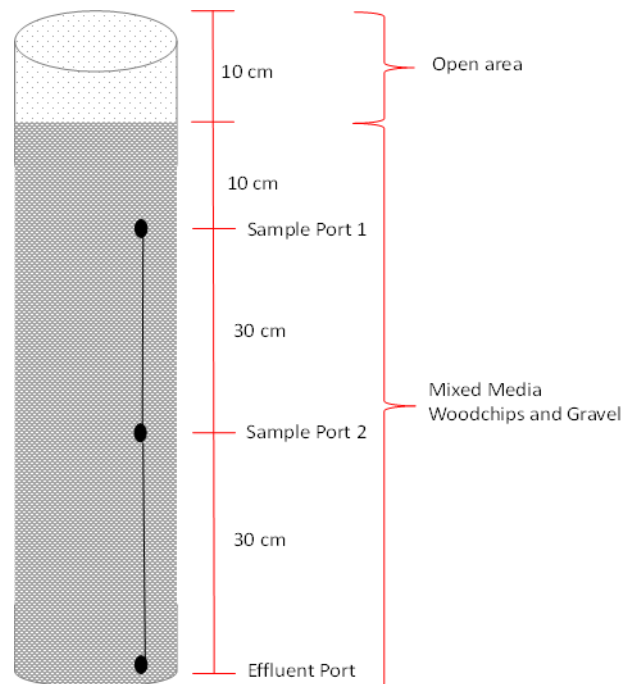
Figure 2-1 Model bioretention column design as shown in Peterson et al. (2015) to establish the presence of denitrification and characterize denitrification kinetics.

The first column was constructed according to the procedure as outlined in Peterson et al. (2015) and shown in Figure 2-1. The purpose of this design was to first, verify the presence of denitrification through a series of control tests, and second, characterize denitrification specific rate order and constant. Mixed media was packed to a

height of 70 cm leaving a freeboard of 10 cm in the column. The effluent port consisted of a valve which, constricted flow, where the optimal rate of flow, as determined in Peterson et al. (2015), corresponded to an initial drainage flow of 1.4 mL/min. This is done prior to packing the column with the mixed media; the empty column was filled with deionized (DI) water to a height of 70 cm, and effluent valve was adjusted accordingly. Sample Ports 1 and 2 were not used in this set of column experiments.

The second column was designed to mimic the drainage configuration of an internal water storage zone (IWSZ). Thus, the valve-restricted effluent sample port was replaced by an unrestricted upturned elbow-configured tube (MasterFlex L/S 18) as shown in Figure 2-2. The mixed media was packed into the column until it reached a height of 45 cm (Figure 2-2) as suggested by (Brown and Hunt 2011; Hunt et al. 2012; Lynn et al. 2015a). Influent stormwater vertically travels through the depth of the column and the sampling location (effluent port) is at height of the elbow. Remaining results, such as many discussed in Chapter 3 refer to this column configuration. Sample Port 1, as in Figure 2-1, is not used; Sample Port 2 was the location of an oxidation reduction potential (ORP) probe as to continuously monitor the redox conditions of the IWSZ environment both during and between simulated storm events.
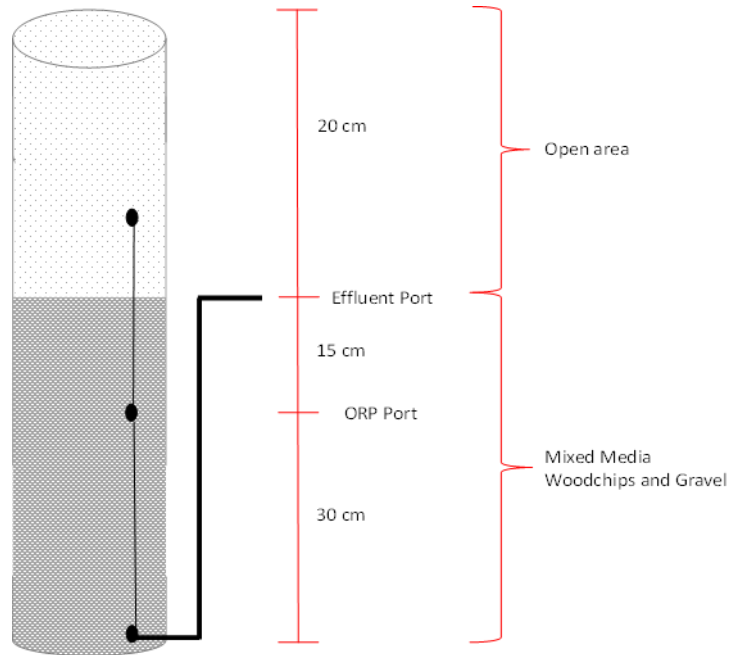
Figure 2-2. Model IWSZ as to quantify nitrate removal performance with a height of 45 cm (18 in.).

2.1.2. Media Preparation

Two specific media preparations are described. The *Control Media* refers to the mixed pea gravel and Willow Oak woodchip media as outlined in Peterson et al. (2015), henceforth known as control mixed media. This media is used in both column configurations (Figure 2-1 and Figure 2-2). The only difference is the height of the packed media. The *Treatment Media* refers to woodchips that were subjected to dilute alkaline pretreatment as used specifically for the Batch Study set of experiments only. The purpose of this treatment was to investigate if and how the bioavailability of carbon in woodchip limits the observed denitrification rate, as to be discussed in Chapter 3 results.

Control Media

The media used in the columns contained a mixture of woodchips and pea gravel.

Willow Oak wood samples were collected from the University of Maryland campus; wood was chipped and provided by the University of Maryland Campus Facilities Management. Woodchip samples were sieved through 25.5 mm, 19 mm, 13 mm, 9.5 mm, and No. 4 (5 mm) sieves as done on an automatic shaker for 15 minutes. Only chips retained on the No. 4 sieve were used in the mixed media (Peterson et al. 2015). Woodchips were stored in sealed non-transparent plastic bags. Pea gravel (0.3 to 9.5 mm) was purchased from a local home supply store, and prepared by thoroughly rinsing with tap water and then heating for 4 hours at 600°C to burn off organic matter (Peterson et al. 2015).

Mixed media contained 4.5% (by mass) or equivalently, woodchips were 20% of the volume of pea gravel (Peterson et al. 2015). This corresponded to a porosity of 0.34. Prior to packing the mixed media into the column, woodchips were soaked in synthetic stormwater (Table 2-1) for two days (Lynn et al. 2015a; Peterson et al. 2015). Afterwards, woodchips were completely rinsed with DI water and thoroughly mixed with the pea gravel. For the column design 1 (Figure 2-1), mixed media was packed to a height of 70 cm, whereas column design 2 (Figure 2-2), mixed media was packed to a height of 45 cm.

Treatment Media

In some cases, 5-mm Willow Oak woodchips were subject to dilute alkaline and subsequent acid pretreatment prior to inoculation for batch experiments. Woodchips were completely dried for a minimum of 24 hours at 105°C prior to pretreatment. Woodchips were placed in 2-L glass beakers and immersed in 1% NaOH (w/v) solution with a solid to liquid ratio of 1:10 (Wang et al. 2008). Beakers were covered with aluminum foil and

placed in autoclave at 121°C for 30 minutes. After alkaline pretreatment, woodchips were thoroughly washed with DI water. Subsequently, woodchips were soaked in synthetic stormwater (Table 2-1), where pH measurements exceeded the acceptable range for denitrification (pH > 8). Without acid addition, batch studies revealed negligible denitrification activity due to pH inhibition. In order to reduce the pH, 1N H_2SO_4 was added to the soaking solution, as adopted by Chaudhary et al. (2012). The pH was closely monitored to account for the natural buffering capacity of the pretreated woodchips, and acid was slowly added until reaching a target pH between 5.5 and 6.0. At this point, woodchips remained immersed in the acid-modified soaking solution for a minimum of 2 days before the start of batch studies, where the final solution pH was within the optimal range of 6.0-8.0.

2.1.3. Synthetic Stormwater Preparation

The baseline concentrations and constituents of all synthetic stormwater components are outlined in Table 2-1. Baseline stormwater specifically refers to a constant nitrate concentration at 3 mg-N/L to represent a typical event mean concentration (EMC) of a first-flush event (Pitt and Morquecho 2005; Han et al. 2006; Li and Davis 2014). Nitrate, in the form $NaNO_3$, was the only nitrogen species added; assumingly, at this lowest layer of bioretention, nitrate is the dominant N species whilst other forms would have been removed and/or biologically transformed into nitrate. Also, at this depth, most suspended solids, metals, and hydrocarbons would be removed (Hunt et al. 2012). Thus, the only remaining stormwater constituents of interest are phosphate and dissolved solids. Phosphate, as Na_2HPO_4, was added at urban runoff levels (0.1 mg-P/L) to encourage bacterial growth. Calcium chloride ($CaCl_2$) was added at 80 mg/L in

order to fix the ionic strength. Nason et al. (2012) measured highway runoff DOC

ranging from 1.81 to 10.8 mg/L in Oregon. However, DOC was not added to synthetic

stormwater so that woodchips were the only carbon source. Additional stormwater

constituents as added for specific experiments are listed in Table 2-2.

Table 2-1 Chemical composition of synthetic stormwater runoff as to be applied under constant baseline conditions

Pollutant Type/Name	Chemical	Manufacturer	Concentration
Nutrient/Nitrate	Sodium Nitrate	Fisher Scientific	3 mg-N/L
Nutrient/Phosphate	Dibasic sodium phosphate	J.T. Baker	0.1 mg-P/L
Dissolved Solids	Calcium Chloride	J.T. Baker	80 mg/L

Table 2-2. Additional synthetic stormwater and preparatory chemicals as needed for specific experiments

Experiment Designation	Pollutant Type/Name	Manufacturer	Concentration
Sodium Azide Control Test	*Pollutant/*Sodium Azide	Fisher Scientific	1000 mg-N/L (Prep) 50 mg-N/L (Test)
Tracer Test	*Dissolved Solids/*Sodium Chloride	VWR	100 mg/L
Salt-Spiked Toxicity Test			5 g/L
Treatment Media Preparation	Sodium Hydroxide	Sigma Aldrich	1% w/v (2g)
	Sulfuric Acid	Fisher Scientific	1N
Deoxygenated-Reduced Baseline	*Pollutant/*Sodium Sulfite	Fisher Scientific	30 mg-SO_3/L

2.2. Experimental Tests

2.2.1. Batch Study

Woodchips and baseline influent stormwater were added at a solid to liquid ratio

of 1:3 (by volume) in a 1-L container wrapped in aluminum foil, as to be consistent with

the woodchip to pore volume ratio of the IWSZ. No pea gravel was added to batch

studies. 40 mL grab samples were collected over the course of the entire experiment,

approximately 50 hours to characterize the first-order approximated kinetics. Upon

collection, all batch samples were tested for pH, nitrate, TN, and TOC.

Batch studies are defined by the woodchip preparation method. A summary of all

batch study materials are outlined in Table 2-3.

Table 2-3. Materials for the control and treated woodchips for batch study analysis. Both batches were conducted in triplicate for three weeks.

	Control Woodchips	Treated Woodchips
Pea Gravel Volume (cm^3)	0	0
Woodchip Volume (cm^3)	250	250
Stormwater Volume (mL)	750	750
Seed Volume (mL)	0	75

The first set of experiments was a control, or untreated media. This was designed

to ensure that denitrification could occur in a batch scale, and also, to verify that the

associated first-order rate constant, k, is consistent with prior determination in the

Column 1 design. The second set of batch studies focused on additional woodchip

pretreatment in attempt to increase the rate constant (as outlined in Treatment Media).

However, since methodology required autoclaving the woodchips, and presumably killed

the native denitrifying-bacteria population in the woodchips, such batches were

supplemented with an external source of denitrifiers. To ensure sufficient inoculation of

the bacteria, effluent from the IWSZ (Figure 2-2) was provided to the batches at a 1:10

ratio of the influent stormwater prior to start of the weekly experiment. Synthetic

stormwater was prepared and pumped into the IWSZ until 75 mL of the effluent was

collected and transferred to the three replicate treated batches.

In all batch studies, three replicates were run per week; this was repeated for three weeks to ensure that the acclimation period subsided and denitrification rates were representative of maximum achievable values.

2.2.2. Column 1 Experimental Design

Establishing Denitrification Set-Up

Two sets of control tests were designed to verify that nitrate removal was biologically-mediated denitrification in the Column 1 (Figure 2-1) configuration. In both control tests, the 70-cm packed media column was loaded with 2.5 L of artificial stormwater, as prepared in Table 2-1, once the effluent valve was properly set to drain at an initial rate of 1.4 mL/min. Composite grab samples were collected over the course of 2.8 days.

The first was performed without a carbon source (woodchips), i.e., the media was only pea gravel. The second control test required a modification to the artificial stormwater preparation with the addition of sodium azide. Control mixed-media included the addition of sodium azide into woodchip preparations as woodchips were soaked in synthetic stormwater containing 1000 mg-N/L NaN_3 prior to column packing. The column was loaded with 2.5 L of synthetic stormwater containing 50 mg-N/L NaN_3.

Denitrification Kinetics Set-Up

Control mixed media was packed into the Column 1 design (Figure 2-1) to analyze denitrification kinetics. 2.5 L of synthetic stormwater was added to the column and over the course of 2.8 days, composite samples were collected and analyzed for nitrate. The first week of nitrate data was not used for denitrification kinetic analysis; this was denoted as the acclimation or lag-phase period (Lynn et al. 2015a; Peterson et al.

2015). The subsequent weeks represented well-acclimated media. Each week the influent

nitrate concentration was varied to determine a denitrification rate order and associated

constant, *k*. The variable nitrate concentrations were 1.0 mg-N/L, 3.0 mg-N/L, and 6.0

mg-N/L. The column was fully drained by the end of the 2.8 days and was left

undisturbed between experiments.

2.2.3. Column 2 (Model IWSZ) Experimental Design

An experimental set-up of the Column 2 (Figure 2-2) is presented in Figure 2-3.

This set-up is specific for constant 3.0 mg-N/L influent stormwater concentrations and a

constant flowrate. Dynamic inflow nitrate concentrations and corresponding rates were

conducted by replacing the large single reservoir with 5 smaller reservoirs.
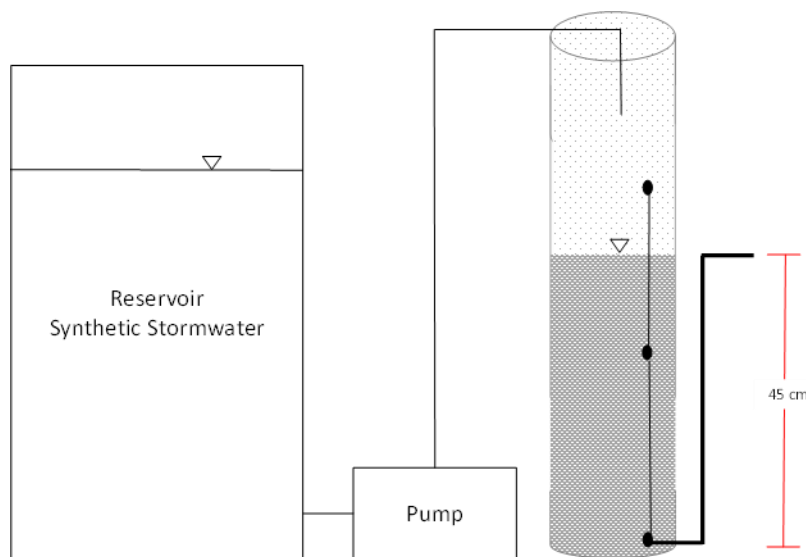
Figure 2-3. Experimental Set-Up of the Column 2, model IWSZ design, including the reservoir of prepared stormwater and peristaltic pump.

Tracer Tests

Tracer tests allow for the comparison of the (theoretical) hydraulic retention time

(HRT) to the (actual) constituent residence time (t_c) in order to evaluate the extent of

mixing, i.e., characterization of hydrodynamic behavior. Tracer tests were performed at HRTs of 1.8, 0.9, and 0.5 hours, correspond to flowrates of 11, 22, and 38.5 mL/min, respectively.

Prior to the start of each tracer test, the entire column was completely flushed with DI water at 80 mg/L of $CaCl_2$ as to ensure the removal of any interfering compounds. The tracer test proceeded by spiking the influent stormwater (Table 2-1) with 100 mg/L NaCl. Electrical conductivity (EC) measurements were taken first, of influent salt-spiked stormwater, and continuously, throughout the sample collection period. Influent salt-spiked stormwater entered the column at the predetermined uniform flowrate and continued until effluent sample EC measurements consistently ($n \geq 5$) was equal or greater than 95% measured influent NaCl-spiked stormwater; average EC reading of the NaCl-spiked synthetic stormwater was 284 µS/cm. At this point, the influent salt-spike stormwater stopped, and baseline influent entered the column at the same uniform flowrate continuing until effluent sample EC measurements consistently ($n \geq 5$) was equal to or greater than 95% of the influent baseline reading. Average EC reading of the synthetic stormwater was approximately 130 µS/cm.

F-Curves were generated by normalizing the EC measurements and plotting against elapsed time as defined by the start of influent spiked or baseline stormwater pumping began (Fogler 2011). As such, 2 separate F-Curves were produced from one tracer test; one that showed the EC normalized value going from 0 to 1, and a second, showing the reverse. Specifically, the first curve was used to quantify the following dispersion parameters - (1) constituent residence time, (2) variance, (3) dimensionless variance, and (4) n-CMFRs.

<u>Nitrate Removal and Hydraulic Retention Time</u>

Runoff was applied first, at a constant velocity of 16.8 cm/hr corresponding to an approach flowrate, Q, of 22.0 mL/min, using a peristaltic pump, based on a typical rainfall duration and rainfall intensity-to-runoff application rate. This velocity was regarded as baseline nitrate application rate, with a nitrate concentration of 3.0 mg-N/L. The baseline rate was presumed a reasonable estimate of well-established media, as it is within the range of proposed interval hydraulic loading rates for a 45-cm IWSZ in Lynn et al. (2015b). After each simulated event, the column was left undisturbed for the following two days or more. In other words, the IWSZ was subjected to at least a 2-day antecedent dry condition (ADC), where media remained in contact with stormwater.

In order to minimize macroscale environmental disturbances, i.e., the presence of dissolved oxygen in stormwater and redox measurements of non-reduced conditions, incorporated additional preparatory steps of the influent stormwater. Stormwater nitrate concentration was 3.0 mg-N/L and applied at baseline conditions for 6-hours, unless otherwise specified. Prepared stormwater influent was deoxygenated overnight with nitrogen gas, and this set of experiments was denoted as Deoxygenated Baseline. Some baseline experiments also included the addition of 30 mg-SO_3/L of sodium sulfite prior to the storm event. This set of experiments is denoted as Deoxygenated-Reduced Baseline. Additional measurements included dissolved oxygen (DO) and ORP of the stormwater influent, in addition to the regular sample analysis. At the time of sampling, a DO probe and ORP probe was placed in the reservoir of prepared stormwater and measured accordingly (Figure 2-3).

To evaluate the variable nitrate effluent patterns with respect to influent flow

rates, i.e., hydraulic retention times, multiple events were simulated. Each storm was replicated at least once, again with a minimum of 2-day ADC. The additional baseline storms are summarized in Table 2-4. Some HRT storms were conducted for 72 hours, as opposed to 6 hours, to assess steady state nitrate removal conditions.

Table 2-4. Summary of Baseline Storms with Corresponding Hydraulic Retention Time in Laboratory-Scale IWSZ

Approach Velocity (cm/hr)	Flow Rate (mL/min)	HRT (hrs)	Storm Duration (hrs)
1.9	2.5	8.0	72
2.5	3.3	6.0	72
3.8	5.0	4.0	72
8.4	11.0	1.8	6
16.8	22.0	0.9	6
29.4	38.5	0.5	6

Toxicity Effect: Nitrate Removal and Increased Salt Loading

In order to investigate the toxicity effect of increased salt concentrations on denitrifiers, synthetic stormwater was prepared with the addition of 5 g/L NaCl. This corresponds to a 0.5% NaCl solution to mimic stormwater salinity after winter road salt application(s). Stagge et al. (2012) reported that a small number of deicing treatments in winter are responsible for elevated chloride concentrations in highway runoff. Combined with measured runoff influent chloride EMCs ranging from 5 to 6423 mg/L in Natarajan and Davis (2015), equivalently 8 to 10581 mg/L NaCl, the highest concentrations may be correlated with road salt application. Experimental design followed steady state 3-day storm event with a corresponding 8-hour HRT.

Application to Maryland Type Storm Events

In an attempt to mimic the variability in hydrograph and pollutant concentrations for stormwater runoff systems, input pollutant loading rates, along with storm duration were varied from the baseline of 3.0 mg-N/L at 16.8 cm/hr for 6 hours. The inflow was

separated in discrete intervals with a triangular hydrograph and a "first flush" declining pollutant concentration. Five discrete flow and pollutant concentration increments were used for each experiment (Figure 2-4).
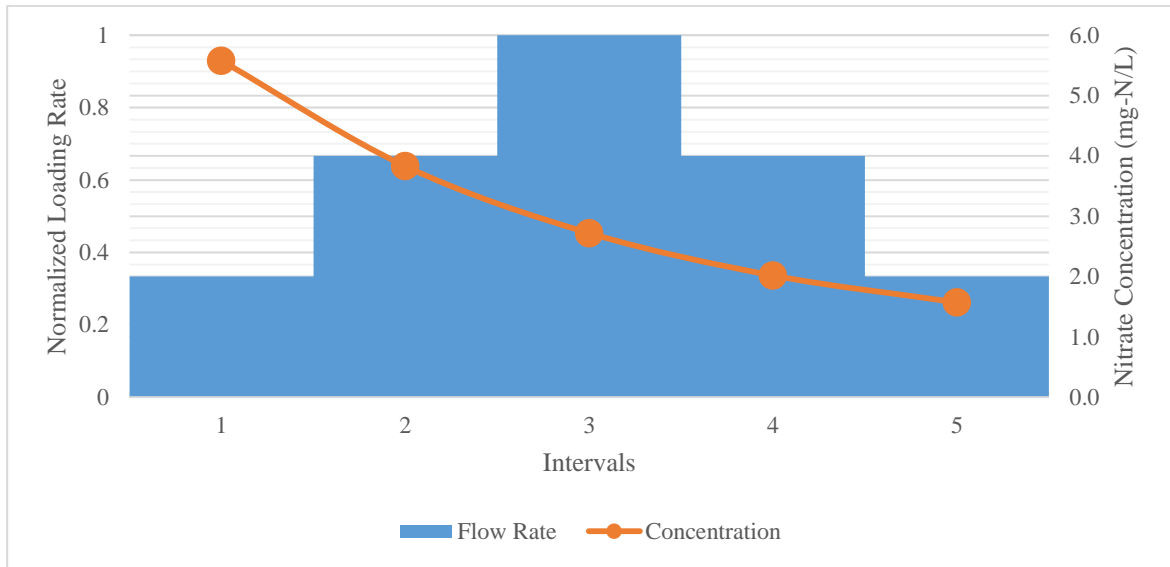
Figure 2-4. Normalized first-flush simulated storm event, with a flowrate derived from the Rational Method and an exponentially declining nitrate concentration.

Experimental input flows and storm durations were derived from recorded Maryland storm events, where the intensities were organized by intervals and presented along with their probability of occurrence (Kreeb 2003). Rainfall depth and duration was averaged for each interval to characterize a single storm; for the largest storm, the duration was assumed to be 36 hours. The depth was determined to be 3.0 inches based on the following assumptions below:

1. Maryland, on average, receives 102 cm (40 inches) of rainfall per year (US Climate Data 2016).

2. Maryland, on average, accumulates this total rainfall depth over the course of 60 rainfall events

3. The depth of all storms is represented as the midpoint of the interval range as provided.

Such field-scale intensities were then translated for laboratory based application through the adaption of the Modified Ration Method (Iowa SUDAS 2013). The peak runoff rate, Q_p, is calculated in Equation 2-1. Complete derivation with corresponding flowrates for each interval of all storms shown in Table 2-5 are compiled in Appendix III.

$$Q_p = C * i * A_{catchemnt} \hspace{3cm} \text{2-1}$$

1. The runoff coefficient, C, is 0.9. This assumes that the catchment area is highly urbanized/impervious (McCuen 2005).
2. The cross-sectional area, i.e., bioretention footprint, represents 5% of the total catchment area (Department of Environmental Resources, P.G. County 2007).
3. The intensity, i, is defined by the rainfall depth (cm) over the entire storm duration (hours).

Each event is characterized by a rainfall depth, total runoff application, and probability of occurrence (Table 2-5). Rainfall depth is in units of cm; corresponding units in inches is shown in parentheses. The two numbers below each rainfall depth correspond to the theoretical applied volume of runoff (mL) and the normalized applied pore volume based on IWSZ storage volume of 1200 cm^3 (mL), respectively, in Table 2-5.

Table 2-5. *Summary of Maryland Rainfall Distributions as Adopted from Kreeb (2003) for Laboratory-Based Simulation. Runoff application is assumed to be twice as long as rainfall duration, with a time of concentration equal to the rainfall duration, resulting in a triangular hydrograph. Associated total theoretical applied runoff volume and normalized applied pore volume are presented below the corresponding rainfall depth.*

Runoff Application	Rainfall Depth, cm (in)				
	0.140 (0.055)	0.445 (0.175)	0.956 (0.375)	1.905 (0.750)	7.620 (3.000)
	237, 0.20	754, 0.63	1616, 1.35	3232, 2.69	12927, 10.77
2.0 hr	0.2857	0.0214	0.0167	0.0043	0.0008
5.0 hr	0.0164	0.0257	0.0221	0.0089	0.0025
7.0 hr	0.0085	0.0223	0.0198	0.0083	0.0038
11.0 hr	0.0099	0.0351	0.0475	0.0221	0.0087
20.0 hr	0.0058	0.0337	0.0629	0.0528	0.0266
37.0 hr	0.0024	0.0070	0.0397	0.0611	0.0515
72.0 hr	0.0000	0.0009	0.0043	0.0172	0.0435

In order to incorporate a variable influent pollutant concentration, each discrete flow interval corresponded to a specific nitrate concentration. This was derived to represent a first-flush scenario, whereby the pollutant concentration followed an exponential decay with an event mean concentration (EMC) of 3.0 mg-N/L. The other assumptions necessary to determine the first-flush concentrations were first, an initial concentration, $C_0 = 6.0$ mg-N/L, and second, the modeled equation approaches an asymptote of 0.8 mg-N/L. The higher initial nitrate loading accounted for the accumulated nitrate that had been flushed from the upper media between and/or during the initial flows of a storm event. Concentrations are expected to decrease throughout the storm duration. Thus, the nitrate concentration can be calculated based on the following system of equations for each simulated storm event:

$$C_i = 6.0 \exp(-at_i) + 0.8 \qquad\qquad \text{2-2}$$

$$EMC = 3.0 = \frac{Event\ Duration * \sum_{i=1}^{5} Q_i * C_i}{Total\ Applied\ Volume} \qquad \text{2-3}$$

where C_i is the nitrate influent concentration of discrete flow interval i

Q_i is the flowrate of discrete flow interval i

t_i is the elapsed time from the beginning of the storm to the end of interval i

a is a parameter to characterize the rate of concentration reduction per unit of time

Solving for a for each simulated storm event and C_i for each provides results summarized in Table 2-6, where the C_i was constant regardless of storm intensity and a was adjusted to meet the desired EMC.

Table 2-6. First-Flush Simulated Nitrate Concentrations for All Maryland-Type Simulated Storms

Discrete Flow-Interval No.	Target Nitrate Concentration (mg-N/L)
1	5.58
2	3.83
3	2.72
4	2.02
5	1.57

2.3. Analysis

2.3.1. Chemical and Physical Analysis

Stormwater samples were tested for nitrate using Standard Method 4500-NO_3^- Ion Chromatographic method (APHA 1992). A Dionex ICS-1100 Ion Chromatography instrument was used for nitrate measurements with an IonPac AS22 column. Eluent contained 4.5mM Na_2CO_3 and 1.5 mM $NaHCO_3$. Nitrite measurements were conducted using Standard Method 4500-NO_2^- B - Colorimetric method; ammonium measurements followed Standard Method 4500-NH3 F. Phenate (APHA 1992). Total Nitrogen (TN)

was measured using the Shimadzu TOC/TN Analyzer.

$$\text{Organic N} = \text{TN} - (NO_3 - N) - (NO_2 - N) - (NH_4 - N) \qquad \text{2-4}$$

Oxidation/reduction potential (ORP) was measured in situ in the columns at each sampling time. When applicable, regular measurements of dissolved oxygen (DO) and ORP were measured and recorded for the influent stormwater. The pH and 2 ORP probe measurements were read from a Thermo Scientific Orion pH/mV 3-Star meter.

Measured values below detection limits or the lowest standard were reported as half of the lowest standard. Best practices were followed in regards to quality assurance and quality control. Regular standard checks were conducted. If the standard check(s) was not within 10% of the expected value the system was recalibrated. Standard laboratory and data handling and analysis procedures were practiced. All instruments are listed in Table 2-7 and undergo regular and continued maintenance according to instrument operation manuals.

Table 2-7. Compiled list of analytical methods and corresponding Standard Methods (when applicable), instruments and detection limits.

Method	Instrument	Measured	Detection Limit
4500-NO3- Ion Chromatographic	Dionex ICS-1100	Nitrate	0.05 mg/L-N
4500-NO2- B - Colorimetric	Shimadzu UV160U	Nitrite	0.01 mg/L-N
	Shimadzu TOC-5000	Total Nitrogen	0.1 mg/L-N
4500-NH3 F. Phenate	Shimadzu UV160U	Ammonium	0.05 mg/L-N
505 Organic Carbon (Total)	Shimadzu TOC-5000	Total Organic Carbon	0.5 mg/L
	Orion pH Meter Model 520A	pH	-2.00
	Fisher Scientific Epoxy Low Maintenance ORP/ATC Triode	Oxidation/Reduction Potential	± 1999.9 mV
	sensION+ DO6 Portable Dissolved Oxygen Meter	Dissolved Oxygen	0 – 20 ppm
	YSI Model 35 Conductance Meter	Electrical Conductivity	Cell constant, K = 1.0/cm 0.1 μ Ω/cm

2.3.2. Biological Analysis

Scanning electron microscopy (SEM) imaging of woodchip samples from batch study experiments was used to investigate the effects of dilute alkaline pretreatment on woodchips. All SEM work was conducted at Montana State University by Ms. Laura Kellerman. Upon sample arrival, one control and treated woodchip were attached to a SEM mount using double sided tape and left to fully air dry. Samples were coated with Iridium at 20 mA for 60 seconds using an Emitech K575X sputter coater to make the surface conductive. Samples were imaged in the SEM using a Zeiss Supra 55VP Field Emission Scanning Electron Microscope operated at a 1.0 kV. The dehydration and coated chemical conductive material result in the collapse of the three dimensional biofilm and significant sample distortion viewed on the two dimensional plane (Abed et al. 2012).

Prior to batch study trials, initial comparison of SEM images of untreated (control) and pretreated (treatment) woodchips offered visual confirmation of a woodchip physical deformation. One site of the treated woodchip and control woodchip was selected for additional detailed imaging after viewing 500X magnification. This selected site was considered representative of the entire surface that was not charging. For both samples, a 1000X site was further imaged at two locations under 2,000X and 5,000X magnification as it showed vivid brightness and contrast for easier viewing. Scaling of treated SEM images ranged from 10µm to 100 µm, whereas control SEM images ranged from 3µm to 100µm. After three weeks of incubation, a control and treated woodchip was subject to SEM imaging. This set of imaging results aimed to identify biofilm formation and offer a semi-quantitative analysis of cell density. For both samples, six sites were viewed at 8,000X magnification, whereby one site was selected for further imaging. The treated woodchip site was viewed under 14,000X, 15,000X, 18,000X, and 24,000X magnification; the control woodchip site was viewed under 15,000X, 22,000X, 23,000X, and 26,000X magnification. Scaling of both woodchip SEM images ranged from 1 to 2 µm.

DNA extraction followed by metagenomic 16S rRNA sequencing was performed on woodchips following one-year of continuous operation in the Column 2 assembly. Three wet woodchip samples, weighing a total of 0.8662 g, were removed from the middle of the IWSZ. The chips were sonicated in order to remove and resuspend biofilm cells into a 2 mL 80 mg/L $CaCl_2$ buffer solution (Stoodley et al. 1998). The buffer solution was selected because it is also the background stormwater salt concentration for most experimental work. Woodchips were sonicated in a Branson 2210 Ultrasonic

cleaner for five minutes in a water bath. Woodchips were removed from the 15-mL centrifuge tube container. The remaining liquid was thoroughly mixed. 1-mL samples of homogenized liquid sample were prepared and frozen until DNA extraction.

DNA was extracted according to the manufacturers' instruction in the PowerSoil DNA Isolation Kit (MoBio Laboratories). The sample was thawed and centrifuged for one minute at 20°C and RCF of 10.000 G (Thermo Scientific Sorvall Legend Micro 21R Microcentrifuge). A 0.2421 g pellet of each sample was collected by pipetting at 60 µL increments.

Extracted DNA was used as a template for PCR amplification. Results confirmed that the DNA exhibited sufficient quality as to allow for V3-V4 sequencing and any present inhibitors from the IWSZ environment did not impact PCR amplification. DNA was amplified using the 341F/907R universal primers and DreamTaq PCR MasterMix (ThermoFisher Scientific) on a Thermocycler.

DNA was sent to the BioAnalytical Services Laboratory at the Institute of Marine and Environmental Technology, at the University of Maryland Baltimore County. Ms. Sabeena Nazar was responsible for the 16S rRNA Metagenomics Report using an Illumina-based platform.

Chapter 3 Laboratory Results and Discussion

Denitrification was the primary nitrate removal mechanism in the laboratory-designed IWSZ. Experimental results are discussed as to first establish the environmental conditions required for microbial-mediated denitrification. Second, laboratory work investigated the role of contact time between the denitrifying bacteria, whom are responsible for nitrate acquisition and consumption, and the influent nitrified stormwater.

3.1. Environmental Conditions for Denitrification

In order to validate that denitrification was the primary means of nitrate removal, two control tests were performed (Figure 3-1) in the *Column 1* design (Figure 2-1). The first, *Pea Gravel Control,* corresponded to IWSZ media only composed of pea gravel. Influent concentration measured 2.74 mg-N/L and average effluent concentration measured 2.94 ± 0.05 mg-N/L. This verified that denitrification required woodchips to serve as an external carbon and energy source for the denitrifying bacteria (Schipper et al. 2010; Lynn et al. 2015a; Peterson et al. 2015). Second, *Sodium Azide Inhibition* incorporated 50 mg-N/L NaN_3 to the artificial stormwater. Stormwater influent nitrate concentration measured 3.16 mg-N/L and average effluent concentrations measured 3.14 ± 0.15 mg-N/. The addition of NaN_3 created an inhibitory effect on the denitrifying microbes (Bremner and Yeomans 1986; Peterson et al. 2015). Results of the *Pea Gravel Control* and *Sodium Azide Inhibition* tests indicated a -4% and 1.6% mass removal, respectively. Thus, heterotrophic denitrification was not only a biologically mediated process, but the woodchips could not be responsible for any nitrate physiochemical transformations (Peterson et al. 2015).
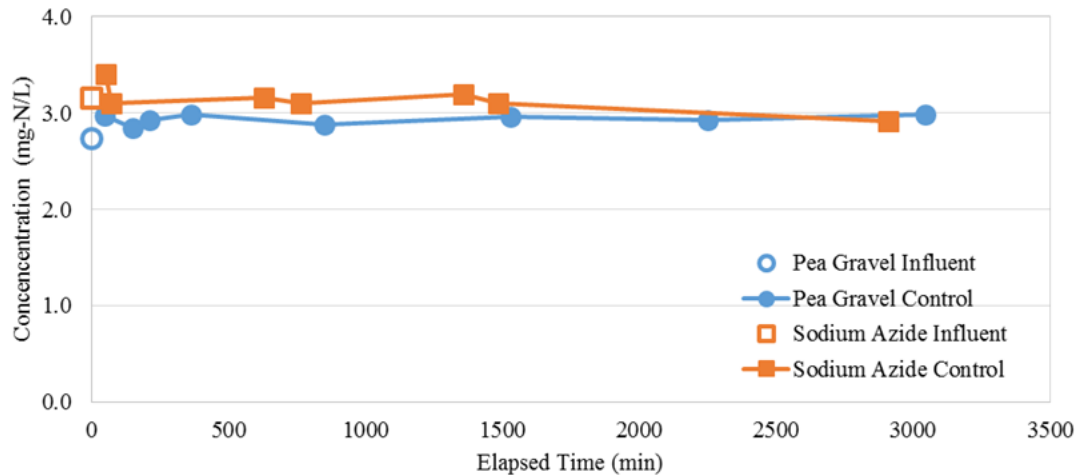
Figure 3-1. Establishing environmental conditions to confirm the presence of microbial denitrification - (1) absence of an external carbon source (woodchips), and (2) inhibition of denitrifying microbes with the addition of 50 mg-N/L NaN₃ in stormwater influent.

Nitrate removal was evaluated in the IWSZ containing a mixture of woodchips (4.5% by mass) and pea gravel, and loaded at variable nitrate influent concentrations (

Figure *3-2*). The Column *1* design was successfully able to reduce synthetic stormwater influent nitrate concentrations of 6.0, 3.0, and 1.0 mg-N/L to below the 0.05 mg-N/L detection limit within 4000 minutes, or approximately 2.8 days (

Figure *3-2*). The concentration of nitrate shown at time 0 minutes represents the influent stormwater nitrate concentration; composite grab samples were collected over 4000 minutes, so that reported elapsed time is the average of the collection period (

Figure *3-2*). The first effluent sample was often lower than its expected value. This can be attributed to a slight dilution with stormwater that had been retained in the column a week prior. While Run 1 and Run 2 were loaded under the same influent nitrate concentration, the effluent nitrate profile did not follow the same trend (

Figure *3-2*). Rather, the sampling times between 500 and 1500 minutes indicated a concentration difference of at least 1 mg-N/L. Run 1 was representative of a lag phase,

i.e., the media was neither well-established nor were the denitrifiers exhibiting optimal performance (Robertson 2010; Lynn et al. 2015a; Peterson et al. 2015), thus, it was not indicative of an accurate denitrification rate. Comparison of Run 2 with subsequent variable influent nitrate concentrations, e.g., 1.0 and 6.0 mg-N/L, demonstrated similar removal patterns. Nitrate concentrations consistently were reduced to below 0.05 mg-N/L without any noticeable lag phase and therefore, media was considered well-acclimated. The 3.0 mg-N/L Run 2, 1.0 mg-N/L and 6.0 mg-N/L loaded column experiments were included to characterize the denitrification rate order and quantify the associated rate
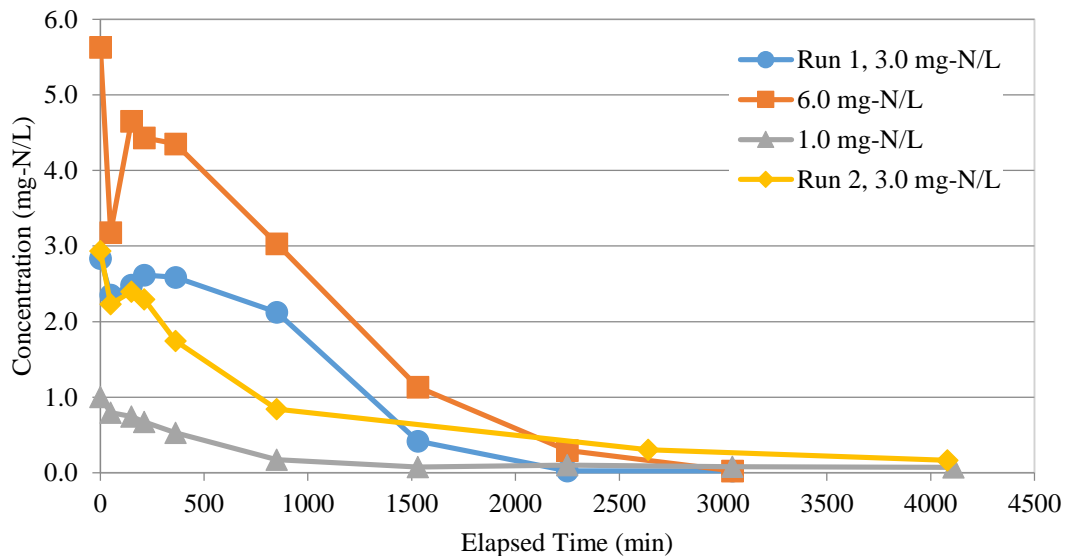
Figure 3-2. Nitrate loss (mg-N/L) in the Column 1 design containing a mixture of woodchips and pea gravel. Composite samples are collected over the 4000 minutes and nitrate concentrations are plotted at the average time.

constant.

The bacteria responsible for the observed nitrate reduction in

Figure *3-2* and throughout the remainder of Chapter 3 were investigated via

Illumina 16S rRNA Metagenomic sequencing. The report compiled all bacterial genome

data present in the sonicated woodchip sample. The sample had 239,921 total read counts

with 87.34% passing quality filtering. Data were arranged by classification status beginning with the bacterial kingdom. All information specific to the phylum, class, order, family, genus, and species was also compiled into a pie chart and table displaying the top results, i.e., the 8 most abundant of the specific classification levels, where the "other" category represents the sum of all classifications with less than 3.50% abundance.

Figure 3-3 shows the class-level taxonomic results. At this taxonomic level, 78.89% of the total 165,135 reads could be classified. Specifically, the class level classifications were investigated to assess their potential for denitrification and/or anaerobic lignocellulose degradation. Previous studies have identified class-level denitrifiers via PCR-amplification targeting denitrifying enzyme reductases, or denitrifying functional genes as shown in Figure 1-2 (Jones et al. 2008; Bai et al. 2013; Tsitko et al. 2014; Saarenheimo et al. 2015; Ren et al. 2016) amongst other molecular tools, e.g., fluorescence in situ hybridization (FISH), pyrosequencing, and qualitative-PCR (q-PCR).

Acidobacteria, Clostridia, Betaproteobacteria, and Alphaproteobacteria have the ability to denitrify as demonstrated in other denitrifying environments, such as wastewater treatment plants (Broszat et al. 2014; McIlroy et al. 2014), activated sludge (Morgan-Sagastume et al. 2008), lakes (Saarenheimo et al. 2015), and sand filters (Bai et al. 2013). All of the identified classes contain the final nosZ gene, so the production of N_2O was not expected but not confirmed in this study.
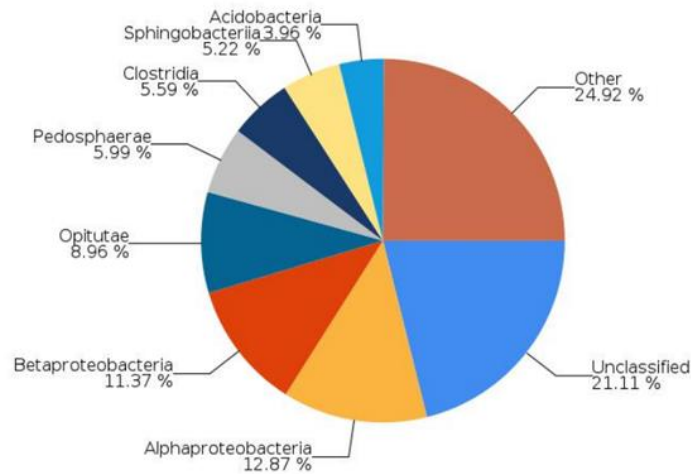
Figure 3-3. Taxonomic classification of the 8 most abundant bacterial classes present in the woodchips after 1-year of operation in the Column 2 IWSZ design.

Remaining class levels have the ability to breakdown lignocellose under anaerobic conditions. This is of important interest since the IWSZ is permanently saturated to promote anoxic conditions (Kim et al. 2003) and woodchips are a lignocellulose-based material. The lignocellulose must be hydrolyzed into soluble compounds prior to oxidation during denitrification (Desvaux 2006). Opitutae and Pedosphaerae belong to the Verrucomicrobia phylum; this phyla contains fermentative anaerobes that have the ability to degrade lignocellulose and fix nitrogen gas (Tsitko et al. 2014). Sphingobacteria were identified in the cooling and maturation phase of the co-composing of cow manure and rice straw (Ren et al. 2016). This suggested that members of this class were involved in the degradation of lignocellulose.

Combining results of known denitrifiers and anaerobic lignocellulose degraders further reinforces the presence of a mature biofilm in and/or around the woodchip structure. Most likely, some bacteria supplied soluble bioavailable carbon. Subsequently, denitrifiers oxidized preferred carbon substrates coupled with the reduction of nitrate.

Thus, the analysis of present bacterial class-level taxonomy may reveal a synergistic relationship between the two active metabolic pathways.

However, additional molecular-based analysis tools are necessary to draw more definitive conclusions. Specifically, work should integrate water quality observations, e.g., denitrification rates, and microbial community activity and dynamic response. For example, q-PCR targeting denitrifying functional genes coupled with current metagenomic data may be of interest. Similar to the experimental work of Warneke et al. (2011b), a more thorough analysis of the denitrifying bacterial community with respect to temperature and carbon substrate may account for differences in denitrification kinetics and production of N_2O. Moreover, the proportion of denitrification genes to the total bacterial DNA (16S rRNA) genes can reflect the carbon uptake used for denitrification as opposed to non-denitrifying carbon utilization. A non-invasive approach may employ stable-isotope probe in combination with microautoradiography (MAR)-FISH can be adopted to identify and characterize unrecognized active denitrifiers as in McIlroy et al. (2014).

3.2. Contact Time Requirements

Results established by Herbert (2011) suggested that laboratory experiments could quantify the role of flow rate with respect to denitrification kinetics and mass transfer parameters. In particular Herbert (2011) acknowledged the coupling of heterotrophic denitrification and oxidation of organic matter. This study did not verify complete denitrification, i.e., water quality and/or biological assessment tools to analyze for nitrous oxide production was not employed. Previous laboratory and field-scale

woodchip denitrifying systems have reported some release of nitrous oxide (Schipper et al. 2010; Herbert 2011; Warneke et al. 2011a).

Fundamental mass transfer mechanisms for any solute refer to diffusion, advection, and dispersion. Interaction between the macro and microscale environment is dynamic and dependent on such mass transfer parameters.

Figure 3-4 identifies the three major "zones" of interest as follows:

1. Bulk liquid phase

2. Denitrification biofilm

3. Boundary Layer

The bulk liquid phase, in this case the stormwater, is representative of the macro-scale environment and was the only quantifiable phase within this study. Therefore, nitrate effluent profiles coupled with other dynamic nutrient and environmental system measurements, e.g., pH and ORP, helped to develop a contact time equation and identification of critical limiting parameters.

The microscale environment consisted of the biofilm that was assumed to form and mature around the woodchips, and the boundary layer, as defined by the thickness, δ, and the concentration gradient that existed between the bulk-liquid and the biofilm (Figure 3-4). The system is best characterized as a dual porosity continuum (Herbert 2011). In such a system, it can be expected that large contrasts in hydraulic conductivity (K_H) exist over short distances. In other words, K_H of the porous woodchip-pea gravel media was significantly larger than the K_H of the biofilm. Therefore, a single porosity, homogenous environment would not properly characterize the physical processes that occurred during and between storm events (Herbert 2011).
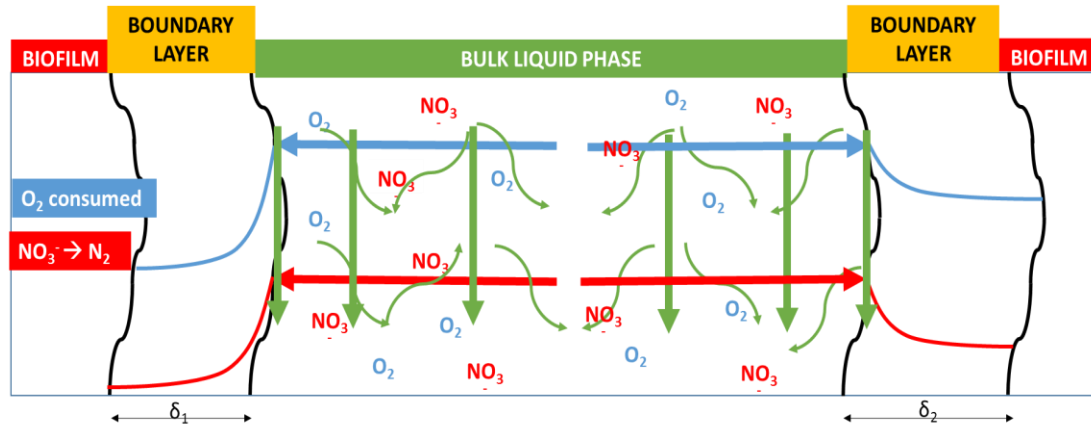
Figure 3-4. Conceptual depiction of macro and microscale environmental interactions and fate of solutes during simulated storm event. The macroscale is confined to the bulk liquid phase, or stormwater, whereas the microscale environment consists of the biofilm and boundary layer separating the porous phase from the biofilm.

One may expect that advective-dispersive transport was confined to the mobile bulk liquid region, and the presence of a solute in the immobile phase (biofilm) was solely dependent on diffusion from the mobile to the immobile liquid (van Genuchten and Wagenet 1989). However, in reality, both the boundary layer δ will adjust with changes in flowrate, and the biofilm may be physically sloughed from the woodchip lattice during high flow events. Sloughing events, in particular, may cause variations in the biofilm's physical shape and metabolic activity, and thus, the associated kinetics may not reflect the optimal rate (Costerton et al. 1995). The biodegradation of the solute, i.e., nitrate via denitrification, or the consumption of the solute, i.e., oxygen via aerobic respiration, was assumed confined to the biofilm itself.

3.2.1. No-Flow Condition

When the system was at rest, i.e., subjected to a *no-flow* condition, the necessary contact time for nitrate concentrations to fall below detection limit and signify complete denitrification was represented as follows:

$$\text{Minimum Contact Time } = \frac{1}{k} + D_t + t_{anoxia} \qquad \text{3-1}$$

where k is the first-order rate (time^{-1}) denitrification rate constant

D_t is the time required for diffusion of nitrate across the boundary layer and into the biofilm

t_{anoxia} is the time associated with the complete consumption of oxygen in the biofilm to ensure anoxic conditions
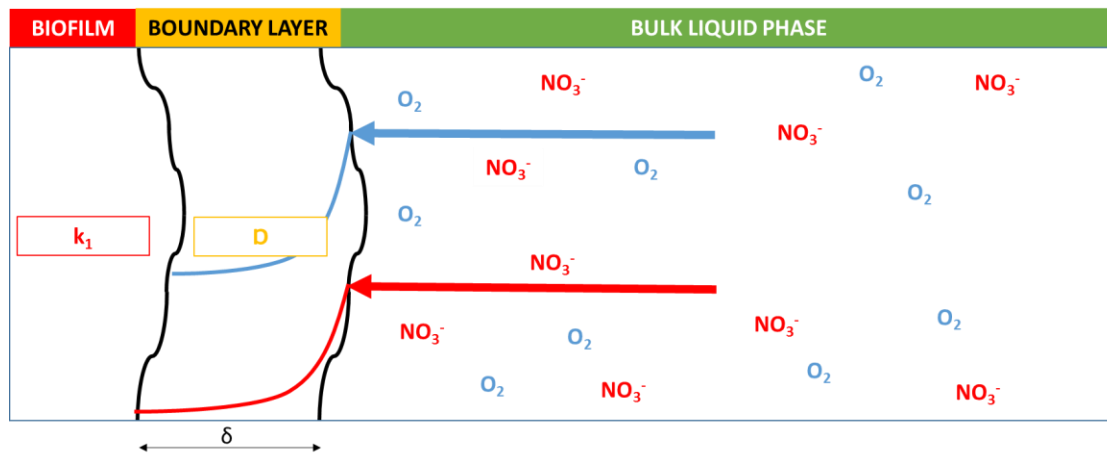
Figure 3-5. Conceptual depiction of contact time under the no-flow condition. Contact time is the sum of (1) establishment of anoxic conditions, (2) diffusional mass transport (D) of nitrate across the boundary layer, and (3) denitrification kinetics (k₁) restricted to the biofilm layer.

As shown in Figure 3-5, diffusion is the transfer process responsible for the movement of oxygen and nitrate out of the bulk liquid and in contact with the biofilm (Stewart 2003). The boundary layer, as defined by δ, accounts for mass transfer resistance and is regarded as the immobile, if not slow-moving, fluid adjacent to the biofilm. This study acknowledges the presence of a dynamic δ, and the nutrient gradients that exist between the macro/microenvironment and within the biofilm itself (Bishop et al. 1995; Sternberg et al. 1999). However, δ was never quantified, nor was the corresponding diffusional time, D_t, known to be a function of both boundary layer thickness and solute (Stewart 2003).

This introduced a new term into Equation 3-1, the apparent rate constant, k_{app}. Therefore, the reported denitrification rate constant accounts for both microscale processes, e.g., diffusion across the boundary layer and nitrate reduction within the biofilm. The antecedent dry condition (ADC) was quantified by measuring stormwater nitrate effluent concentrations when the system was under a *no-flow* condition. As defined by Lynn et al. (2015b), the ADC is defined as the number of whole days between storm events. Collectively, the minimum contact time equation can be revised (Equation 3-2).

$$\text{ADC} \approx \text{Mininum Contact Time} = \frac{1}{k_{app}} + t_{anoxia} \qquad \text{3-2}$$

Summed Denitrification Kinetics and Diffusional Mass Transport

Lynn et al. (2015a) determined that a maximum denitrification rate could be achieved when the IWSZ media was well-established and subjected to permanently saturated conditions. Following the experimental set-up of Peterson et al. (2015), the *Column 1* configuration was modeled as a sequencing batch reactor to determine the reaction rate order and associated constant, k_{app}.

Three influent nitrate concentrations were selected to determine a reaction order and k_{app} value: 1.0, 3.0, and 6.0 mg-N/L. Both zero-order and first-order reaction kinetics were fit to the compiled data. The mass balance and derivation of k for a sequencing batch reactor following zero and first-order is shown below:

$$\frac{dM}{dt} = V\frac{dC}{dt} + C\frac{dV}{dt} = Q_0 C_0 - QC \pm rV \qquad \text{3-3}$$

where   V is the system volume

                C is the effluent concentration

t is time

Q_0 is the influent flowrate

Q is the effluent flowrate

r is the reaction rate that can either consume or generate C

Column 1 is modeled as a sequencing batch reactor, so that $Q_0 = 0$ mL/min and Q = 1.2 mL/min by a constricted effluent valve

This simplifies to the mass balance equation to

$$V\frac{dC}{dt} = -rV$$

$$\frac{dC}{dt} = -r$$

When r is a zero-order equation, r = -k

When r is a first-order equation, r = -kC

$$\frac{dC}{dt} = -k$$

$$\frac{dC}{dt} = -kC$$

Including the boundary conditions of the integration,

$$\int_{C_0}^{C} dC = -k\int_{0}^{t} dt$$

$$\int_{C_0}^{C} \frac{dC}{kC} = -\int_{0}^{t} dt$$

Integrating and solving to C yields, for zero-order and first-order, respectively,

$$C = C_0 - kt \qquad\qquad 3\text{-}4$$

$$C = C_0 \exp(-kt) \qquad\qquad 3\text{-}5$$

By fitting the experimental data to zero-order and first-order equations, goodness-of-fit statistics suggest data were better represented by first-order kinetics. Thus,

remaining denitrification kinetics discussion resides on the assumption that it follows a first-order reaction. The first-order denitrification rate constant that best fit experimental nitrate reduction under different influent nitrate concentrations is 0.0011 min^{-1} (Figure 3-6).
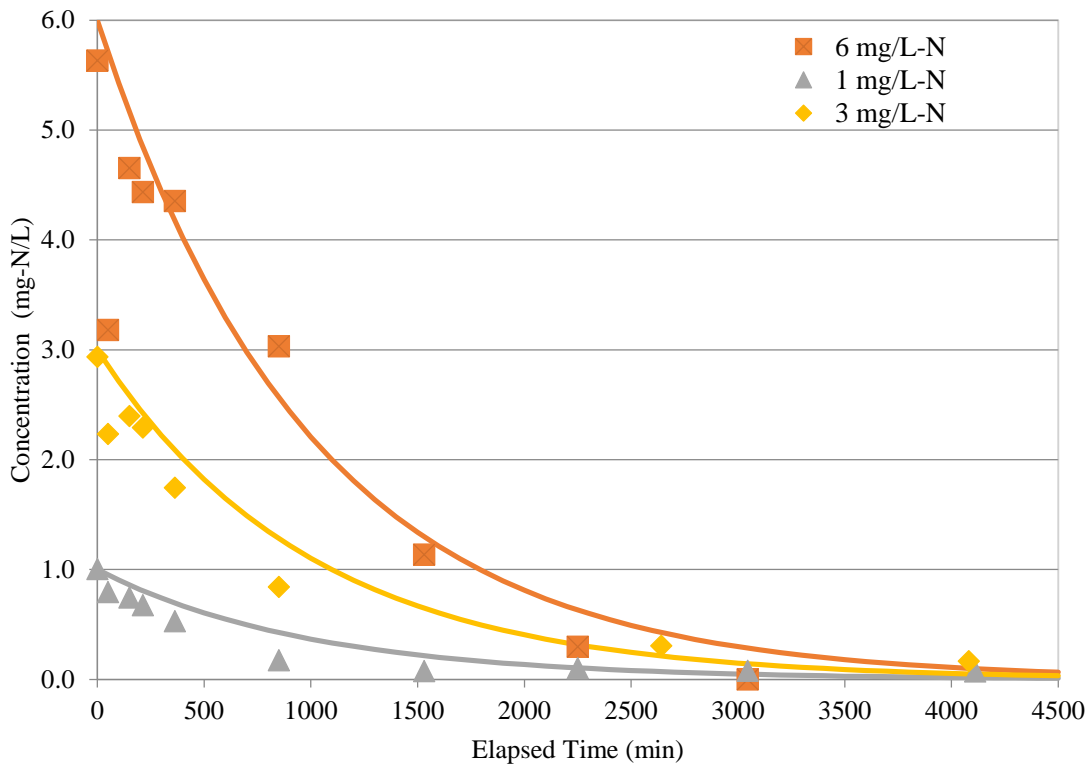
Figure 3-6. Pseudo-First Order k Data-Fitting, where k_{app}=0.0011 min^{-1}, as determined by minimizing the sum of squares under variable nitrate influent concentrations. The quantified rate constant is assumed to be the total time associated with diffusional mass transport and biodegradation of nitrate time.

Table 3-1 summarizes published order and associated *k* values for denitrification. If researchers classified *k* as zero-order and the influent nitrate concentration was available, *k* was converted to first-order with units of min^{-1} for comparison. This study's reported *k* value is on the same order of magnitude as some previous work (Chun et al.

2009; Leverenz et al. 2010; Peterson et al. 2015). It is interesting to note that while these reports were all conducted at the laboratory scale, the denitrifying environment contained (presumably) different wood characteristics and nitrate influent concentrations were much greater than 6.0 mg-N/L. Chun et al. (2009) reported two *k* values within 15% of this study's *k* determination at nitrate concentrations of 11.2 and 21.1 mg-N/L; Leverenz et al. (2010) designed a wetland for nitrified wastewater treatment that removed influent nitrate concentrations ranging from 53 to 82 mg/L-N at a rate approximately 50% higher than this reports. Other *k* determinations for other woodchip-based systems were on the order of 10^{-4} min^{-1} revealing that this study's IWSZ configuration was capable of nitrate removal at faster rates.

The quantified k_{app} indicated that the use of a lignocellulose-based carbon source exhibits a slow denitrification rate, where retention time is on the order to days to ensure measured nitrate concentrations were below the 0.05 mg-N/L detection limit. Experimental work quantified the contact time for complete denitrification to be 4000 minutes, or 2.8 days (Figure 3-2). Rearranging Equation 3-5 based on the quantification of *k*, the estimated the contact time, *t*, was 3722 minutes or 2.6 days for complete denitrification assuming an influent of 3.0 mg-N/L.

$$t = -\frac{\ln\left(\frac{C}{C_0}\right)}{k} \qquad \text{3-6}$$

Therefore, if an IWSZ does not retain stormwater for a minimum of 2.6 days, denitrification will not be complete. Furthermore, a retention time of this length reveals a fundamental challenge in the context of bioretention or any other nature-based stormwater technology. Such sustainable treatment technologies are traditionally

designed to intercept high flow stormwater runoff rates. The designed contact time

should reflect the ability of the SCM to meet hydrologic and water quality goals (Davis et

al. 2010, 2012b).

Table 3-1. Summary of previous research classification of denitrification rate order and constant using woodchips as the external provided carbon source for denitrification.

Reference	Environment	Woodchip Species	Influent N Source and Concentration	Reaction Order	Presented k Value	k (min^{-1})
This study	Lab Scale – Sequencing Batch IWSZ Zone	Willow Oak	Variable – 1, 3, and 6 mg/L-N NaNO$_3$	First Order	0.0011 min^{-1}	0.0011
Peterson et al. (2015)	Lab Scale – Sequencing Batch IWSZ Zone	Willow Oak	3 mg/L-N NaNO$_3$	First order	11.4 day^{-1}	0.0079
			3 mg/L-N NaNO$_3$	Zero order	6.6 mg N/L-day	0.0015
Lynn et al. (2015a)	Lab Scale - Microcosms	Eucalyptus	2.14 mg/L-N, Spiked KNO$_3$ stormwater pond	First Order	0.58 hr^{-1}	0.0097
				Zero Order	9.24 mg N/L-day	0.0030
Robertson (2010)	Lab Scale – Bioreactor simulated columns	Hardwood fresh	3.1 mg/L-N, Spike KNO$_3$ Avon stream water	Zero Order	11 mg N/L-day	1.96E-4
		Hardwood fresh	13.2 mg/L-N	Zero Order	13.8 mg N/L-day	6.64E-4
		Hardwood fresh	23.7 mg/L-N	Zero Order	13.8 mg N/L-day	4.04E-4
		Hardwood fresh	48.8 mg/L-N	Zero Order	18.6 mg N/L-day	2.65E-4
Chun et al. (2009)	Lab Scale - Bioreactor	Not specified	Creek water 11.2 mg/L-N, Spiked KNO$_3$	First Order	0.074 h^{-1}	0.0012
			Creek water 10.4 mg/L-N, Spiked KNO$_3$	First Order	0.131 h^{-1}	0.0022
			Creek water 25.7 mg/L-N, Spiked KNO$_3$	First Order	0.037 h^{-1}	6.2E-4
			DI 33.7 mg/L-N, Spiked KNO$_3$	First Order	0.024 h^{-1}	4E-4
			DI 21.1 mg/L-N, Spiked KNO$_3$	First Order	0.075 h^{-1}	0.00125
Chun et al. (2010)	Field Scale - Bioreactor	Not specified		First Order	0.01 h^{-1}	1.7E-4
Warneke et al. (2011a)	Field Scale – Denitrification Bed	Mixture of woodchips and saw dust	>100 mg/L-N nitrified wastewater effluent	Zero Order	7.6 mg N/L-day	
Leverenz et al. (2010)	Lab Scale –SSF Wetland	Recycled pallet woodchips	Nitrified wastewater, 53-82 mg/L-N (unplanted)	First Order	2.28 d^{-1}	0.0016
			Nitrified wastewater, 53-82 mg/L-N (planted)	First Order	1.30 d^{-1}	9.0E-4

<u>Establishment of Anoxic Conditions</u>

To complete the Minimum Contact Time Equation (3-2) under the *No-Flow* condition, the required time to establish anoxic conditions must be quantified.

Prior to the OPR measurements presented in Figure 3-7, a constant 3.0 mg-N/L nitrate concentration was applied for 3 days at v = 1.8 cm/hr (2.5 mL/min). The ORP measurement of 80.1 mV at time 0 signaled beginning of a *No-Flow* condition. Initial measurements indicated an aerobic environment most likely due the presence of oxygenated stormwater in system. ORP decreased at a rate of 0.5 mV/min (n=10; R^2=0.9956) until it reached 0 mV. At this point, the rate nearly doubled at an ORP reading of -0.97 mV/min (n=11; R^2=0.9909) until it approached -250 mV (Figure 3-7). This trend is expected to continue until the environment approached its maximum reducing potential where the ORP will plateau until disturbed.
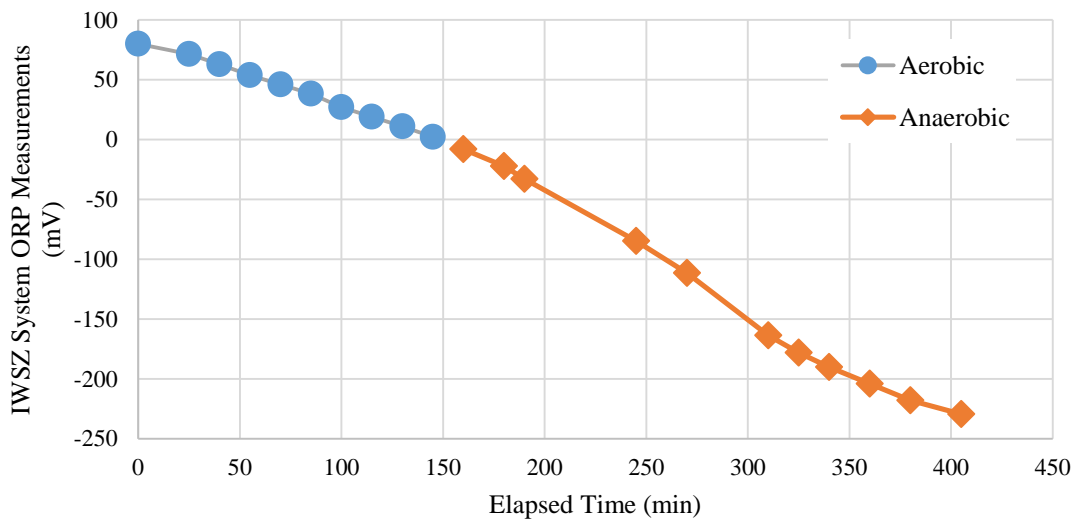
Figure 3-7. Continuous ORP Measurements of the IWSZ System under no-flow condition directly after the continuous 3-day application of 3.0 mg-N/L stormwater. Starting ORP is 80 mV and the redox potential is recorded for 400 minutes.

While the ORP measurements were only reflective of the macro-scale reducing potential, there are two possible assumptions – (1) the macro-scale paralleled the biofilm environment, i.e., it continually became more reduced, or (2) the macro-scale was not reflective of the biofilm environment. Anoxic microniches within the biofilm may have developed, both inside and/or at the woodchip surface (Partheeban and Kjaersgaard 2014). Stewart (2003) proposed that anaerobic microorganisms can thrive in aerated waters assuming that such anaerobes resided at biofilm depths on the order of 10 µm. It is at this depth that the aerobic bacteria locally deplete the oxygen resulting in concentrations below 1-2 ppm, and allow for the coexistence of the two (Stewart 2003; Rivett et al. 2008).

Results of Figure 3-7 revealed that the macro-scale environment was below 0 mV within 2.5 hours. According to Stumm and Morgan (1995) denitrification occurs between -200 and 200 mV. Assuming initial ORP measurements were 400 mV and a declining rate of 0.5 mV/min, the time required to reduce the redox potential to 200 mV is approximately 400 minutes (0.28 days). Robertson (2010) estimated oxygen depletion in a laboratory column to occur within 1 hour. In either case, the time associated to deplete oxygen, and establish anoxic conditions, is noticeably less than the 2.6 days required for complete denitrification. Accounting for t_{anoxia} into Equation 3-2 based on this study's experimental findings suggests that stormwater must be retained up to 2.9 days to ensure first, the establishment of reduced conditions, and then, observe nitrate concentrations below 0.05 mg-N/L. Regardless of whether the first condition is necessary for denitrification, the addition of 0.28 days to the 2.6 day contact time will not increase the

2-day ADC. Therefore, the time for oxygen depletion is neglected and Equation 3-2 can be further simplified to:

$$\text{Minimum Contact Time} = 2.6 \text{ days} \qquad \text{3-7}$$

<u>Effect of Lignocellulose Material on Denitrification Kinetics</u>

Woodchip-based media is a lignocellulose material, which has been widely used in denitrifying systems to serve as a long-lasting carbon source/reducing agent and substrate for microbial biofilms (Kim et al. 2003). Previous work has estimated the longevity of woodchip denitrifying systems to exceed a decade (Robertson 2010; Lynn et al. 2015a; Peterson et al. 2015) due to the recalcitrant nature of lignin that restricts the cellulose accessibility. Alkaline pretreatment of the woodchips was proposed as an alternative media treatment method; the major effect is the delignification of the biomass, thereby exposing the cellulose to enzymatic hydrolysis and increase the bioavailable carbon (Wang et al. 2008). A three-week batch study experiment of control (untreated) media and treated (subjected to dilute alkaline pretreatment) media revealed differences amongst nitrate reduction rates and system longevity. Compiled batch study TOC and pH measurements are shown in Figure 3-9 and Figure 3-10.
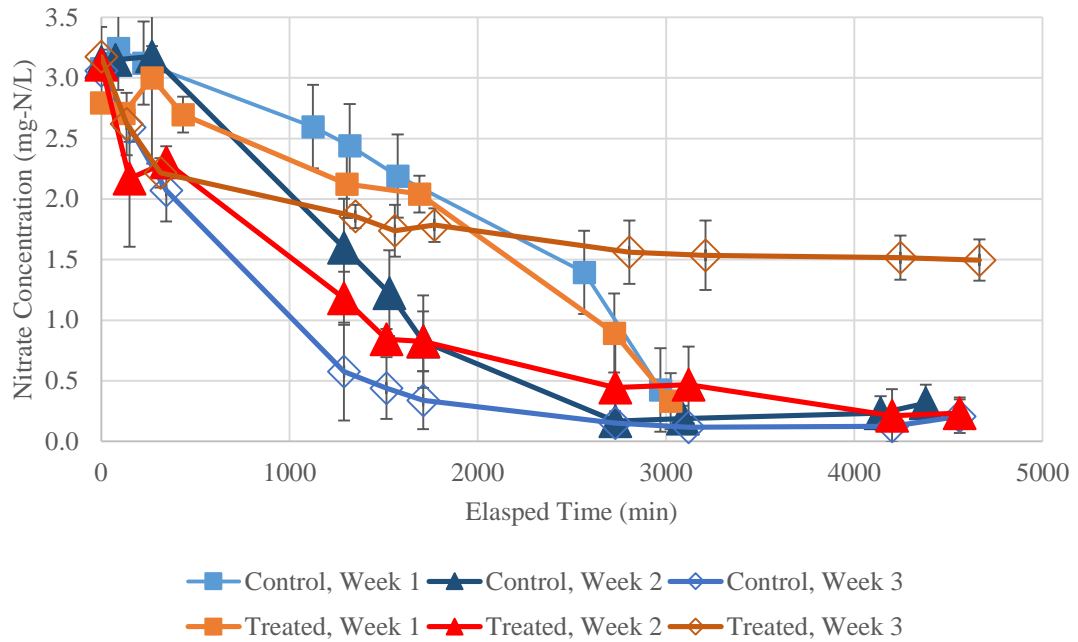
Figure 3-8. Nitrate-N concentrations from Control and Treated Woodchip Batch Studies. Average values from all 3 runs for each sampling point are shown. Error bars show one standard deviation from the mean.
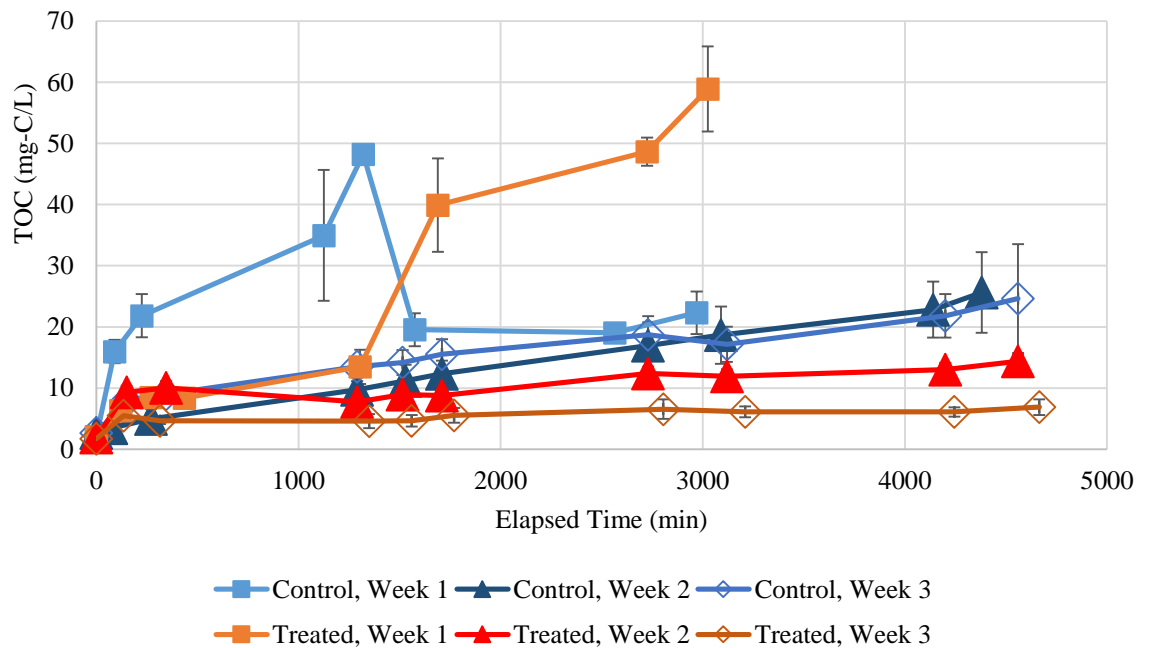
Figure 3-9. Total Organic Carbon concentrations from Control and Treated Woodchip Denitrification Batch Studies. Average values from all 3 runs for each sampling point are shown. Error bars show one standard deviation from the mean.

49
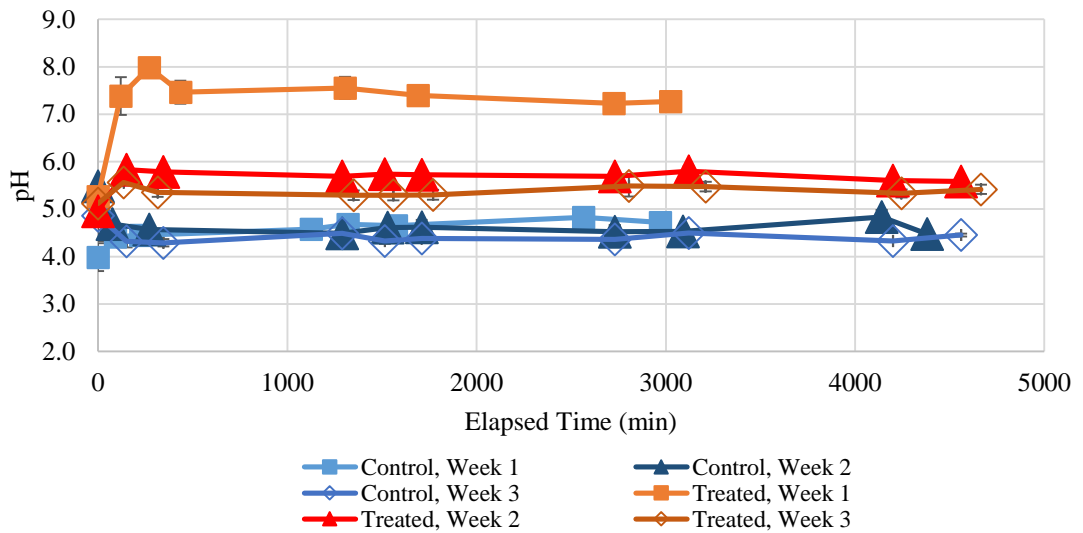
Figure 3-10. Compiled pH measurements of Control and Treated Woodchip Batch Studies. Average values from all 3 runs for each sampling point are shown. Error bars show one standard deviation from the mean.

For *Week 1* experiments, initial nitrate measurements of the both batch studies did not reduce more than 10% of the reported influent concentration until almost one day of contact time. In the control batch, nitrate reduced from 3.08 mg-N/L ± 0.09 mg-N/L to 2.60 mg-N/L ± 0.13 mg-N/L in 1125 minutes; the treated batch nitrate reduced from 2.79 mg-N/L ± 0.06 mg-N/L to 2.13 mg-N/L ± 0.28 mg-N/L in 1305 minutes. Therefore, independent of woodchip treatment, both *Week 1* nitrate data appeared to exhibit a lag period (Figure 3-11). The observed lag phase was consistent with the *Column 1* denitrification kinetic analysis, where one week was necessary for biofilm acclimation and maturation with respect to the synthetic stormwater nutrient contents. A t test confirmed a statistically significant difference between the control and treated *Week 1* nitrate profiles ($p < 0.05$). In other words, the lag phase itself was specific for the control and treated woodchip media.

Both media types demonstrated maximum TOC concentrations during *Week 1*. The treated *Week 1* TOC values steadily increased up to 58.9 mg-C/L in 3000 minutes. In

50

comparison, the control media steadily increased to a maximum TOC concentration of 48.2 mg-C/L at 1320 minutes and then abruptly declined and remained at 20.3 mg-C/L $\pm$ 1.76 mg-C/L for remainder of the experiment. However, a paired t test comparing the average control and treated batch *Week 1* TOC measurements did not indicate a significant difference (p > 0.05). Most likely, the treated *Week 1* TOC reflected high concentrations of reduced sugars and subsequent acid-formation that led to the observed pH drop between *Week 1* and *2* (Figure 3-9). Reducing sugars may have further degraded to formic, acetic, and levulinic acid (Palmqvist and Hahn-Hägerdal 2000). Presumably, the higher control *Week 1* TOC measurements were due to leached nutrients from the woodchips as observed in previous studies (Lynn et al. 2015a; Peterson et al. 2015). Treated *Week 1* pH values ranged from 7.2 to 8.0 (Figure 3-10). Glass and Silverstein (1998) suggested an aquatic environment with a pH around 8.0 was optimal for denitrification. Despite pH conditions more conducive to denitrification, the treated media did not appear remove nitrate faster than the control media (Figure 3-8). However, the *k* value was not determined for the *Week 1* values as to be consistent with previous kinetic determinations (Lynn et al. 2015a; Peterson et al. 2015).

The pH measurements of the control samples were between 4.0 and 5.0 for all three weeks (Figure 3-10). Galbe and Zacchi (2002) determined that this pH range was optimal for most cellulose enzyme performances.

This hypothesis is supported by SEM imaging analysis of the control and treated woodchip structures prior to batch incubation (Figure 3-11). SEM imaging was used to investigate the effects of dilute alkaline pretreatment on woodchip cell wall disruption, composition, and surface properties (Kristensen et al. 2008). Figure 3-11 shows control

51

and treated woodchips prior to batch study experiments as viewed under 500X (A and B) and 1000X (C and D) magnification. The images were not analyzed for biofilm formation since woodchip samples were not exposed to the synthetic nitrified stormwater environment. Figure 3-11 (A and B) offer visual confirmation that the alkaline pretreatment physically deformed and disturbed the organized structure of the woodchip cell wall. Similar to the SEM images of the eucalyptus-derived biochar in Hina et al. (2010), untreated samples exhibited a number of hollow channels from the plant cells with honey comb structures. Upon alkaline pretreatment, many of the honey comb structures collapsed, leaving a highly disorganized structure.
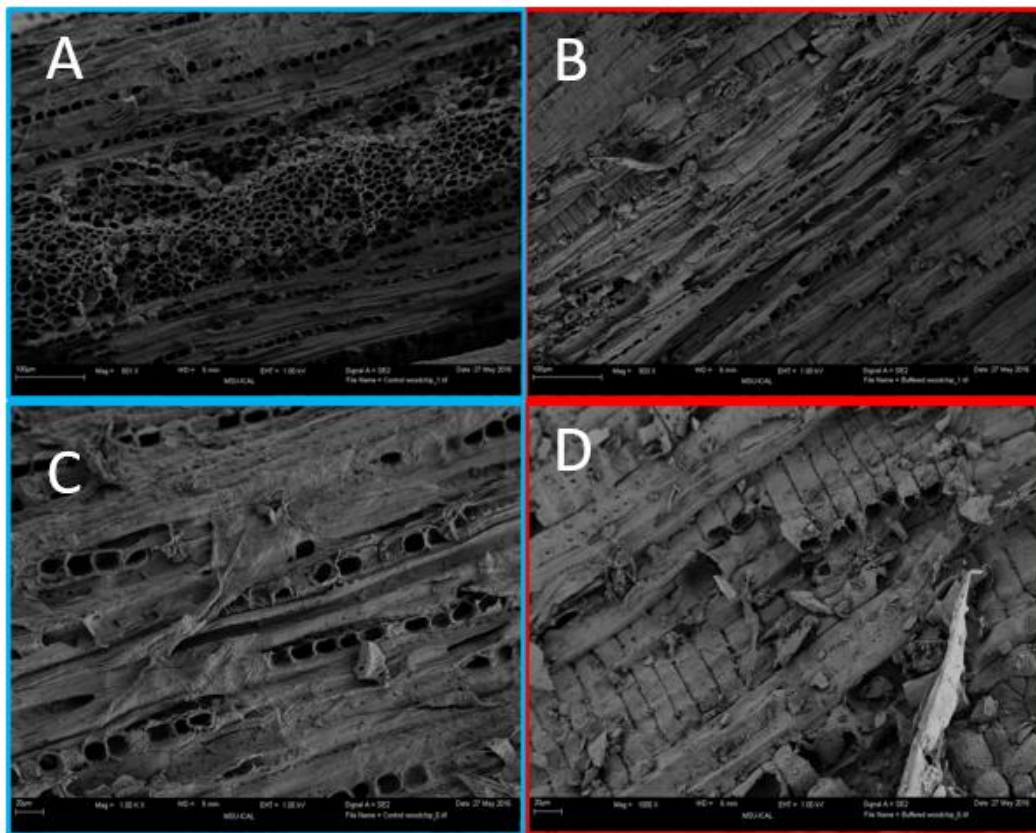
Figure 3-11. Comparison of control (A and C) and treated (B and D) woodchip. A and B are viewed at a 500X magnification. Scale is 100 μm. C and D are viewed at a 1000X magnification. Scale is 20 μm.

As shown in Figure 3-11 (C and D), the alkaline pretreatment physically removed an outer layer of the woodchip structure, and exposed a cross-hatched aligned structure. Presumably, the cellulose fibers were still intact, but now, unprotected by the lignin, cellulose was more susceptible to enzyme degradation and increased bioavailable carbon as observed in this study and others (Selig et al. 2007, 2009; Kristensen et al. 2008).

Once the media was well established, e.g., *Weeks 2 and 3*, denitrification kinetics should be representative of the maximum denitrification rate. Table 3-2 compiles the reported first-order denitrification rate constant based on the 3-Run average nitrate concentrations at each sampling time. The system was modeled as a batch reactor with a constant volume and the denitrification rate constant was assumed first-order (Equation 3-8).

$$\frac{dM}{dt} = V\frac{dC}{dt} + C\frac{dV}{dt} = Q_0 C_0 - QC \pm rV$$

where $Q_0 = 0$ mL/min

$Q = 0$ mL/min

$r = -kC$

Including the boundary conditions for integration and solving for C

$$C = C_o \exp(-kt) \qquad\qquad 3\text{-}8$$

Table 3-2. Compilation from Batch Study First-Order Denitrification Kinetic Rate Constant Using Minimization of Least Squares Regression.

Experiment		k (min^{-1})	SSE
Control	*Week 2*	6.40E-04	0.9179
	Week 3	1.20E-03	0.2809
Treated	*Week 2*	7.60E-04	0.5919
	Week 3	2.30E-04	1.0524

The average control *Week 2* influent concentration was 3.1 mg-N/L ± 0.06 mg-N/L and reduced to 0.3 mg-N/L ± 0.16 mg-N/L over 4000 minutes. Similarly, average treated *Week 2* began at 3.1 mg-N/L ± 0.10 mg-N/L and ended at 0.2 mg-N/L ± 0.13 mg-N/L. Comparison of the two nitrate profiles did not indicate the difference was statistically significant ($p > 0.05$). The associated first-order rate constant for the control and treated batch studies was 6.40×10^{-4} min^{-1} and 7.60×10^{-4} min^{-1} respectively (Table 3-2). Both values were on an order of magnitude lower than the previously reported *k* of 0.0011 min^{-1}.

Control and treated *Week 2* TOC measurements consistently increased over time. Initial average control TOC measurements were 4.98 mg-C/L ± 1.14 mg-C/L and steadily approached a maximum value of 25.6 mg-C/L ± 6.59 mg-C/L (Figure 3-9). The observed TOC behavior of the control media is consistent with prior studies (Peterson et al. 2015). In similar fashion, results of Peterson et al. (2015) measured *Week 1* maximum TOC values approaching 50 mg-C/L, whereas *Weeks 2* and *3* measurements gradually increased up to 20-30 mg-C/L upon the establishment of well-acclimated media. Initial average treated TOC measurements were 10.0 mg-C/L ± 1.33 mg-C/L and slightly increased to a maximum value of 14.4 mg-C/L ± 7.17 mg-C/L (Figure 3-9). The reduced TOC measurements from the treated woodchip *Weeks 1* and *2* indicate that microbes consumed reduced sugars. A paired t test of the two TOC profiles did not suggest that a statistical difference was present ($p > 0.05$). The pH measurements over the entire experiment exhibited little variance specific to the media-type batches (Figure 3-10). Average control pH values were 4.59 ± 0.11 whereas average treated measurements were 5.72 ± 0.08.

Week 3 treated nitrate concentrations plateaued at values greater than 1.5 mg-N/L (Figure 3-11). This corresponded to a calculated rate constant of 2.30×10^{-4} min^{-1}. However, the minimized SSE increased from *Week 2* to *Week 3* of operation as the system was unable to reduce nitrate below the 0.05 mg-N/L detection limit, and the reported *k* value did not well represent the observed nitrate removal (Table 3-2). Moreover, the rate constant for the treated batches decreased between *Weeks 2 and 3* by a factor of 3.3. The TOC values from *Week 2* to *Week 3* exhibited less intra-weekly variability; *Week 3* measurements only marginally increased from 5.5 mg-C/L ± 1.2 mg-C/L to 6.9 mg-C/L ± 1.28 mg-C/L. Collectively, nitrate and TOC results suggest that the ability of treated woodchip for nitrate removal was exhausted after two weeks of operation.

In comparison, the *Week 3* control batch *k* value of 0.0012 min^{-1} (Table 3-2) was found to be within 10% of the previously reported denitrification kinetic rate constant, 0.0011 min^{-1}. This indicates that the media is acclimated and representative of maximum denitrification rates after three weeks of operation in a batch-scale system. Average pH measurements varied between 4.29 ± 0.08 to 4.50 ± 0.01. *Week 2* and *Week 3* TOC profiles are relatively consistent with one another (p-value = 0.048). However, SEM imaging of the control woodchip batch did not exhibit visible biofilm growth and maturation (Appendix I). Part of the biofilm formation process includes the synthesis of extra-cellular polymeric substances (EPS), which are known to be energetically demanding and carbon-expensive (Allan et al. 2002). In this system, the recalcitrant nature of the woodchip may prompt minimal EPS production since bacterial already need to invest energy in enzymes for lignocellulose degradation. Previous studies have shown

that cells favor carbon conservation by minimizing carbon usage for EPS production (Allan et al. 2002). Similar to the findings of Allan et al. (2002), the biofilm wet mass and enzyme specific activity were reduced in nitrogen-limited cultures, which may explain the visibly undetectable biofilm growth in this study.

As expected, there is a statistically significant difference between treated and control *Week 3* nitrate time series ($p < 0.05$) and TOC time series ($p < 0.05$). The significant difference in observed nutrient content and nitrate removal performance can be explained by microbial economics. In general, economic theories of microbial metabolism predict enzyme production as dependent on availability of simple and complex resources. Production should increase when simple nutrients are limited and complex nutrients are in excess; production should decrease when the situation is reversed (Allison and Vitousek 2005). Essentially, the treated woodchip batch supplied the system with simple and complex C-resources. The control woodchip batch provided the system with only complex C-resources, thus, motivating microbes to invest in C acquisition. Allison and Vitousek (2005) postulated that the measured denitrification kinetic response was related to the demand and availability for carbon and nitrogen enzyme synthesis. The control media was designed to optimize the C:N ratio for microbial denitrification without sacrificing excessive organic leaching as previously determined in Peterson et al. (2015).

However, the treated media only demonstrated increased available carbon during *Week 1*. Biofilm growth, activity and heterogeneity is a direct response to the amount of nutrient, e.g., carbon and nitrogen, available for cell replication and metabolic activities (Costerton et al. 1995). An accelerated carbon breakdown should encourage faster

adhesion since the surface in question is itself a nutrient (Costerton et al. 1995). With a greater abundance and diversity of carbon-utilizing bacteria, it is likely the overall demand for carbon increased. Also the initial surplus of TOC may have promoted the growth of other microorganisms that outcompeted denitrifiers for the available carbon. Microbial economic theory suggests that denitrifiers may not have been motivated to invest in the production of N reducing enzymes. In the presence of certain carbon sources, e.g., pyruvate, glucose, and oleic acid, known denitrifiers may utilize other metabolic pathways in which oxygen is the terminal electron acceptor (Morgan-Sagastume et al. 2008). Also, previous studies indicated that denitrifiers prefer alcohol-based substrates, e.g., methanol, rather than the products of cellulose hydrolysis, e.g., simple sugars (Kumar and Lin 2010). The rapid depletion of TOC coupled with poor nitrate removal rates suggested that nutrient deficient conditions triggered the biofilm loss (Hunt et al. 2004). In doing so, starved cells may begin a search for a fresh source of nutrients to adapt to the dynamic environment (O'Toole et al. 2000). Therefore, it was not surprising that the SEM imaging after three week batch study incubation did not reveal significant biofilm growth (Appendix I).

3.2.2. Effect of Flow Conditions

Evaluating the nitrate behavior during flow conditions increases the complexity of the system (Figure 3-12). This study followed a heuristic approach to evaluate system performance as suggested by Delay et al. (2013). Measured nitrate removal was confined to the macroscopic scale, i.e., stormwater nitrate measurements coupled with certain dispersion parameters can indicate the potential for in-storm denitrification. Analogous to

the *No-Flow Condition*, the driving force of denitrification is the contact time between

the mobile, or bulk-liquid phase, and the immobile phase (Delay et al. 2013).

BIOFILM	BOUNDARY	BULK LIQUID
k_1	D	**Advection and Dispersion** • System geometry • Variable *K* gradients/Preferential flow paths = f(media) • Q
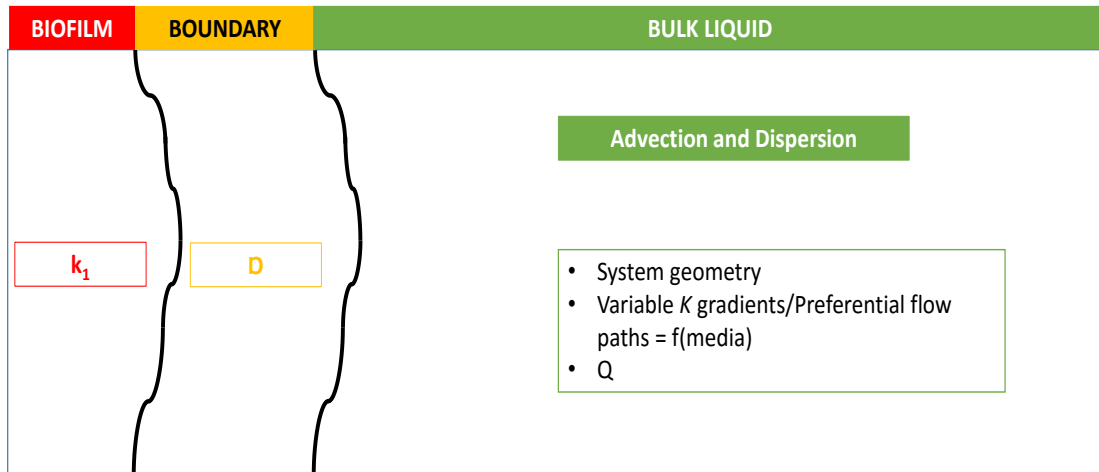
Figure 3-12. During-storm scenario, the identification of the three major zones, and important governing parameters that impact nitrate fate, transport behavior, and removal.

While subjected to flow conditions, nitrate movement is affected by advection

(moving with the direction of flow), dispersion (mixing within the surrounding

stormwater), and diffusion (transferring from the stormwater to the biofilm) (Figure

3-12). Both the spatial distribution and mixing of the mobile phase is a function of the

system geometry (Lynn et al. 2015b), the expected hydraulic conductivity gradients

between media and biofilm, introduction of preferential flow paths (Stephens 1995;

Herbert 2011), and the approach velocity, or flowrate (Q). Experimental work focused on

manipulating Q as to identify the prevailing mass transfer processes. In order to

encourage nitrate reduction under flow conditions, advection and dispersion must be

minimized for diffusion and biodegradation to occur.

Tracer tests were conducted on a 1.9, 0.9, and 0.5-hour HRT, corresponding to an

influent Q of 11.0, 22.0, and 38.5 mL/min. Dispersion parameters, e.g., constituent

residence time (t_C), variance (σ), and dimensionless variance (σ_D) were calculated to estimate a n-CMFRs in series model (Table 3-3). An *n* value of 1 represents a perfect CMFR model whereas an *n* value of infinity is a perfect PFR model. All parameters were quantified by normalizing the electrical conductivity measurements (μS/cm) corresponding to 0-1 (Figure 3-13). Initially the system only contained synthetic stormwater with a background 80 mg/L $CaCl_2$ content and at time 0 spiked-NaCl stormwater was added to the system until it completely replaced the baseline stormwater.
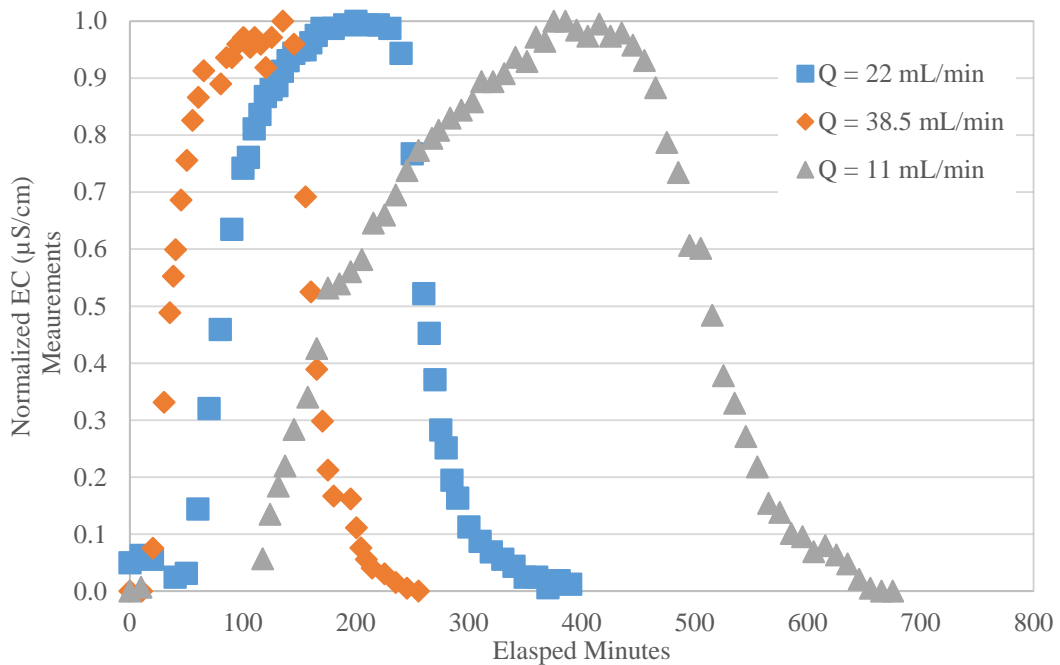
Figure 3-13. F-Curve for the 1.9-hr, 0.9-hr, and 0.5-hr HRT designed tracer studies as constructed from normalized electrical conductivity measurements to quantify dispersion parameters.

Figure 3-13 presents a second F-Curve to show the reverse situation, although this was not used in dispersion parameter calculations. Results corroborated the findings of Herbert (2011) such that increased pore water velocities coincide with increased dispersion coefficients. As the stormwater was prone to more advective-dispersive movement, the system increasingly deviated from a plug flow reactor (PFR) model. In

59

other words, as the system was characterized by a smaller number of n-CMFR in series, it exhibited more mixing as characteristic of a CMFR model (Table 3-3). In this study, it assumed that an HRT of 2.0 hours or more, the reactor model is better representative of a PFR model, as the *n* number of CMFR reactors in series is increasingly greater than 10. To maintain consistency, the IWSZ will be modeled as a PFR to evaluate parameters including the denitrification rate constant, *k*, and expected nitrate concentration removal, for flow events corresponding to an HRT of at least 2.0 hours.

Table 3-3. Summary of the relevant dispersion parameters used to evaluate the extent of mixing within the system under various flowrates. Constituent residence time, variance, and dimensionless variance were all calculated using the 0-1 portion of the F-Curve to characterize the system as n-CMFRs in series.

Flow Rate (mL/min)	HRT (hrs.)	t_C (min)	σ (hrs²)	σ	n-CMFRs
11.0	1.82	211.2	4375.1	0.10	10.19
22.0	0.91	89.8	1190.1	0.15	6.78
38.5	0.52	46.0	592.9	0.28	3.56

As to be discussed, *low flow* events are representative of in-storm nitrate removal; *high flow* events do not allow for measurable in-storm nitrate removal as the system was dominated by advective-dispersive transport.

The contact time is defined for the *Flow Condition:*

$$\text{Contact Time} \approx \text{HRT} = \frac{V}{Q} \qquad \text{3-9}$$

If the HRT is characteristic of a low flow event, then the contact time may be used as a predictive measure of nitrate removal as it is limited by the denitrification rate constant:

$$\text{Contact Time} \propto \frac{1}{k_{app}} \propto \frac{C}{C_0} \qquad \text{3-10}$$

where $\frac{C}{C_0}$ is the nitrate concentration recovery

If HRT is characteristic of a high flow event, then in-storm denitrification will not occur, and the nitrate recovery is considered negligible.

Subsequent experimental work focused first, to quantify the HRT threshold that separated *low flow* from *high flow* event. The defined HRT corresponds to an 80% concentration recovery. If the concentration recovery is greater than 80%, differences between measured influent and effluent concentrations do not reflect in-storm denitrification. Second, experimental work aimed to identify and quantify other relevant environmental and/or system parameters that could be used to predict nitrate fate and behavior within an IWSZ.

Implications of Low Flow

The contact time between the stormwater and biofilm was reduced by increasing the flowrate to correspond to 8.0, 6.0, and 4.0-hour HRT storms. Influent stormwater contained 3.0 mg-N/L and was continuously applied for 72 hours to establish a steady state nitrate removal (Figure 3-14). In all events, clean water was first washed out, then nitrate exhibited steady state in-storm denitrification removal. The average effluent nitrate concentrations at steady state for the 8.0, 6.0 and 4.0-hour HRT were 1.92 ± 0.17 mg-N/L, 2.14 ± 0.15 mg-N/L, and 2.59 ± 0.06 mg-N/L, respectively (Figure 3-14). This suggests that low Q would limit advective-dispersive transport so that nitrate diffusion and reduction could simultaneously occur. As previously quantified, the first-order rate constant of 0.0011 min^{-1} indicated that effluent nitrate concentrations of 0.05 mg-N/L would require a contact time of 4000 minutes. Thus, with contact time on the order of hours, rather than days, only partial denitrification was expected. Therefore, the steady-state nitrate profile was now limited by first-order denitrification kinetics.
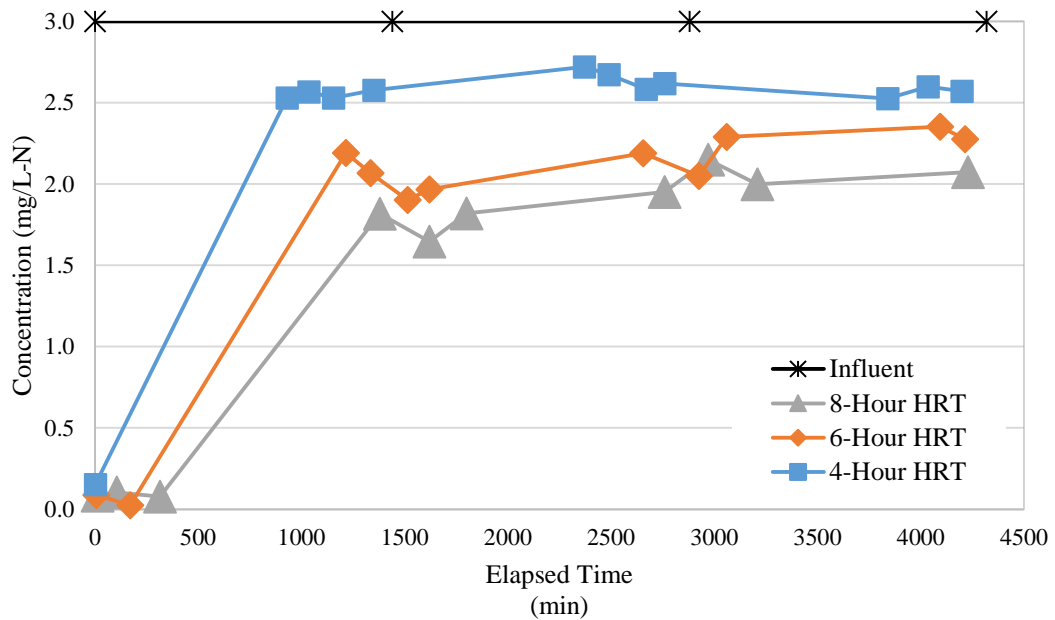
Figure 3-14. Nitrate behavior when the IWSZ system reached apparent steady state over 4000 minutes at 8.0, 6.0, and 4.0-hour HRT. The designed HRTs correspond to an influent Q of 2.5, 3.3, and 5.0 mL/min, respectively.

Nitrate removal is inversely proportional to the diffusivity time (D_t) and proportional to the first-order rate constant (*k*). Therefore, a longer contact time, as created by an increased HRT, allows for more nitrate removal, i.e., reduced concentration recovery (Table 3-4).

The associated rate constant was developed based on an assumed steady-state plug flow reactor model. 4.0-, 6.0- and 8.0-hour HRTs suggests an n-CMFR in series model with n greater than 10 (Table 3-3), which is considered to be well-representative of a PFR reactor model. The resultant equation is as follows:

$$C = C_0 \exp(-k\tau) \qquad \text{3-11}$$

where C_0 is the measured influent concentration

C is the meaured effluent concnetration

k is the first-order reaction rate constant

τ is the hydraulic retention time

The associated rate constant, k, was determined based on the average nitrate concentrations for each HRT event at steady state. The k determination for the 8.0-hour, 6.0-hour, and 4.0-hour were 7.98 x 10^{-4} min^{-1}, 9.40 x 10^{-4} min^{-1}, and 5.51 x 10^{-4} min^{-1}, respectively. Such variation in reported k values may reflect dispersion in the system, as it was not accounted for in Equation 3-11.

An average k value was calculated in attempt to represent the denitrification rate constant under all simulated flow conditions based on the results of events (Table 3-4). This corresponded to a value of 7.63 x 10^{-4} ± 1.94 x 10^{-4} min^{-1}. Therefore, assuming an 80% nitrate concentration recovery (20% removal) with an upper and lower bound for the average k of 9.60 x 10^{-4} min^{-1} and 5.66 x 10^{-4} min^{-1}, respectively, Equation 3-11 yields a corresponding HRT (τ) range of 3.87 to 6.57 hours.

Thus, to propose a single value to define the minimum HRT, the values from Table 3-4 were considered, along with the previously reported batch value of 0.0011 min^{-1}. With consideration of all data, the 6.0-hour HRT k value of 9.40 x 10^{-4} min was selected. This was considered a better representation of the *flow*-defined denitrification kinetics and is within 20% of the batch value. Using this constant, assuming an 80% recovery, the minimum denitrification contact time is found to be 237 minutes, or approximately 4.0 hours. This value may be somewhat conservative, corresponding to a 20% removal.

For this study, the remainder of the discussion defines the separation between *low* and *high flow* events at an HRT of 4.0 hours. Specific to this laboratory-designed IWSZ (Figure 2-2), a depth of 45-cm, circular cross-sectional area with a 10-cm diameter, and media porosity of 0.34, a 4.0-hour HRT corresponds to a Q = 5.0 mL/min and v = 3.8

cm/hr. Specific to this column design, any of these three values may be used to distinguish between *low* and *high flow* events.

Table 3-4. Steady-state nitrate concentration recovery as a function of HRT and the corresponding denitrification kinetics assuming an ideal PFR-mode system.

HRT (hrs.)	k (min^1)	Concentration Recovery	Nitrate Removal
4.0	5.51E-04	88%	12%
6.0	9.40E-04	71%	29%
8.0	7.98E-04	68%	32%

Throughout the duration of all three simulated events, ORP measurements were greater than 0 mV (Figure 3-15). ORP measurements of the 4.0-hour and 6.0-hour HRT storm did not exhibit much inter-storm nor intra-storm variability with one another (Figure 3-14). At steady state, the average 8.0-hour HRT ORP measurements were 122.7 $\pm$ 22.8 mV. In comparison, average 4.0-hour HRT ORP measurements were 233.4 $\pm$ 5.2 mV and average 6.0-hour HRT ORP measurements were 243.6 $\pm$ 17.9 mV. More reduced conditions during the 8.0-hour HRT event may suggest more oxygen was consumed via aerobic respiration, as the contact time between the stormwater and biofilm increased. The ORP measurements support the assumption that a heterogeneous biofilm structure formed around the woodchips, where a dissolved oxygen concentration gradient along biofilm depth allowed for aerobic and anaerobic metabolic activity (Stewart 2003).
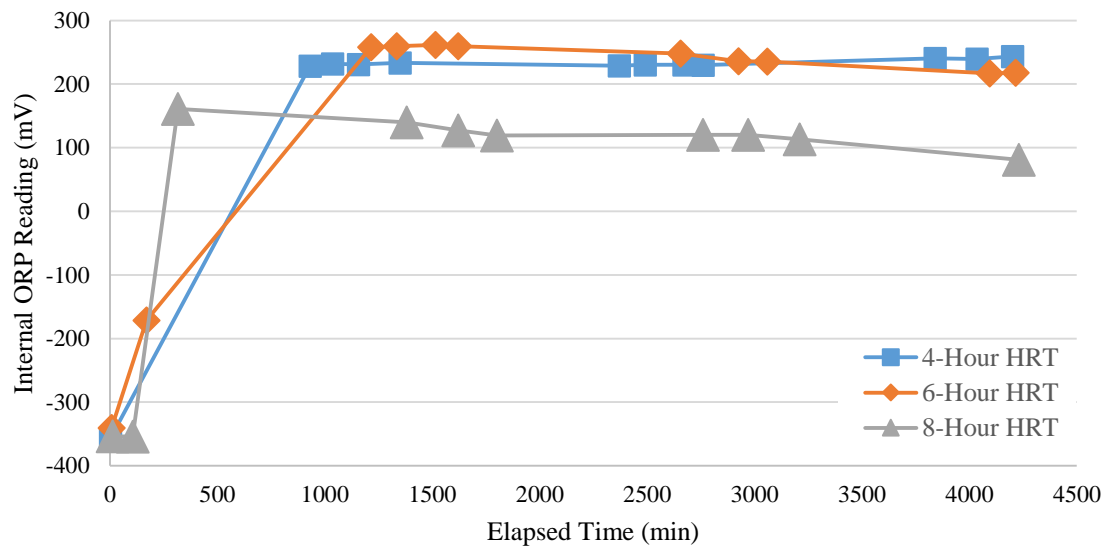
Figure 3-15. The internal ORP measurements during steady-state nitrate removal storms.

Evaluation of nitrate concentrations (Figure 3-14) and corresponding redox potential of the system (Figure 3-15) suggest that the macroscale measurements were not necessarily indicative of microscale processes responsible for nitrate removal. It is possible that the matured biofilm structure, responsible for denitrification and oxygen consumption, was highly stratified due to substrate competition, effective diffusivity of the respective solutes through the biofilm, and space limitations (Bishop et al. 1995). Microniches may have developed within the biofilm so that denitrifiers and other heterotrophic microorganisms can coexist and utilize available carbon (Schipper et al. 2010). Thus, while oxygen and nitrate may be subjected to similar diffusive movement across the boundary layer, their ultimate fate within the biofilm was quite different. Conversely, the same microorganisms responsible for oxygen depletion may also be capable of nitrate reduction. Since denitrifiers are facultative aerobes, thermodynamically, bacteria would select oxygen rather than nitrate as the terminal

65

electron acceptor (Partheeban and Kjaersgaard 2014). As compiled in Rivett et al. (2008), previous field studies suggested a threshold between 1 and 2 $mg-O_2/L$, below which the presence of oxygen did not impede denitrification. While not quantified in this study, microbial community composition and dynamics coupled with oxygen consumption rates and dissolved organic carbon conversion may help to verify either of these explanations (Peter et al. 2011).

Effect of High Salt Concentration

It is important to consider the seasonality effect of spiked salt concentrations for the environmental fate of surface-water ecosystems. Road salt as sodium chloride (NaCl) is heavily applied during the winter months for deicing roads. To mimic this scenario, synthetic stormwater was spiked at a concentration of 0.5% NaCl (or 5 g/L), and applied to the IWSZ for 3 days at an 8.0-hour designed HRT. Average influent concentrations were measured to be 1.77 ± 0.01 mg-N/L while average effluent concentrations were 1.65 ± 0.59 mg-N/L, corresponding to a 93% recovery (Figure 3-16). In comparison, when the synthetic stormwater, with a background 80 mg/L $CaCl_2$ was applied at an 8.0-hour HRT, the system demonstrated a 40% mass removal at steady state (Table 3-4).
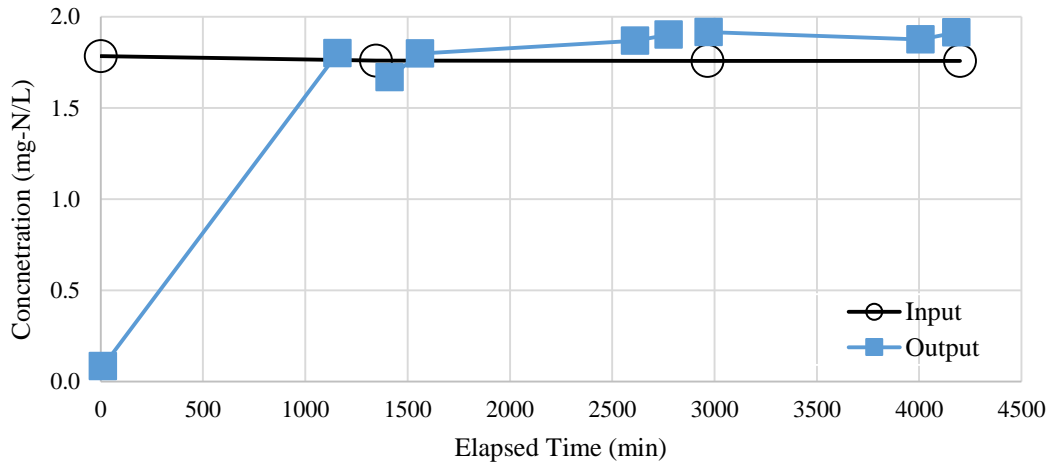
Figure 3-16. Spiked 0.5% NaCl stormwater nitrate effluent profile when applied at an 8.0-HRT continuously for 3 days.

Seitzinger (1988) compiled reports of nitrate removal via denitrification in freshwater and marine sediments. However, results of Figure 3-16 show a conservation of nitrate under a steady state 8.0-hour HRT, thus, suggesting an inhibitory effect. Park et al. (2001) observed a 10-day acclimation period with respect to denitrification from a freshwater to marine system. By diluting seawater with tap water at different ratios, initial effluent nitrate measurements demonstrated an indirect relationship between salt concentration and system efficiency. The 10-day recovery period indicated that the denitrifiers were successful in their adaptation to new environmental conditions. It is possible that if the experiment was conducted over a 10-day period, or more, after the establishment of steady state conditions, nitrate removal would resemble the findings of Figure 3-14 at 8.0-hour HRT.

Previous studies show that elevated salt concentrations can affect chemical and physical soil properties; this can be detrimental to microbial health and functionality (Rietz and Haynes 2003). Increased salinity resulted in smaller, more stressed microbial communities that were less metabolically efficient (Rietz and Haynes 2003; Yuan et al.

2007). Furthermore, salinity can restrict organic matter decomposition. The production of cellulase, enzymes necessary to catalyze celluloysis can be inhibited when subject to a highly saline environment (Badran 1994). It is possible that the salinity directly affected the available organic C and thus, denitrification was inhibited due to the lack of an external electron donor.

Regardless of either explanation, the ability for bioretention to effectively manage N loading in the winter months appears may be severely restricted due to road salt application

Implications of High Flow

Storms characterized by *high flow* events did not exhibit measurable nitrate reduction during events when the HRT was less than 4.0 hours. Specific to this study's column design, a *high flow* event corresponds to Q > 5 mL/min or v > 3.8 cm/hr. For this discussion, negligible nitrate removal, henceforth known as nitrate washout behavior, was characterized by at least 80% recovery of influent nitrate. Results indicated that *high flow* nitrate removal was dictated by the allocated IWSZ storage. Thus, *high flow* events could either be completely captured by the IWSZ, or exhibit washout behavior independent of macroscale environmental measurements, e.g., redox potential and dissolved oxygen content.

Experimental results incorporated baseline storm events, i.e., constant flowrate and influent nitrate concentration of 3.0 mg-N/L, and also, dynamic storm events. Baseline events were conducted at 1.9, 0.9, and 0.5-hour HRT as to be consistent with previous tracer study determinations. Dynamic events were characterized by typical Maryland storm depth and rainfall duration (Kreeb 2003). Events were then translated via

a Modified Rational Method and a first-flush nitrate concentration to define the pollutant loading rates, as described in Appendix III.

Effect of Storm Size

Figure 3-17 shows if the size of the event was less than the IWSZ storage capacity then the rate of incoming stormwater did not affect nitrate removal. A simulated 0.44-cm (0.175-inch) storm event corresponded to total applied runoff volume of 750 mL; in comparison, the total storage volume of the IWSZ is 1200 mL (cm^3). All effluent nitrate measurements were below the 0.05 mg-N/L detection limit (Figure 3-17) despite a first-flush input loading. In this simulated event, all flowrates: 7.0, 14.0, and 20.9 mL/min – suggested that advective-dispersive transport dominated nitrate movement. However, since the total applied volume to the system was less than the IWSZ storage capacity, no nitrate was detected in the effluent in either experimental run. This was expected because prior to storm simulation, the column was left undisturbed for at least 2.6 days; therefore, all stormwater should be completely denitrified according to the denitrification rate constant of 0.0011 min^{-1} and previous input concentration of 3.0 mg-N/L.
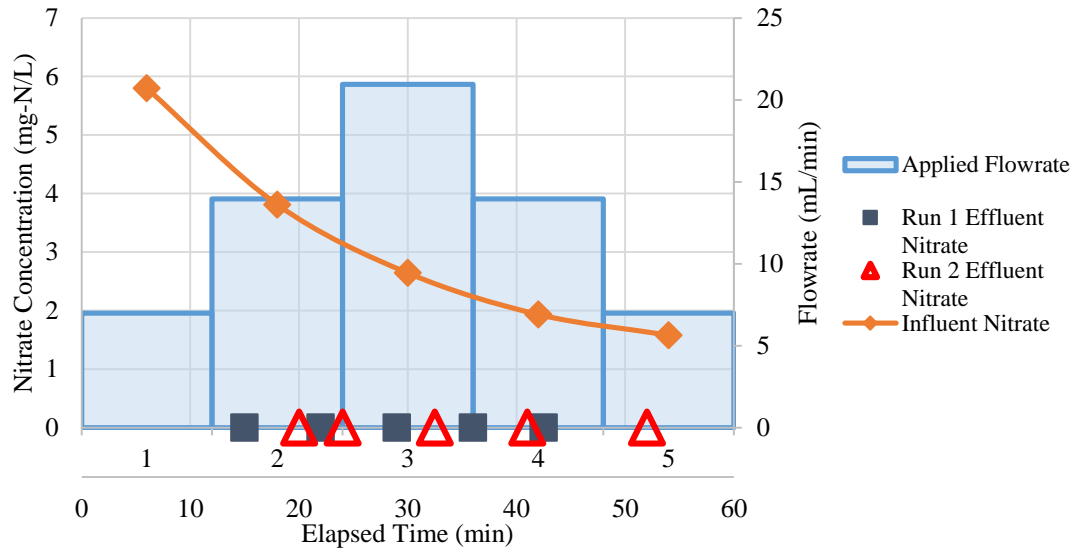
Figure 3-17. Two simulated dynamic storm events of 0.44 cm were applied to the IWSZ over 1 hour. Increments labeled 1-5 separate the 60 min event into 5 equal periods to apply triangular hydrograph shaped flowrate with an associated first-flush pollutant loading to the system.

Effect of Incoming Runoff Rate

When the runoff volume applied exceeded the storage capacity of the IWSZ and the rate of incoming flow signified a *high flow* event, nitrate exhibited a washout behavior. Therefore, the capture of a storm event, and consequently, reported nitrate mass removal, was dictated by the relationship between storm size, i.e., applied runoff volume, and IWSZ storage capacity. This was investigated under constant and dynamic pollutant loading rates.

Constant Pollutant Loading Rate

Baseline storm events were conducted at constant flowrate over 6-hours at a targeted constant influent nitrate concentration of 3.0 mg-N/L (Figure 3-18). Measured influent nitrate concentrations for 1.8, 0.9, and 0.5-hour HRT designed events were 3.05 ± 0.14 mg-N/L, 3.19 mg-N/L, and 2.79 mg-N/L, respectively; measured effluent maximum nitrate concentrations were 2.559 mg-N/L, 2.618 mg-N/L, and 2.995 mg-N/L,

respectively (Figure 3-18). All events demonstrated at least 80% recovery of the measured influent nitrate.
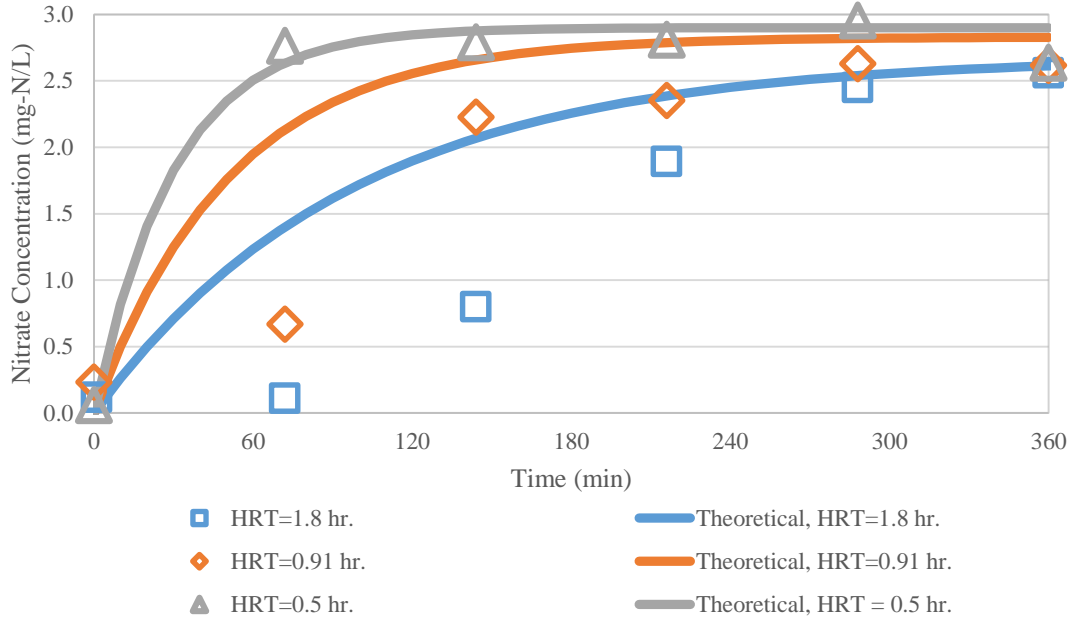
Figure 3-18. Experimental results of measured nitrate effluent concentrations under 3 HRTs at constant flow and 3.0 mg-N/L input concentration. Predicted non-steady state CMFR-modeled nitrate concentrations are shown by solid lines.

Another method to examine the assumed washout behavior of the three experiments is to compare measured nitrate concentrations with predicted values derived from a non-steady state CMFR model. Tracer studies indicated that increased flows better resembled a CMFR model (Table 3-3). Presumably, the deviation between experimental and predicted values will decrease with a shorter HRT event. The expected nitrate concentration, C, as a function of time, t, was determined to be in Appendix II:

$$C = \frac{\frac{C_{IN}}{\tau} - \left[\frac{C_{IN}}{\tau} - C_O\left(\frac{1}{\tau} + k\right)\right] exp\left[-\frac{t}{\tau} - kt\right]}{\frac{1}{\tau} + k} \qquad 3\text{-}12$$

where C_{IN} is the influent concentration

τ is the HRT (min)

C_0 is the initial concentration in the system at time 0

k is the first-order rate constant

t is time

Figure 3-18 plots the predicted C (mg-N/L) as a function of time (min) as presented in Equation 3-12 and corresponding experimental nitrate measurements. In the washout prediction curves, *k* was 0.0011 min^{-1} to be consistent with this study's prior determination.

Table 3-5 shows statistical measurements to quantify the differences between the reported nitrate concentrations and predicted washout behavior. As the HRT decreased, Equation 3-12 better predicted the measured nitrate concentrations. The statistical measurements, e.g., bias, average bias, and SSE, all decreased with a reduced HRT-designed event. While Equation 3-12 predictions always included some error, this is result of an assumed perfect CMFR reactor and restriction of nitrate movement to mobile bulk liquid phase.

Table 3-5. Statistical measurements to assess the difference between model-derived washout behavior and experimental nitrate results. Measurements are based on the selected events as presented in Figure 3-18.

	HRT = 1.8 hr	HRT = 0.9 hr	HRT = 0.5 hr
Bias	3.077	2.493	0.190
Average Bias	0.513	0.415	0.032
SSE	3.542	2.647	0.108

The 6-hour baseline events shown in Figure 3-18 were run multiple times (Appendix I). From influent and effluent nitrate measurements of each event, Table 3-6 compiles the mass removal. As the HRT increased, the nitrate mass removal was larger. However, since the influent flowrates were characterized as *high flow events*, in-storm denitrification is not expected to be responsible for the observed differences in nitrate

mass removal. Over a 6-hour period, 0.5-hour HRT applied 39.16 ± 0.68 mg-N, while a

1.8-hour HRT event applied 11.99 ± 0.15 mg-N. Cumulative mass exports for the 1.8-

hour HRT and 0.5-hour HRT event were 5.47 ± 0.35 mg-N and 33.39 ± 0.34 mg-N,

respectively. The difference between input and output masses of the two 1.8-hour and

two 0.5-hour designed HRT events was not considered to be statistically significant ($p >$

0.05). Therefore, rather than relying on the relative mass removal (%) as presented Table

3-6, the actual mass removed (mg-N) should be compared, i.e., the difference between

mass input and mass output. This is because relative removal is biased towards lower

applied influent mass. Collectively, results of Figure 3-18 and Table 3-6 suggest a nitrate

washout behavior of all simulated events.

Table 3-6. Compilation of Nitrate Mass Percentage Removal as a Function of HRT of the IWSZ.

HRT (hrs.)	Q (mL/min)	Experiment ID	Mass In (mg-N)	Mass Out (mg-N)	Difference (mg-N)	Removal (%)
1.8	11	Run 1	12.09	5.21	6.88	57%
		Run 2	11.88	5.72	6.16	52%
0.9	22	Run 1	21.83	14.82	7.01	32%
		Run 2	21.55	14.27	7.28	34%
		Run 3	25.01	14.74	10.27	41%
		Run 4	21.29	13.87	7.42	35%
0.5	38.5	Run 1	39.64	33.63	6.01	15%
		Run 2	38.68	33.15	5.53	14%

Dynamic Pollutant Loadings

Figure 3-19 shows the nitrate effluent profiles of two 1.9-cm (0.75-inch) depth

storm events. For a 3.5-hour runoff application, nitrate was applied at 6.5, 13.1, and 19.6

cm/hr (8.5, 17.1, and 25.6 mL/min), whereas a 5.5-hour event corresponded to 4.1, 8.3,

and 12.5 cm/hr (5.4, 10.9, and 16.3 mL/min) loading rates. Initial effluent concentrations

were below 0.05 mg-N/L and 0.12 mg-N/L for the 3.5-hour and 5.5-hour event, respectively. The measured nitrate effluent never equaled the highest initial input nitrate concentration of 5.8 mg-N/L, but reached a maximum concentration of approximately 3.05 ± 0.1 mg-N/L for the two storms. The mixing of the stormwater in the system, especially during peak application rates, may be responsible for the observed plateau as the first-flush pollutant application was designed based on an EMC of 3.0 mg-N/L (Equation 2-3). As shown in Figure 3-19, a more intense storm can be characterized by a slightly faster approach from a concentration at or near the 0.05 mg-N/L detection limit to the design EMC. Mass removal totals for all simulated storm events were not statistically different from one another ($p > 0.05$) (Table 3-7). In other words, since all applied flowrates in both simulated storm events exceeded the 3.8 cm/hr (5.0 mL/min) threshold, nitrate was behavior was unaffected by the dynamic pollutant loadings.
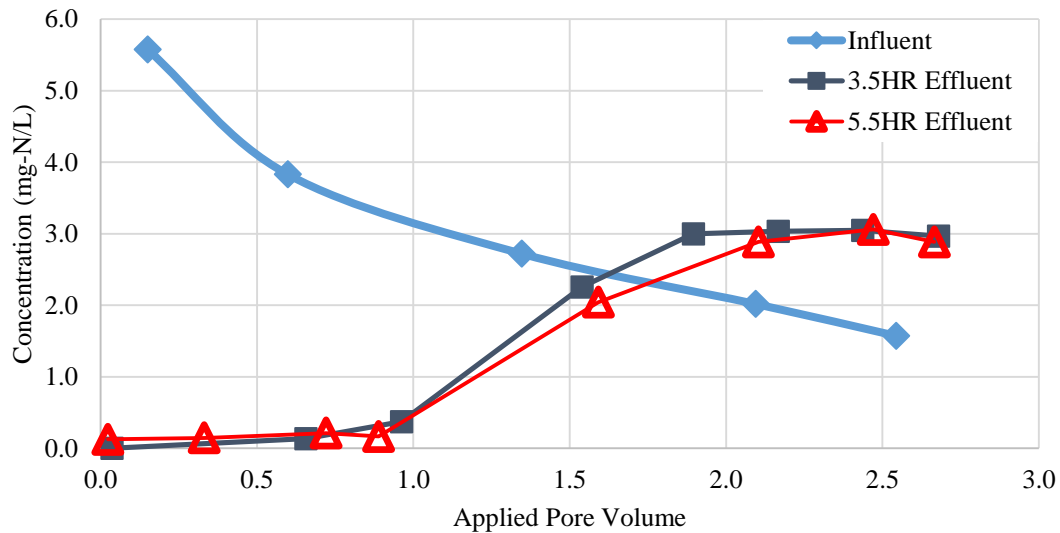
Figure 3-19. Comparison of two 1.9-cm storms showing the nitrate effluent profiles. Stormwater was applied to simulate a first-flush pollutant curve and applied at a dynamic rate of 5 equally spaced flowrates as developed by the Modified Rational Method.

Table 3-7. Experimental results of 0.75-inch (1.9-cm) storm-simulated events as to quantify nitrate mass removal. The three flowrates correspond to the interval numbers 1, 2, and 3, respectively. The HRT values are calculated based on 1200 cm^3 IWSZ storage capacity and the flowrates listed, respectively.

Experiment	Flowrates (mL/min)	HRT (hrs.)	Mass In (mg-N)	Mass Out (mg-N)	Difference (mg-N)	Removal (%)
3.5-hr Run 1	8.5, 17.1, 25.6	2.3, 1.2, 0.8	10.09	4.34	5.75	57
3.5-hr Run 2			10.47	4.09	6.38	61
5.5-hr Run 1	5.4, 10.9, 16.3	3.7, 1.8, 1.2,	9.87	3.79	6.08	62
5.5-hr Run 2			10.20	3.97	6.23	61

Effect of Macroscale Environmental Conditions

In order to evaluate the effect of disturbed macroscale environmental conditions on nitrate performance, two additional storm events were simulated. Prior to each storm event, modifications of unamended stormwater included - (1) deoxygenate with nitrogen gas overnight, and (2) the addition of 30 mg-SO_3/L as $NaSO_3$. All stormwater was applied over two 6-hour durations at 16.8 cm/hr (22 mL/min), which correspond to a 0.9-hour designed HRT, with a targeted nitrate influent concentration of 3.0 mg-N/L. Figure 3-20 shows the nitrate effluent profiles of each of the three storm events. All three nitrate curves followed a similar trend, as to suggest that additional stormwater amendments did not affect nitrate behavior (Figure 3-20). Measured influent nitrate concentrations of the unamended (baseline), deoxygenated, and deoxygenated-reduced stormwater were 2.76 mg-N/L, 2.96 ± 0.01 mg-N/L, and 2.96 ± 0.02 mg-N/L, respectively; maximum measured nitrate concentrations corresponded to 2.48 mg-N/L, 2.71 mg-N/L, and 2.75 mg-N/L. Average initial effluent nitrate readings were 0.06 ± 0.04 mg-N/L which indicated that complete denitrification had occurred prior to the storm event. For all three events, effluent concentrations corresponded to at least 80% recovery of the influent concentrations, as to indicate a nitrate washout behavior.
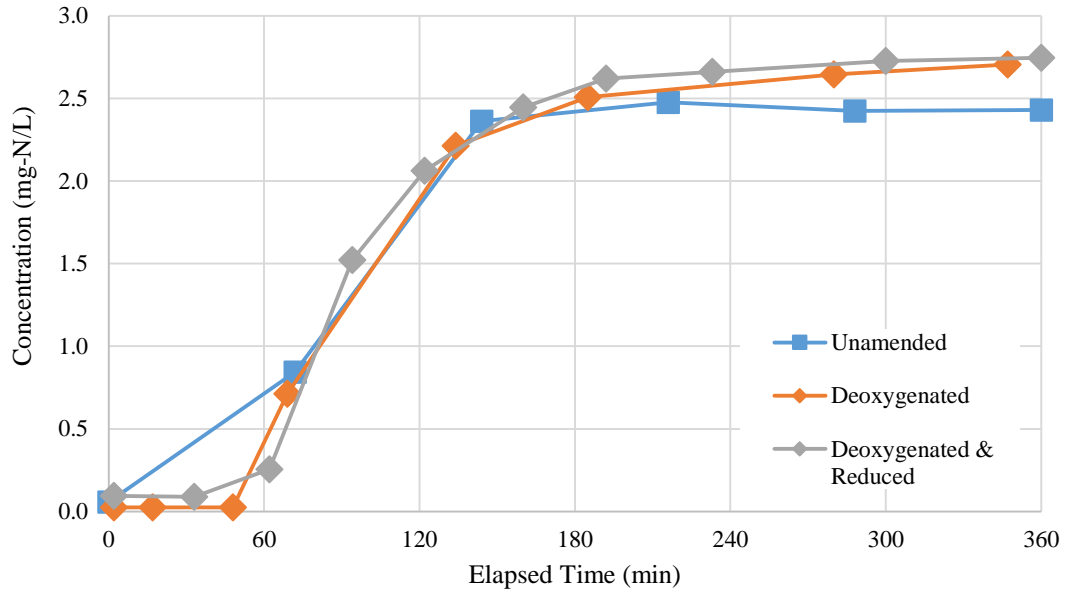
Figure 3-20. Comparison of nitrate effluent profiles (mg-N/L) of unamended stormwater, deoxygenated, and deoxygenated-reduced. Stormwater was deoxygenated overnight with nitrogen gas. Reduced stormwater also contained 30 mg-SO₃/L. All events were conducted for 6-hours at constant Q = 22 mL/min and influent nitrate concentration of 3.0 mg-N/L.

Table 3-8 reports the nitrate mass removal for all simulated storm events that were performed at a constant nitrate loading corresponding to a 0.91-hour HRT. Storms were replicated to ensure accuracy and allow for statistical analysis. The F-test confirms that the variances between the unamended and deoxygenated mass removal variances were statistically the same ($p > 0.05$). A two sample of equal variance t-test verified that there is not a significant difference between the unamended and deoxygenated reported mass removals ($p > 0.05$). Average unamended stormwater mass removal was $35 \pm 4\%$. Since the 6-hour reported deoxygenated-reduced mass removal of 34% was within one standard deviation of the average unamended standard results, there was not a significant difference in reported mass removal for all three storms.
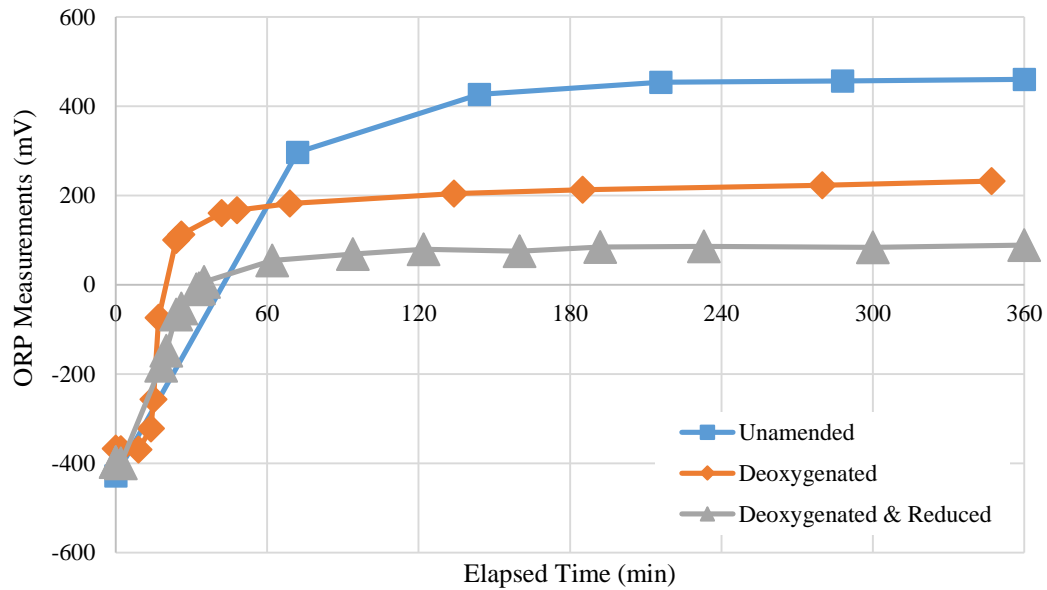
Figure 3-21. Comparison of ORP measurements (mV) of unamended stormwater, deoxygenated, and deoxygenated-reduced. Stormwater was deoxygenated overnight with nitrogen gas. Reduced stormwater also contained 30 mg-SO₃/L. All events were conducted for 6-hours at constant v = 16.8 cm/hr and influent nitrate concentration of 3.0 mg-N/L.

Table 3-8. Compiled nitrate mass removal for stormwater designed event of HRT=0.92 hr., Q=22 mL/min with constant nitrate influent concentration of 3.0 mg-N/L. Storms designed with a [*] were conducted for 4-hours instead 6 hours.

Deoxygenated	Reduced	Experiment	Mass In (mg-N)	Mass Out (mg-N)	Difference (mg-N)	Removal (%)
No	No	Run 1	21.83	14.82	7.01	32%
		Run 2	21.55	14.27	7.28	34%
		Run 3	25.01	14.74	10.27	41%
		Run 4	21.29	13.87	7.42	35%
Yes	No	Run 1	22.46	15.04	7.42	33%
		Run 2	23.38	14.26	9.12	39%
	Yes	Run 1*	15.92	7.81	8.11	51%
		Run 2*	16.19	8.40	7.79	48%
		Run 3	23.44	15.53	7.91	34%

For the storm events shown in Figure 3-21, initial ORP measurements ranged from 367.0 mV to -427.7 mV. However, the maximum redox measurements were dependent upon the stormwater preparatory methods. Unamended and deoxygenated stormwater events peaked at an ORP value of 460.1 mV and 232.5 mV, respectively,

reflective of a non-reduced macro-environment. In comparison, deoxygenated-reduced stormwater redox measurements did not exceed 90 mV, and can be considered sufficiently reduced for denitrification (Stumm and Morgan 1995). Average dissolved oxygen (DO) measurements for the deoxygenated stormwater influent and effluents, respectively, were 3.9 ± 0.6 ppm and 1.4 ± 0.3 ppm. Average DO measurements of deoxygenated-reduced stormwater influent and effluents, respectively, were 0.1 ppm and 0.2 ± 0.1 ppm. Based on effluent readings, the system was anoxic as DO readings were below the 2 ppm threshold (Kim et al. 2003). However, the absence of oxygen in the stormwater effluent was not indicative of reduced conditions, as deoxygenated ORP measurements were greater than 200 mV within 2 hours (Figure 3-21). Nitrate effluent profiles (Figure 3-20) coupled with ORP profiles (Figure 3-21) reinforce the hypothesis that the rate of flow through the IWSZ dictated nitrate fate and transport, and preservation of an anoxic (DO < 2 ppm) and reduced (ORP < 100 mV) conditions did not significantly affect nitrate removal.

3.3. Summary

Experimental work verified that a permanently saturated layer can encourage nitrate removal via denitrification. The IWSZ media serves as the external carbon source for denitrification and the substratum for the denitrifying biofilm. Presumably, the native microbial community is responsible for anaerobic lignocellulose degradation, to provide bioavailable carbon, and denitrification. It is necessary to restrict the hydraulic retention time of nitrified stormwater in the denitrifying catchment zone to ensure nitrate diffusion across the boundary layer. Labile DOC may leach from vegetation and permeate through the media layers into the IWSZ, but denitrifiers are confined to the biofilm matrix. Thus,

opportunity for DOC diffusion and microbial uptake was not considered in this system.

First order denitrification kinetics estimated a contact time of 2.6 days to reduce 3.0 mg-N/L to 0.05 mg-N/L with an apparent rate constant, k, of 0.0011 min^{-1}. The incoming rate of stormwater dictated nitrate transport within the IWSZ. A HRT of 4.0-hours was the threshold to separate partial denitrification, or *low flow* conditions, from *high flow* conditions, i.e., nitrate loading events that only exhibited a washout behavior. Nitrate removal was not significantly affected by a dynamic pollutant loading or preservation of macroscale anoxic-reduced conditions.

Chapter 4 Model Development and Field-Scale Performance Predictions

4.1. Model Framework

4.1.1. Single Storm Behavior

Experimental work verified that regardless of a first-flush pollutant loading and triangular-shaped hydrograph, nitrate behavior followed the fundamentals of macro and microscale mass transport mechanisms. As shown in Figure 4-1, nitrate may experience one of three fates depending on the velocity through the IWSZ and the volume storage capacity of the denitrifying zone. If the storm volume is less than the IWSZ storage volume, the storm is completely captured; nitrate is at least 95% removed assuming the temporary storage time in the IWSZ is greater than or equal to the time constraint established by the denitrification kinetic rate constant. If the storm size exceeds storage capacity, stormwater velocity may dictate nitrate fate. A *low flow* event is characterized by the potential for in-storm denitrification, i.e., both macroscale transport and microscale (diffusive) transport could occur. A *high flow,* or washout event, indicates advective-dispersive transport dominated nitrate movement so that nitrate removal is independent of contact time.

Specific to the laboratory design, media containing 4.5% Willow Oak 5-mm woodchips by mass, and pea gravel corresponded to a first-order denitrification rate constant, k, of 0.0011 min^{-1}. Nitrate was continuously applied at 3.0 mg-N/L for 3 days to quantify a threshold to separate *low* and *high flow* events. With a consideration of a batch study (0.0011 min^{-1}) and *low-flow* denitrification rate constants (Table 3-4), the 6.0-hour HRT k value of 9.40 x 10^{-1} min was selected. Assuming a steady-state PFR model and an

80% recovery to separate *low* and *high flow* events, the minimum denitrification contact time is found to be 237 minutes, or approximately 4.0 hours.

For any design, a critical velocity (v_c) can be developed based on a minimum HRT of 4.0 hours and depth. The parameter, v_c, is adjusted according to the IWSZ storage capacity and cross sectional area.

When runoff is applied at *low flow*, $v \leq v_c$, both macroscale (advective-dispersive) transport and microscale (diffusive) transport to the biofilm surface could occur. Thus, the quantified nitrate removal was limited by the apparent rate constant k and the contact time. As both parameters increased, more nitrate removal is predicted. When the contact time approaches 2.6 days, the rate constant predicts 95% removal of influent nitrate; after a contact time of 2.6 days, the kinetics no longer limit nitrate removal.

Under *high flow events*, $v > v_c$, advection and dispersion dominated nitrate transport, so nitrate exhibits minimal removal, independent of contact time (Figure 4-1).
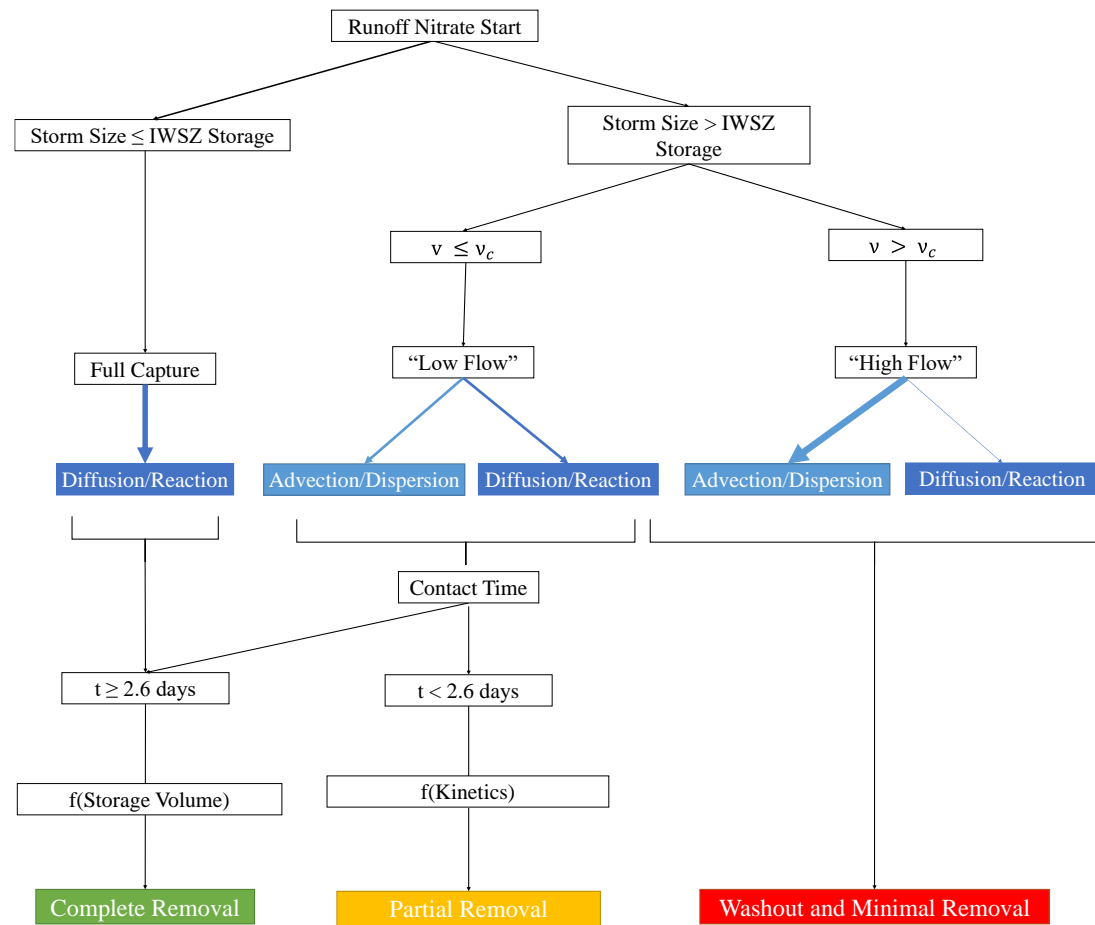
Figure 4-1 Conceptual model to show how IWSZ storage, flow through the IWSZ, and denitrification kinetics can all dictate the fate and extent of nitrate removal during a specific storm event. Contact time of 2.6 days is consistent with this study's calculated denitrification rate constant of 0.0011 min^{-1}.

4.1.2. Annual Nitrate Performance

Kreeb (2003) developed an annual storm distribution based on Maryland precipitation data. Storms were categorized by storm depth and rainfall duration with an expected annual probability of occurrence. For this work, rainfall duration was translated to a runoff application rate as adopted via the Modified Rational Method. If rainfall/runoff depth exceeded the IWSZ storage capacity, then the derived hydraulic loading rates were compared to the critical velocity to classify each storm as a *low* or *high flow event*. Table 4-1 outlines the assumed operational parameters as they are subject to change in the following sections.

Table 4-1. Default Parameter Assumptions for Initial Modified Rational Method Development of Pollutant Loading Rates

Parameter	Value
Minimum HRT	4.0 hours
IWSZ Depth	45 cm
Media Porosity (ε)	0.34
Cross Sectional Area	Circular, D =10 cm
Critical velocity	3.8 cm/hr
Runoff coefficient (C)	0.9
Water Temperature	20°C
Ratio of bioretention footprint to catchment area	5%

Table 4-2 characterizes each storm based on rainfall depth and runoff application duration, where the nitrate behavior can be classified as complete removal, partial removal, or minimal removal, as shown in Figure 4-1 and verified experimentally, in Chapter 3.

Table 4-2 Semi-Quantitative Assessment of Predicted Nitrate Performance based on default parameters (Table 4-1). Green is complete capture of storm. Yellow is partial in-storm denitrification. Red is washout behavior.

Runoff Application	Rainfall Depth (cm)				
	0.140	0.445	0.953	1.905	7.620
2.0 hr	Green	Green	Red	Red	Red
5.0 hr	Green	Green	Red	Red	Red
7.0 hr	Green	Green	Orange	Orange	Red
11.0 hr	Green	Green	Yellow	Orange	Red
20.0 hr	Green	Green	Yellow	Yellow	Red
37.0 hr	Green	Green	Yellow	Yellow	Orange
72.0 hr	Green	Green	Yellow	Yellow	Yellow

While Table 4-2 assesses nitrate behavior with respect to single rainfall event/runoff responses, it is possible to predict the IWSZ performance on an annual basis. A first-flush pollutant application with an nitrate EMC of 1.5 mg-N/L was developed based on field-scale monitoring of a bioretention cell at the University of Maryland campus; Li and Davis (2014) recorded a median TN concentration of 1.55 mg-N/L Assuming all of the influent nitrate is transformed to nitrate preceding the IWSZ, then an EMC of 1.5 mg-N/L is a reasonable estimate. This study's annual predicted loading rate is 16.1 kg-N/ha, comparable to the 14.0 kg-N/ha/yr calculated by Li and Davis (2014).

To quantify nitrate removal, the model assumes there is at least 2.6 days between each nitrate loading period. In other words, once nitrified stormwater is retained in the IWSZ, and the next storm begins, the stored water will be completely denitrified. It is only if the current storm's runoff volume exceeds the IWSZ storage capacity that the effluent will contain some concentration of nitrate. The predicted nitrate concentration, C, is assumed to follow a plug flow reactor model with a steady state concentration as a function of the denitrification rate constant k and a time weighted HRT (Figure 4-2);

HRT$_w$ is an average of the three flowrates developed in the Modified Rational Method formulation. Correspondingly, the mass export is calculated as follows:

$$M = \int_0^t Q_w * C * dt$$

4-1

where   Q$_w$ is the time-weighted average of all three flowrates

C is the steady-state plug flow reactor model concentration (Equation 3-11)

t is time runoff is applied to the IWSZ
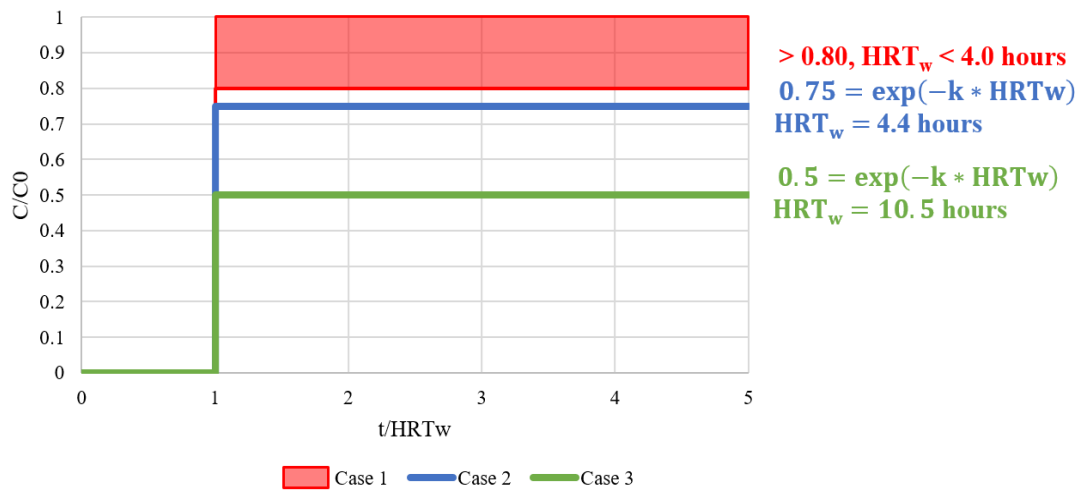
Figure 4-2. PFR Model derivation of the effluent nitrate concentration assuming the runoff volume exceeds the IWSZ storage capacity. The denitrification rate constant, k, is 0.0011 min^{-1}.

The model assumes that all of the runoff volume produced by the storm event will infiltrate the bioretention cell at the flowrates constructed in the Modified Rational Method. Thus, these initial calculations do not account for any stormwater bypass nor the possibility of restricted loading rates due to media infiltration rates or a constricted effluent valve in the drainage pipe, as discussed in Lucas and Greenway (2011a).

Figure 4-3 shows the distribution of expected annual nitrate loading by storm depth. As the size of storm increases, the contribution to the annual input and output pollutant loading increases. This inversely correlates to the annual mass export or nitrate

mass removal percentage. The current IWSZ design is only capable of completely capturing the 0.140-cm and 0.445-cm storms; however, this only constitutes 7% of the total pollutant loading. Remaining storm depths exhibit some nitrogen removal due to in-storm denitrification and the partial capture of the storm. Annually, this IWSZ would export a nitrate loading of 8.6 kg-N/ha/yr, corresponding to an overall 47% nitrate removal.
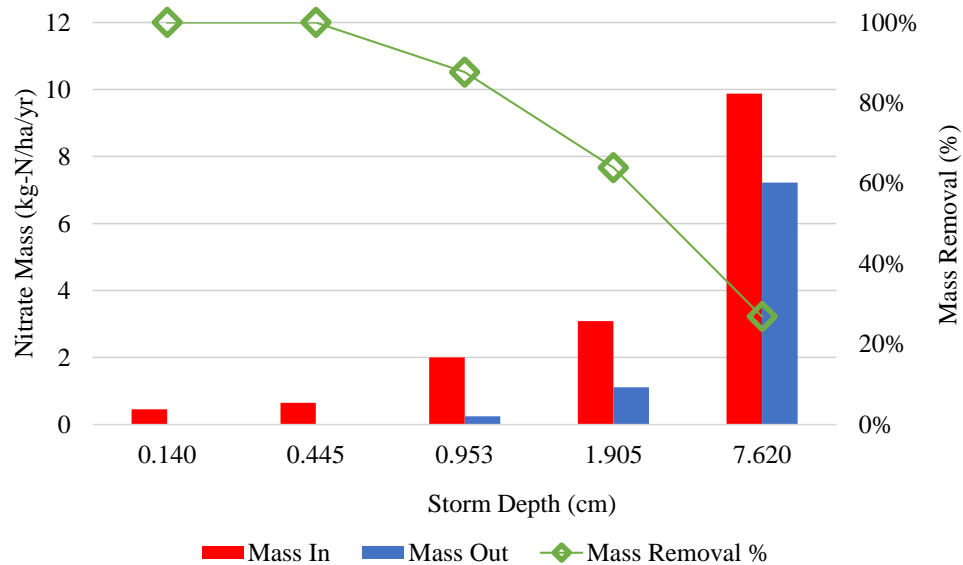
Figure 4-3. Annual predicted nitrate distribution based on default parameters (Table 4-1) and experimental performance of selected storms. Total influent N mass is 16.1 kg-N/ha/yr and total effluent

4.2. Nitrogen Response to Changes in Field-Scale Environment

In order to account for real-world conditions, it is important to predict how the incorporation of an IWSZ will respond to variable environmental changes. Such changes account for the short term, e.g., seasonality, and/or long-term, e.g., climate change and progressive shifts towards highly urbanized environments. Collectively, these impact how bioretention, or any infiltration-based SCM, manage N loadings. Hydrologic and water quality performance cannot be accurately predicted without addressing such changes in the built environment.

4.2.1. Seasonal Temperature Trends

Previous studies have identified seasonal water temperature variation to affect denitrification rates and overall nitrogen management (Bachand and Horne 1999; Warneke et al. 2011a; b). Temperature effects on reaction rates of biological processes are denoted by the Arrhenius Equation (Metcalf and Eddy 1979) (4-2).

$$k = A\exp^{-\frac{E_a}{RT}}$$ 4-2

where k is the rate constant

A is the frequency factor

E_A is the activation energy

R is the universal gas constant

T is temperature (K)

This can be simplified to:

$$\frac{r_T}{r_{20}} = \theta^{T-20}$$ 4-3

where r_{20} is the reaction rate at 20°C

r_T is the reaction rate at water temperature T°C

θ is the temperature-activity coefficient

T is the water temperature (°C)

There is not a uniform value for θ within the context of denitrification, but researchers have proposed a range of probable values. Bachand and Horne (1999) determined θ to be in the range of 1.15 to 1.18, while Metcalf and Eddy (1979) reported activity coefficients between 1.0 and 1.14 for various biological processes. Many researchers have quantified the denitrification rate increase as a response to the measured water temperature. Warneke et al. (2011a) calculated a Q_{10} of 2.0, where Q_{10} is the factor

of the reaction rate increase with every 10°C rise in temperature. Elgood et al. (2010) also

proposed a Q_{10} of 2.0 for nitrate removal in a pine-woodchip streambed denitrifying

bioreactor; Hoover et al. (2015) found Q_{10} ranged from 2.2 to 2.9 for a hardwood chip

denitrifying bioreactor to treat subsurface agricultural drainage water.

Assuming a temperature of coefficient, $\theta = 1.15$, and a 5°C temperature adjusted

for summer and winter months, k is adjusted by approximately a factor of 2.0 (Table 4-3).

A 5°C seasonal variation from default parameters (Table 4-1) was selected based on

observed seasonal effluent temperatures for a denitrifying bed in Karaka, New Zealand

(Warneke et al. 2011a). Temperature measurements ranged from 15.5°C in winter (June)

to 23.7°C in summer (January) The results presented in Figure 4-4 are calculated based

on the rainfall distribution of Kreeb (2003) and model development; the quantified k in

response to assumed water temperature change was incorporated to assess nitrate removal

on an annual basis. Figure 4-4 shows that when k is reduced to account for winter water

temperature, the 0.95-cm, 1.91-cm, and 7.62-cm storms export a larger nitrate mass.

Since k was the only affected parameter, nitrate behavior will adhere to the results of

Table 4-2. That is, the only variable that is affecting the water temperature change is the

extent of nitrate removal under low flow storms. Warmer water temperatures demonstrate

a greater removal efficiency than colder water temperatures under the same nitrate

loading conditions and HRT. For example, assuming nitrified stormwater was applied to

the IWSZ under parameters listed in Table 4-3, then, a winter and summer k predict an

effluent nitrate recovery (C/C_0) of 88% and 59%, respectively.

Table 4-3. The effect of water temperature on the denitrification rate constant. All other parameters represent the default condition. Temperature coefficient was assumed to be 1.15.

Parameter	Value(s)	Effect of T
Minimum HRT	4.0 hours	
IWSZ Depth	45 cm	
Media Porosity (ε)	0.34	
Cross Sectional Area	Circular, D =10 cm	
Critical velocity	3.8 cm/hr	
Runoff coefficient (C)	0.9	
Water Temperature	15°C	$k = 5.47 \times 10^{-4} \text{ min}^{-1}$
	20°C	$k = 1.10 \times 10^{-3} \text{ min}^{-1}$
	25°C	$k = 2.21 \times 10^{-3} \text{ min}^{-1}$
Ratio of bioretention footprint to catchment area	5%	

On an annual basis, results of Figure 4-4 indicate that a 45-cm IWSZ with a summer *k* value removes close to 71% of the annual N loading while a winter *k* only removes 59%.
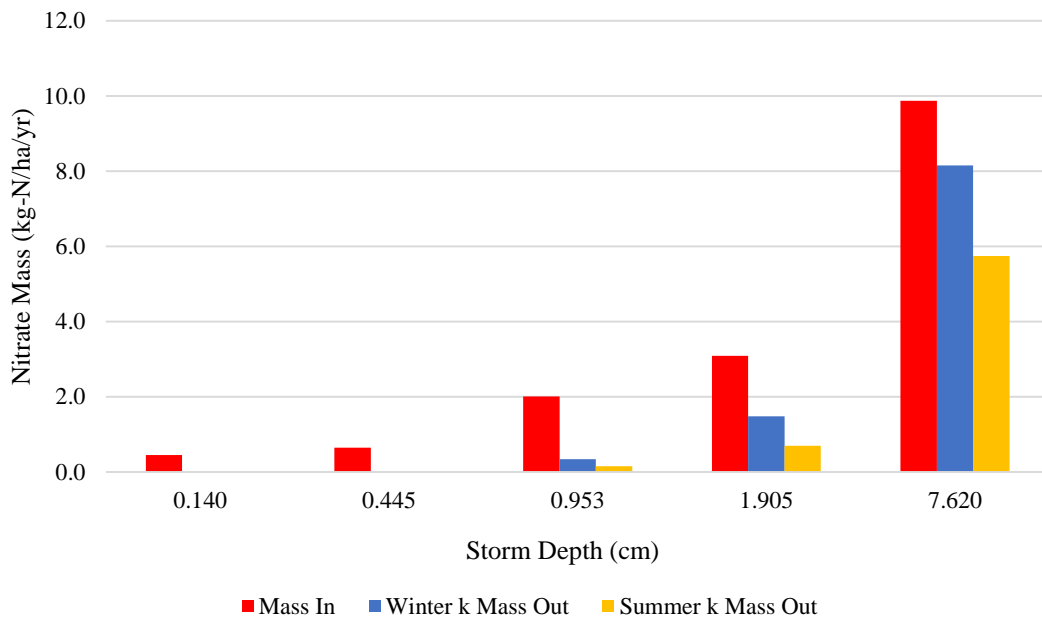
Figure 4-4. The seasonal water temperature effect on the denitrification rate constant k and the predicted nitrate annual export as separated by storm depth, where θ=1.15 and water temperature is 15°C and 25°C in winter and summer, respectively. Other parameters represent the default condition.

While researchers may not agree on an exact value of θ, they have found that other factors besides seasonal water temperature, such as available carbon, cofounded the temperature effect on nitrate removal (Bachand and Horne 1999; Warneke et al. 2011b). Higher ambient and water temperatures may increase denitrification rates when systems are carbon limited due to higher microbial activity that are responsible for the decomposition, and thus, increased bioavailability of C from the woodchips (Warneke et al. 2011a; b). Warneke et al. (2011b) reported that the nitrate removal rate correlated with the copy number of nitrite reductase genes (nirS and nirK). The gene copies (normalized per dry weight of carbon substrate) increased 4-fold with a temperature increase of 10°C whereas the nitrate removal only increased by a factor of 1.2. Warmer temperatures promoted diverse microbial community in all carbon substrates; however, comparison of nitrite reductase gene abundance as a proportion of the total bacteria DNA varied amongst carbon substrate, e.g., green waste, maize cob barrels, and woodchips (Warneke et al. 2011b). This suggested that both carbon substrate and temperature will collectively affect the C availability, denitrifying-specific carbon efficiency, and observed nitrate removal rate.

While this model does not incorporate the variability of k within a single set of output data, it does provide evidence that k will have a strong effect on total nitrate removal performance. Furthermore, this model does not account for lignocellulose degradation rates, and the associated carbon availability and denitrifying microbial response. Future efforts can incorporate these temperature dependent parameters to develop a more comprehensive model with regards to nitrate removal and performance.

4.2.2. Spiked Salt Concentrations

It may be important to consider the seasonality effect of spiked salt concentrations for the environmental fate of surface-water ecosystems. In many areas, road salt as sodium chloride (NaCl) is heavily applied during the winter months for deicing roads.

As previously shown in Figure 3-16, when stormwater was spiked at a concentration of 0.5% NaCl and applied continuously at an 8.0 hour HRT for approximately 3 days, an inhibitory effect as observed.

To account for this inhibitory effect and annual nitrate removal performance, the semi-quantitative analysis of nitrate behavior as presented in Table 4-2 was adjusted. Assuming the frequency of the average 60 Maryland rainfall events is uniformly distributed, i.e., there are 5 precipitation events per month, and the inhibitory denitrification response is in effect one month out of the year, then, 5 storms will exhibit 0% nitrate removal. In addition, one may assume that those 5 storms correspond to the smallest reported storm depth. Prior to this, the model reported an annual nitrate mass of 0 kg-N/ha/yr for 0.140-cm rainfall events assuming that the runoff volume was less than the IWSZ storage capacity.

As shown in Figure 4-5, the performance of 5 storms was adjusted to export a nitrate loading equal to the influent. In total, this added an additional 0.11 kg-N/ha/yr to the winter k that did not account for road salt application. In both cases, the overall nitrate removal is 59%; the impact on the distribution of annual exported nitrate is isolated to 0.140-cm storm depth and is minimal (Figure 4-5). This can be expected because the assumed storms were specific to smallest storm depth, which only contributes 3% of the total annual nitrate mass loading. If larger sized and/or number storms were selected for this inhibitory effect exercise, then difference between winter k reports and incorporation

of road salt application would have a larger difference on nitrate export distribution and overall nitrate mass removal.
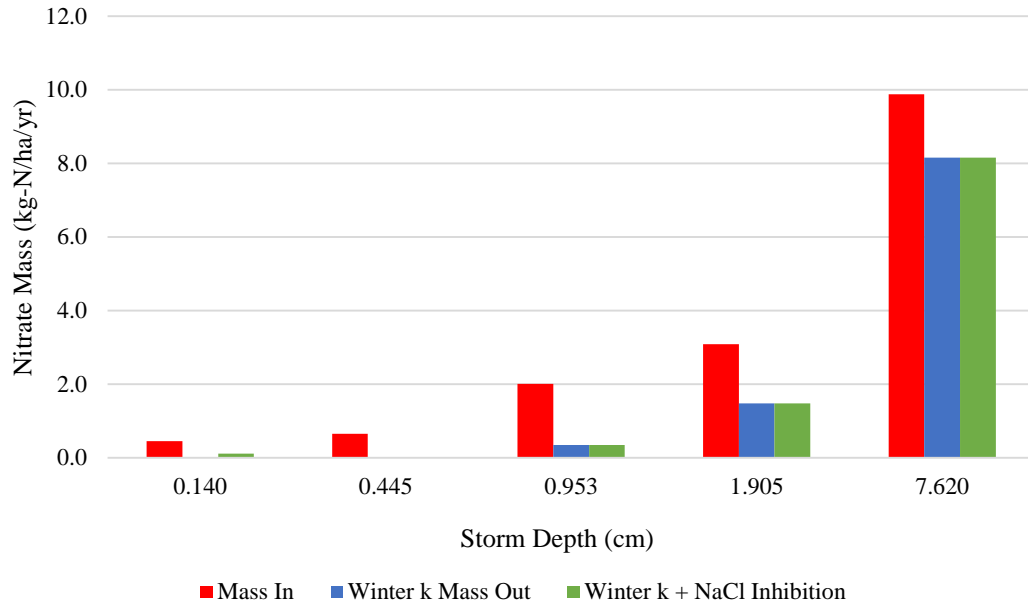
Figure 4-5 Comparison of annual nitrate removal when incorporating a one-month road salt application to inhibit denitrification of 5 0.140-cm storm events. All other model assumptions and parameters are consistent with Figure 4-4.

4.2.3. Rainfall/Runoff Response: Urban Environment

Changes in land use/land development favor increased urbanization. As a consequence, the loss of green space magnifies and accelerates surface runoff (Davis et al. 2012b; Walsh et al. 2012). Hundecha and Bárdossy (2004) developed a conceptual rainfall runoff model to evaluate the effect of increased urbanization at the expense of agricultural land; simulation results indicated that strong urbanization increased the peak flow especially during summer months. In agreement with Davis et al. (2012b), intensified peak flow results from the loss of infiltration and evapotranspiration, as more water was available for runoff. Since precipitation events are translated from a rainfall intensity to runoff application rate via the Modified Rational Method, it is expected that

nitrate performance will be inversely related to the Rational Method C and directly

related to $A_{catchment}$. This is verified through in the simple model by the variation of

parameters C and ratio of cell to catchment area footprint, i.e., adjusting $A_{catchment}$

accordingly.

As urbanized environments are characteristically more impervious, the runoff

coefficient, C will increase; C ranges from 0.05 to 0.98 where the presumed value reflects

the land type/land use (McCuen 2005). A value of 0.98 assumes that the catchment area

is 100% impervious. This simulation adjusts C from 0.75 to 0.98 as to quantify the

change in observed annual nitrate export (Figure 4-6). The input for all values of C was

16.1 kg-N/ha/yr, but the output of varied from 6.4 to 9.3 kg-N/ha/yr when C was equal to

0.75 and 0.98, respectively. Results from Figure 4-6 demonstrate that as the catchment

area becomes more impervious, the observed nitrate performance is reduced. Based on

Rational Method Calculations, the peak flowrate is directly proportional to C. Therefore,

the total number of events that exhibit a washout behavior is magnified in the simulation

results; field studies have reported an accelerated hydrologic runoff response due to

urbanization (Davis et al. 2012a; b).

Table 4-4. Effect of urbanization on runoff response to rainfall patterns and the affected parameters to quantify annual nitrate removal performance.

Parameter	Value(s)	Effect of Urbanization
Minimum HRT	4.0 hours	
IWSZ Depth	45 cm	
Media Porosity ($\mathcal{E}$)	0.34	
Cross Sectional Area	Circular, D =10 cm	
Runoff coefficient (C)	0.75 – 0.98	More impervious land use
Water Temperature	20°C	
Ratio of bioretention footprint to catchment area	3% - 15%	Less available space
Critical velocity	$v = 3.8$ cm/hr	
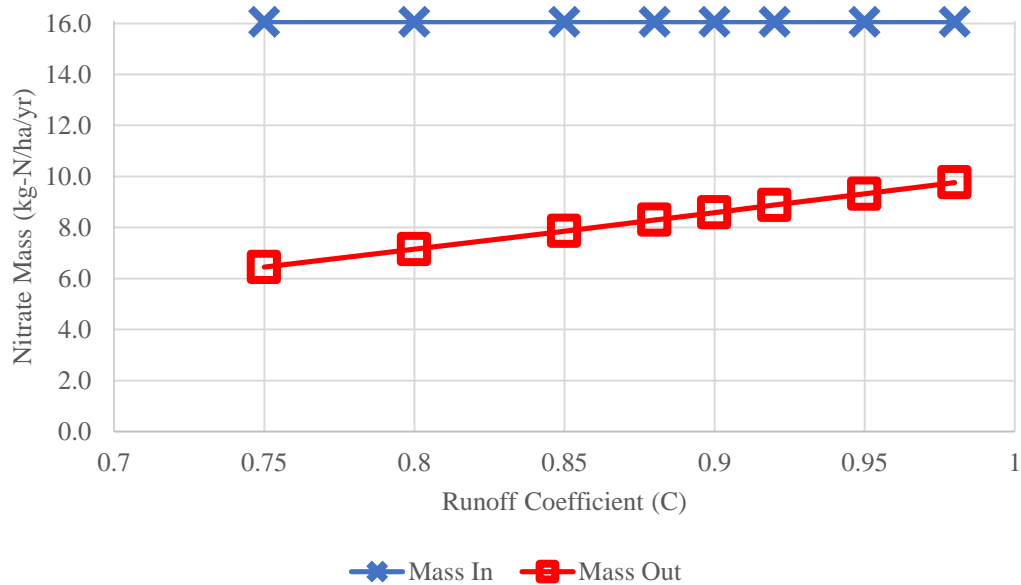
Figure 4-6. Effect of varying the runoff coefficient, C, from 0.75 to 0.98 on the predicted annual nitrate export. All model parameters are presented in Table 4-4, with the exception of a constant ratio of bioretention footprint to catchment area of 5%.

To account for less available greenspace the ratio of the catchment area footprint to bioretention surface area can be adjusted. Typically, this value is 5% (Department of Environmental Resources, P.G. County 2007). Less available space, as characteristic of a dense urbanized environment, is represented by a ratio of 3%. When more space is available for nitrate treatment, the ratio is increased; this model quantifies nitrate removal when ratio is increased up to 15% (Figure 4-7). At a 3% ratio, expected nitrate export is 10.7 kg-N/ha/yr or 33% mass removal. However, as the ratio is increased to 10% and 15%, more nitrate is removed. The model predicts that 10% and 15% ratio exports 5.5 kg-N/ha/yr and 3.71 kg-N/ha/yr, respectively (Figure 4-7). Therefore, reduced space for green infrastructure installment will severely limit nitrate removal. Based on the findings of Figure 4-7, the nitrate removal efficiency is related to the space that a cell can allocate to IWSZ storage.
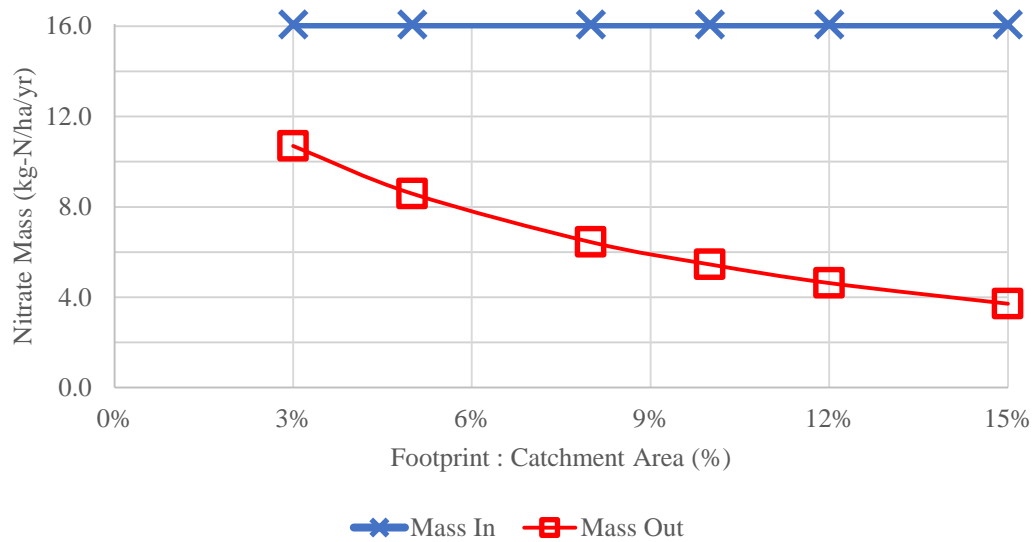
Figure 4-7. Effect of urbanization by changing the allowable space for bioretention installment. This is represented by the ratio between cell footprint and catchment area. All model parameters are presented in Table 4-4, with the exception of a constant C = 0.9.

Collectively, the effects of urbanization, as shown in Figure 4-6 and Figure 4-7, reduce the expected nitrate removal performance as previously demonstrated under default conditions. It is clear that an increase in C and reduction in cell footprint to catchment area ratio will not only increase the intensity but also the frequency of *high flow* events. In other words, reduced nitrate performance is indicative of the IWSZ unable to manage the accelerated rate of pollutant loadings. While not incorporated in the results of Figure 4-6 and Figure 4-7, the infiltration-based SCM may be more susceptible to overflow, whereby a larger volume of untreated stormwater will discharge into receiving waterbodies.

4.2.4. Incorporation of Climate Change

The aforementioned problems – seasonality effect of temperature and increasingly urbanized environments – will only be exacerbated when incorporating the challenges posed by climate change. Climate change does, and will continue to have a profound

effect on contemporary water resource management. Increased frequency in extreme weather events, e.g., droughts and flooding require adaptive water management strategies in order to combat poor surface water quality (Delpla et al. 2009). Presumably, the intensity of first-flush pollutant loadings will be exacerbated based on previous reports of Flint and Davis (2007), Nason et al. (2012), and others.
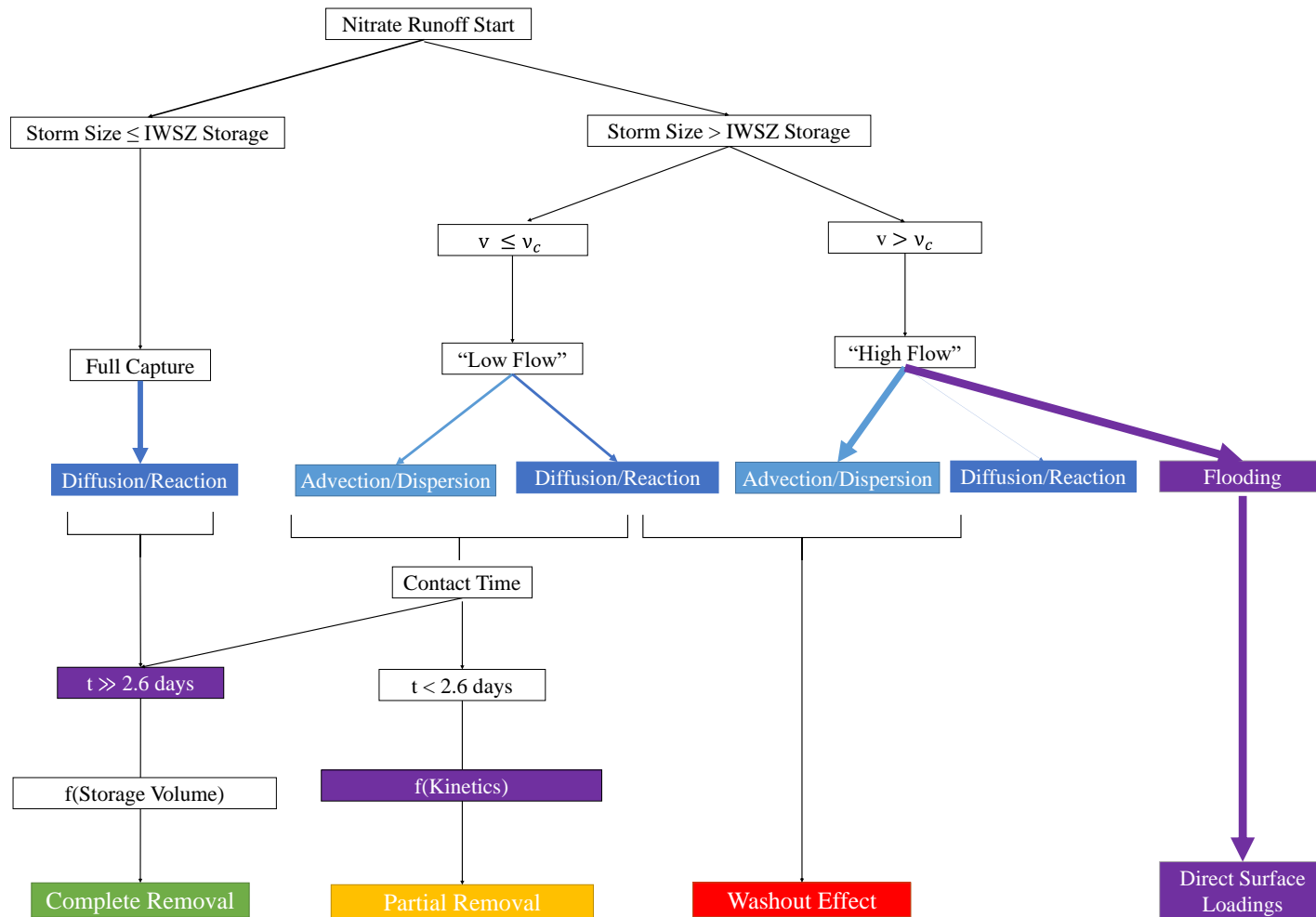
Figure 4-8. Effects of climate change on current N management challenge in bioretention. Purple indicates an expected consequence of climate change with respect to hydraulic loadings and N-targeted treatment in bioretention. Contact time of 2.6 days is consistent with this study's calculated denitrification rate constant of 0.0011 min^{-1}.

Figure 4-8 shows that climate change will not only impact rainfall occurrences, but also rainfall patterns that will be detrimental to traditional bioretention design management strategies.

The simple model accounts for climate change in two scenarios (Figure 4-9). First, the distribution of Maryland storms as compiled in Kreeb (2003) is altered by adding two additional 7.62-cm storms with a runoff duration of 2.0 hours. These two storms increase the input nitrate loading mass from 16.1 kg-N/ha/yr to 18.5 kg-N/ha/yr 20.1 kg-N/ha/yr, respectively. *Case 1* mass input corresponds to a 15% annual increase and *Case 2* corresponds to a 25% annual increase; the variation in annual applied mass is due to the difference in C from 0.9 to 0.98 (Table 4-5). Increased antecedent dry conditions, i.e., drought, will not affect nitrate removal assuming that the retention time of stormwater in the IWSZ is already greater than 2.6 days. Therefore, this was not included in the model simulations for either scenario.

Table 4-5. Effect of climate change on the annual nitrate removal performance. Case 1 only considers an adjusted rainfall distribution; Case 2 also incorporates changes in parameters due to urbanization and water temperature.

Parameter	Values Case 1	Values Case 2
Minimum HRT	4.0 hours	4.0 hours
IWSZ Depth	45 cm	45 cm
Media Porosity (ε)	0.34	0.34
Cross Sectional Area	Circular, D =10 cm	Circular, D =10 cm
Critical velocity	3.8 cm/hr	3.8 cm/hr
Runoff coefficient (C)	0.9	0.98
Water Temperature	20°C	25°C
Denitrification Kinetic Rate Constant	1.10E-03 min^{-1}	2.21E-03 min^{-1}
Ratio of bioretention footprint to catchment area	5%	3%
Rainfall Distribution		
Increased frequency of larger/intense storm events	Added 2 7.62-cm 1-hour rainfall events, totaling 62 annual rainfall events	
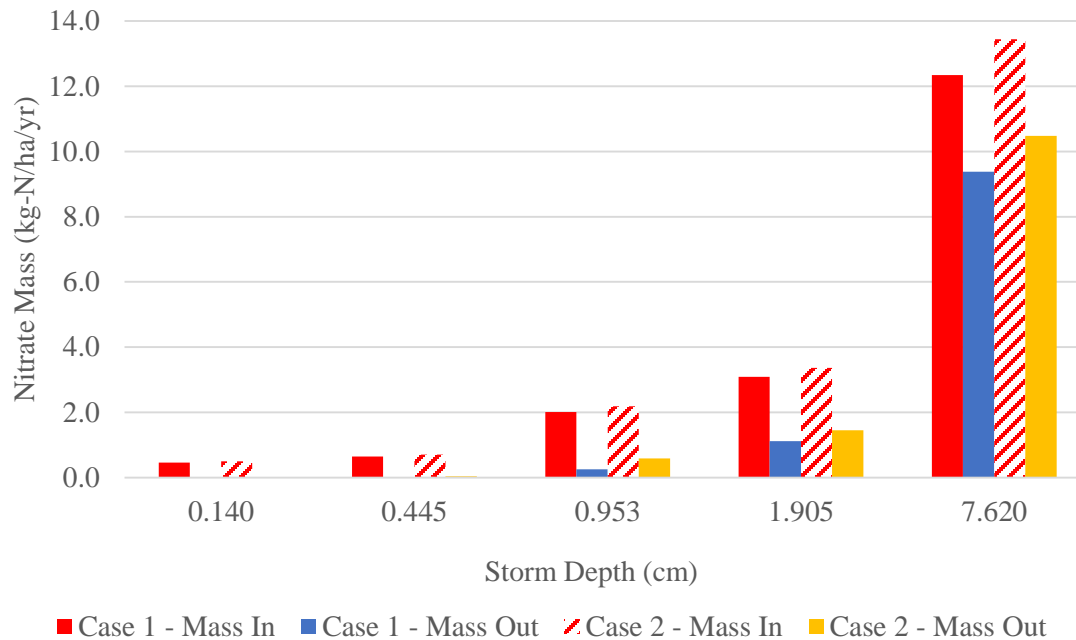
Figure 4-9. Effect of climate change on annual nitrate removal performance. Case 1 only accounts for a change in the rainfall distribution compared to laboratory parameters, whereas Case 2 incorporates additional adjustments due to urbanization and annual water temperature change. See Table 4-5 for details.

Therefore, for the *Case 1* analysis, the only affected response is the 7.62-cm storm nitrate performance. As compared to the results of Figure 4-3, the 7.62-cm annual exported nitrate is increased from 9.9 kg-N/ha/yr to 12.3 kg-N/ha/yr (Figure 4-9).

The *Case 2* analysis also adjusted parameters to reflect a more urbanized catchment area and increased annual water temperatures. As outlined in Table 4-5, the runoff coefficient was increased to 0.98 and the cell to catchment footprint was reduced to 3%; the denitrification rate constant reflects higher annual water temperatures and assumes the previous determination of a *summer k*.

Comparing storm events that are not completely captured by the IWSZ, i.e., 0.953-cm, 1.905-cm, and 7.62-cm storms, the *Case 1* scenario consistently outperformed the *Case 2* scenario by comparing mass recovery. Annually, the nitrate export under *Case*

1 parameters is 10.7 kg-N/ha/yr or 42% removal; *Case 2* parameters increase annual mass export to 12.5 kg-N/ha/yr or 38% removal (Figure 4-9). However, when comparing the predicted mass recovery for each depth, there is not a significant difference between the two ($p > 0.05$). Results of the *Case 1* (Figure 4-9) and default parameters (Figure 4-3) based on predicted nitrate export for each storm depth verify a significant difference between the two results ($p > 0.05$). Therefore, the change in assumed rainfall distribution and incorporation of other environmental parameters both significantly affect the nitrate removal. In *Case 1* and *2,* a majority, 87% and 84%, respectively, of the total exported mass is due to the largest sized storm events.

It is suggested that bioretention, or any infiltration-based SCM design must target these higher flow, or flooding event type storms, that are both a response to intensified rainfall patterns and more highly urbanized catchment areas. This model did not account for stormwater bypass; the opportunity is magnified with larger sized and more intense storm events (Figure 4-8). Pollutant loadings will be carried, accumulated, and deposited in the receiving surface water bodies without any prior water quality treatment (Figure 4-8), thereby, reducing the overall efficiency of the system. That being said, newly installed bioretention must be designed to manage such heightened runoff rates and pollutant loadings. Effective SCM design must incorporate innovative and resilient strategies that will adapt to the changing environment as to be discussed below.

4.3. Adaptive Management Approach

To begin, the simple model assumes a worst-case scenario performance with associated parameters outlined in Table 4-6. This section shall suggest strategies to mitigate the effects of climate change on rainfall distribution, accelerated urbanization,

and denitrification rate constant limitations. Figure 4-10 shows the predicted annual

nitrate removal performance by the default IWSZ configuration. Results of Figure 4-10

do not account for any stormwater bypass of the system nor are the hydraulic loading

rates restricted during infiltration or percolation through the cell.

Parameters to calculate annual applied mass are consistent with the climate

change model *Case 2* analysis (Table 4-5) to yield an influent mass of 20.19 kg-N/ha/yr.

Since the 0.140-cm and 0.445-cm storms contribute less runoff volume than the storage

capacity, the performance of these storms is not affected by the parameter changes.

However, the three larger storm depths demonstrate an increasingly worse efficiency.

The 0.953-cm and 1.905-cm storms export an annual 0.82 kg-N/ha and 1.97 kg-N/ha; the

largest storm leaches 11.64 kg-N/ha. Consequently, when the default IWSZ receives

nitrate pollutant loadings under this worst-case scenario set of parameters, the system

only demonstrates an annual 28% efficiency.

Table 4-6. Parameters account for the worst-case scenario nitrate performance on an annual basis.

Parameter	Values
Minimum HRT	4.0 hours
IWSZ Depth	45 cm
Media Porosity (ε)	0.34
Cross Sectional Area	Circular, D =10 cm
Critical velocity	3.8 cm/hr
Runoff coefficient (C)	0.98
Water Temperature	20°C
Denitrification Kinetic Rate Constant	1.10E-03 min^{-1}
Ratio of bioretention footprint to catchment area	3%
Rainfall Distribution	**Change**
Rainfall distribution of *Case 1* and *Case 2* Climate Change Models	Added 2 7.62-cm 1-hour rainfall events, totaling 62 annual rainfall events
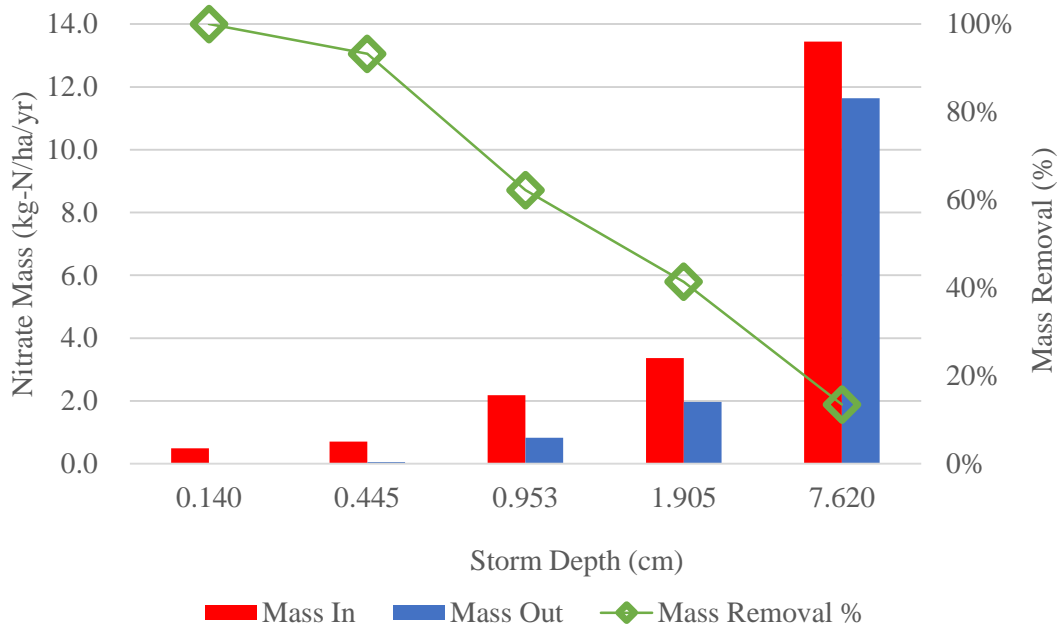
Figure 4-10. Starting point of adaptive management strategies where model development incorporated worst case scenario parameters to quantify nitrate removal performance. See Table 4-6 for details.

While an annual 28% efficiency is much lower than the default parameters (47% efficiency), it is possible to modify current bioretention to best mitigate the challenges posed by field-scale predictions. A novel bioretention shall not only incorporate an IWSZ, but explore multiple design opportunities to target denitrification removal based on enhancing the *no-flow* and *low flow* condition of storms. While the *no-flow* mass removal is limited by the IWSZ storage, the *low flow* is restricted by the contact time and first-order kinetics (Figure 4-1). Thus, adaptive management strategies will focus efforts to integrate alternative designs. Comprehensive design goals target maximize denitrification in-storm removal and larger storage volumes to mitigate the effects of increased pollutant loading rates. Model parameters shall reflect the predicted change with respect to design modifications. Results of annual nitrate performance not only

provide designers with alternative management strategies but also quantify the improved nitrate performance.

4.3.1. Enhanced No-Flow Scenario: Increased Storage Volume

<u>Effect of IWSZ Depth</u>

A modified cell can meet nitrogen water quality goals through the increased volume attenuation. Opportunities for increased nitrate removal is presented and quantified with regards to increased elbow drainage height and additional subsurface catchment zones.

In order to verify the effect of denitrifying storage volume, variable IWSZ depths were selected to quantify annual nitrate performance; in all scenarios, the parameters as defined in Table 4-6 were used. Results show that as the depth increases, the reported nitrate discharge decreases (Figure 4-11). While current 45-cm IWSZ exports 14.5 kg-N/ha/yr, i.e., 28% removal efficiency, a 100-cm depth reduces export to 10.6 kg-N/ha/yr.
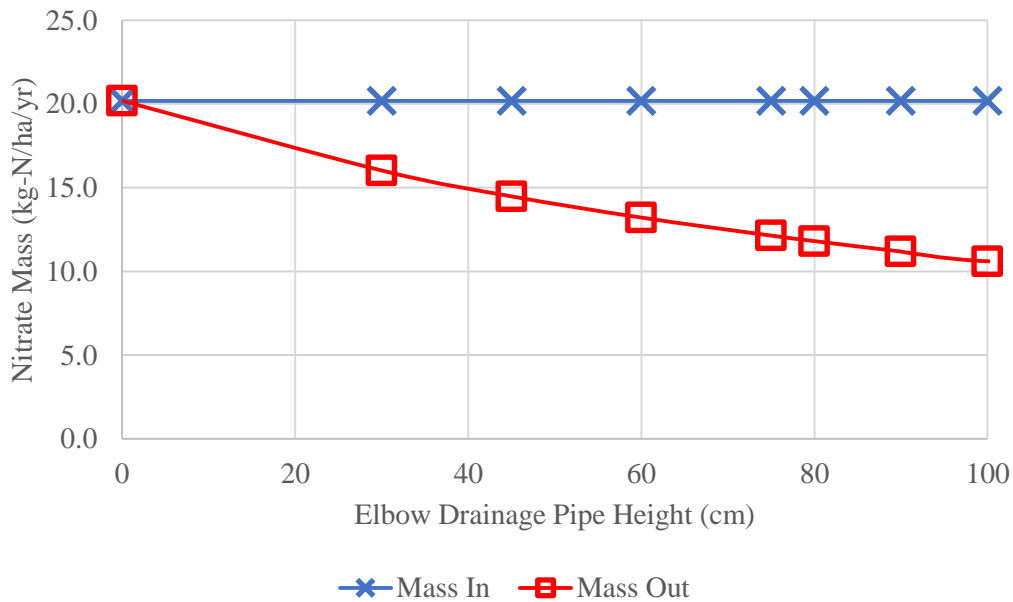
Figure 4-11. Effect of the upturned elbow drainage pipe height on annual nitrate mass export. See Table 4-6 for details.

The IWSZ depth should not be confined to a deeper excavation. Rather, the height of the upturned-elbow configured pipe can simply be raised to a higher elevation within the cell to meet the required storage volume requirement (Figure 4-12). In doing so, more of the bioretention cell is completed saturated and a larger storm depth can be completely captured within the cell. As the height of the elbow approaches the planting layer, the cell resembles a submerged gravel wetland. Regardless of SCM classification, the fundamental biological processes that are inherent to nitrogen transformations are identical.
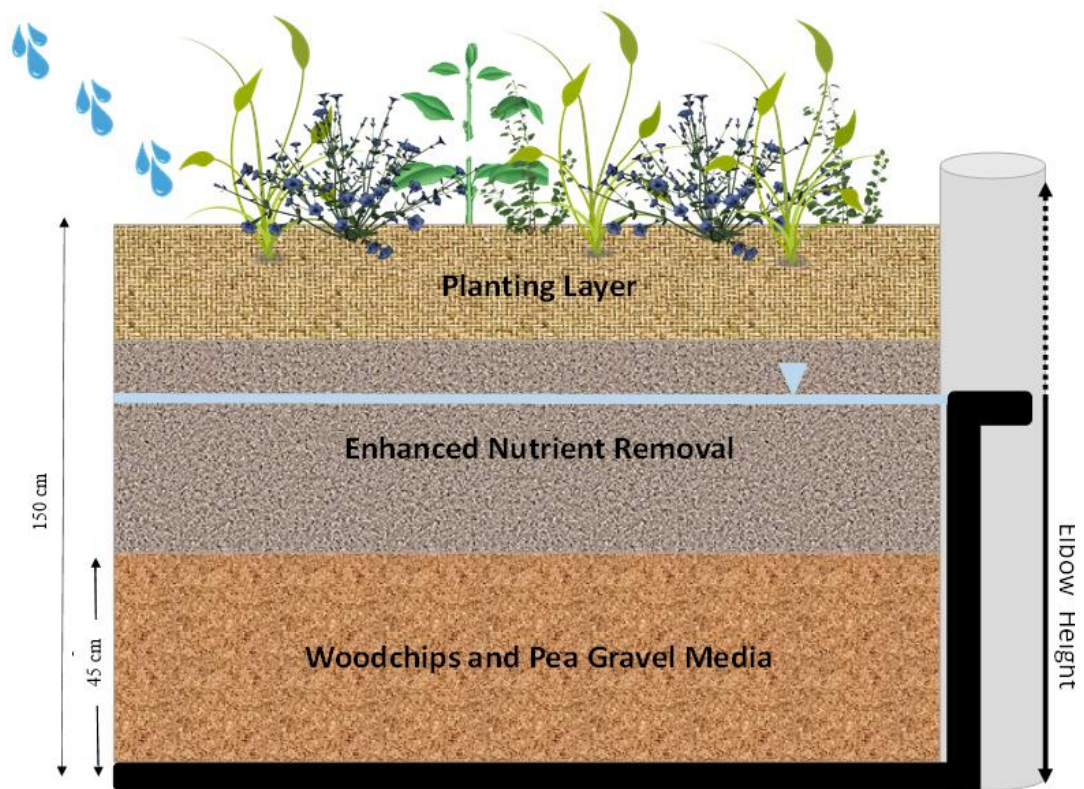
Figure 4-12. Modified Bioretention Cell to Increase Height of the IWSZ to Increase Storage Capacity and Associated Storm Depth. As the elbow height approaches the planting layer, the bioretention cell resembles a submerged gravel wetland.

As shown in Figure 4-12, multiple media layers encompass the IWSZ. While the woodchips are only provided in the bottom most layer, it is possible that natural sources of carbon will be bioavailable for denitrifiers in the upper saturated layers. These include but are not limited to plant litter decomposition, plant rhizosphere deposition products, and macro/micro fauna waste products (Bastviken et al. 2007; Kadlec and Wallace 2008; Wen et al. 2010). Alternative carbon sources will affect the denitrification rates and associated denitrifying community (Warneke et al. 2011a). However, this was not incorporated into model results and additional work may investigate the role of multiple carbon sources on the denitrifying community in efforts to increase the rate of nitrate removal.

Effect of Additional Horizontal Subsurface Storage

Bioretention can also hope to enhance nitrate removal by incorporating additional horizontal subsurface storage space. Underground catchment zones can be installed and connected to the bioretention cell as to increase the nitrate removal without sacrificing additional above ground space. The storage space should be designed so that it is permanently saturated, i.e., the height does not exceed that of the upturned elbow drainage pipe, and filled media that can serve as the electron donor for nitrate removal. While the depth of the storage space is limited by the elbow height, the length and width of the denitrification storage space are not constrained by other cell parameters.

Allocating subsurface horizontal storage for denitrification is analogous to increasing the ratio of bioretention cell footprint to catchment area. For example, increasing the ratio from 5% to 15% is the same as tripling the volume capacity of the denitrifying zone; specific to default parameters, a 5% ratio corresponds to 1200 cm^3

where as a 15% ratio corresponds to 3600 cm^3 of storage volume. Therefore, results of Figure 4-11 are presented similarly to those in Figure 4-7; however, this scenario utilizes all parameters as outlined in Table 4-6 with the exception of varying the cell to catchment footprint ratio. A ratio of 3% corresponds to the previously identified 28% annual efficiency, whereas increasing the ratio to 10% and 15% translates to 8.5 kg-N/ha/yr and 6.3 kg-N/ha/yr, respectively.

Thus, designers may select a maximum allowable nitrate discharge from the bioretention system, and then, allocate the corresponding storage volume. Results of Figure 4-11 and Figure 4-13 verify that increased volume attenuation is an acceptable approach to management nitrate loadings. By increasing the IWSZ storage capacity, the system can capture larger-sized storms and increase the HRT of stormwater through the denitrifying space. Collectively, the findings suggest that multiple design opportunities are available depending on available space and associated costs of excavation, construction, and maintenance. Additional lifecycle analysis may be required to select the most cost effective option when modifying current bioretention design to increase denitrifying storage space.
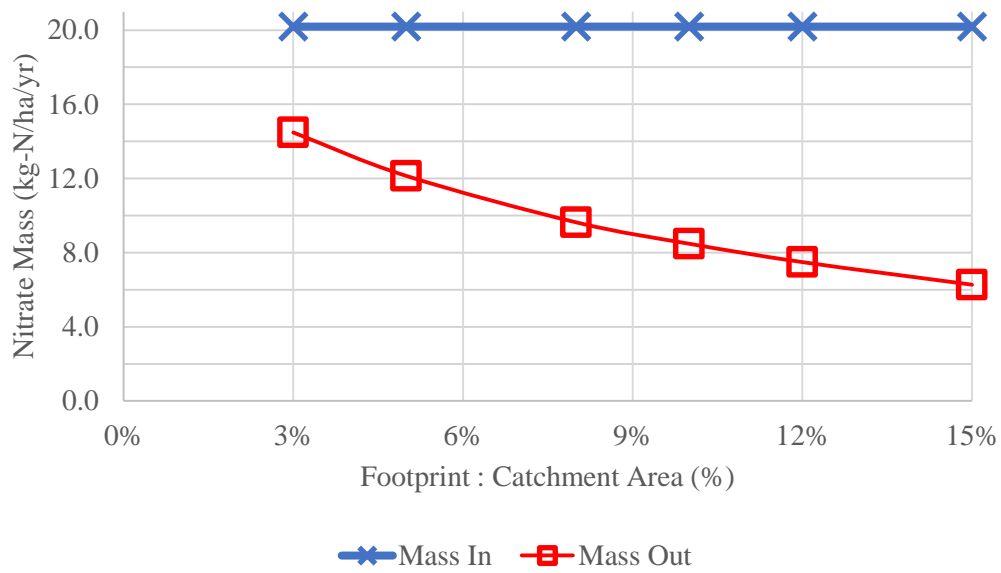
Figure 4-13. Effect of increasing the horizontal subsurface storage for denitrification and the expected annual nitrate performance. See Table 4-6 for details with the exception of varied cell to catchment area footprint ratio.

4.3.2. Enhanced Low Flow Scenario

For bioretention to best meet nitrate removal goals, the rate of stormwater runoff approaching the cell and infiltration rate through the cell must be limited. In addition to increased IWSZ storage volume, other opportunities to enhance the *low flow* scenario, thereby increasing opportunity for in-storm denitrification and nitrate removal response are explored and discussed below.

Restricted Flow in IWSZ

The rate of stormwater flow through the permanently saturated zone can be manipulated by reducing the flow into and/or out of the IWSZ.

To begin, the restricted flow can be targeted through careful selection of overlying media. The media which exhibits the lowest hydraulic conductivity, as dependent on soil matrix characteristics and initial moisture content, will be the rate-

limiting step. The infiltration rate of woodchip-pea gravel media will not limit the rate of stormwater flow (Davis et al. 2009).

Lucas and Greenway (2011a) developed a dual-stage outlet configuration to manage incoming IWSZ flows without sacrificing high infiltration rates of overlying media. An elevated lower outlet constrained flows out of the IWSZ. This offered a novel management strategy for bioretention to mitigate even the most extreme runoff events. A10-cm IWSZ depth with a restricted effluent 8.0 cm/hr flowrate demonstrated nitrate mass removal upwards of 80%. Results indicated a clear relationship between extended retention time and mass removal, although the rate of incoming flow did have some effect; the IWSZ showed 53% and 64% under high flow and 78 to 94% under low flow events (Lucas and Greenway 2011b).

To account for either of these hydraulic loading restrictions, the model incorporated an additional parameter, $v_{restrict}$, to those outlined in Table 4-6. Rather than assume that all hydraulic runoff rates were equal to the flowrate of stormwater through the IWSZ, the model restricted velocity (v), which is independent of surface area of the cell. The allowable infiltration rate of the stormwater through the IWSZ is a function of the media porosity and v (Davis and McCuen 2005) and is calculated as follows:

$$\text{Infiltration Rate} = \frac{v}{\varepsilon}$$

4- 1

where v_c is the critical velocity

ε is the media porosity

In doing so, every storm event is either completely captured by the IWSZ, if runoff volume to storage volume permits, or is a *low flow event* and exhibits in-storm

denitrification. If a design HRT of 4.0 hours in the IWSZ is warranted, then a 45-cm depth and 1200 cm^3 storage corresponds to a restricted v of 3.8 cm/hr.

The added parameter, $v_{restrict}$, allowed for increased nitrate performance because the opportunity for minimal nitrate removal, as characteristic of a washout event, was not present. Figure 4-14 presents the results of annual nitrate removal in two scenarios – (1) unrestricted ponding time, and (2) a restricted ponding time of 24 hours. Excessive ponding should be reduced as possibility of introduced human and environmental repercussions may arise, e.g., mosquito breeding (Hawaii State Department of Health 2015). In both results, the model does not account for the accumulated ponding volume above the cell. In other words, stormwater bypass will only occur if first, the calculated hydraulic loading rates were greater than the restricted v and second, if the total drainage time of the runoff volume was greater than 24 hours. If both scenarios were true, then the stormwater bypass volume was calculated as the difference between the infiltrated volume in 24 hours and the total runoff volume.
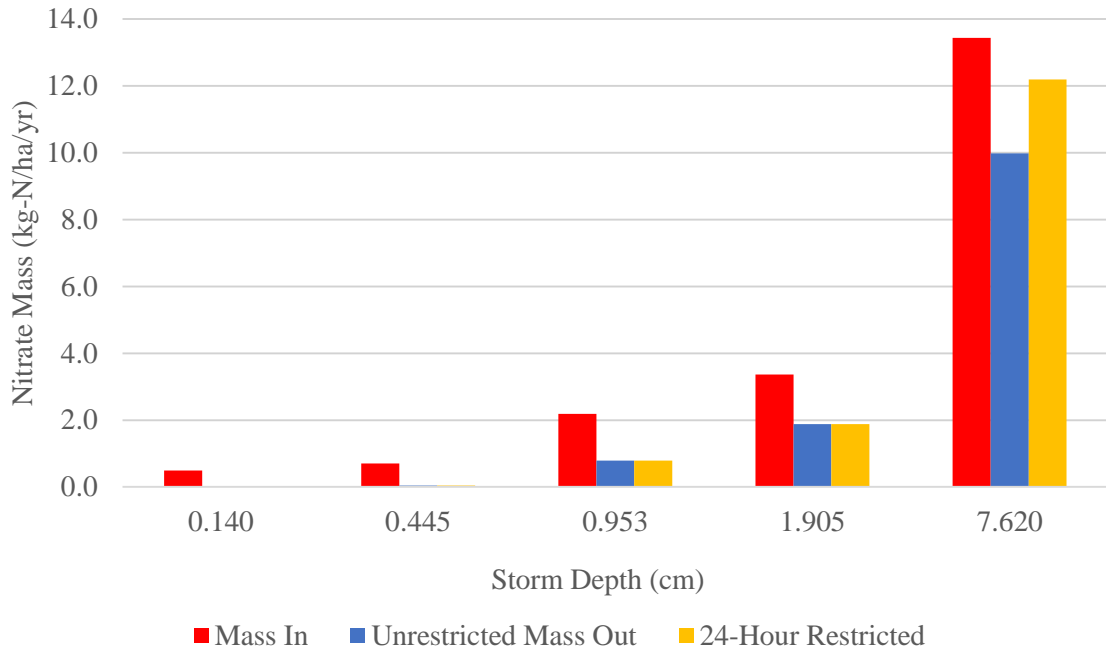
Figure 4-14. Effect of restriction of flow through the IWSZ to maintain a minimum HRT of 4.0 hours and allow for in-storm denitrification. One scenario does not account for the 24-hour constraint of ponded water whereas the second scenario assumes that after 24 hours, stormwater will bypass the system if excess ponding occurs.

With an unrestricted ponding time, the annual nitrate export is 0.05 kg-N/ha, 0.8 kg-N/ha, 1.88 kg-N/ha, and 9.98 kg-N/ha for the 0.445-cm, 0.953-cm, 1.905-cm, and 7.620-cm storm, respectively. In comparison, when the ponding time is restricted to 24 hours, annual nitrate export for the 7.620-cm storm increases to 12.2 kg-N/ha; the smaller sized storms are not affected by this time constraint. Annual mass removal efficiencies for the two scenarios is 37% and 26%, respectively.

Realistically, by restricting incoming and/or outgoing IWSZ flow, the cell may respond with faster, higher volumes of stormwater overflow. This may occur if the intensity of incoming runoff exceeds combined infiltration rate and above-ground storage capacity of the cell. Lucas and Greenway (2008) observed that the bioretention mesocosm was unable to manage incoming hydraulic loadings, which resulted in more

110

bypassed storm volume. It is important to define the above-ground storage constraints, to quantify maximum ponding volume and time, whereas the results of Figure 4-14 only incorporate time. Adoption of cell configuration is shown in Figure 4-15. The included bowl defines the above-ground storage of the cell with a 0.30-m depth.
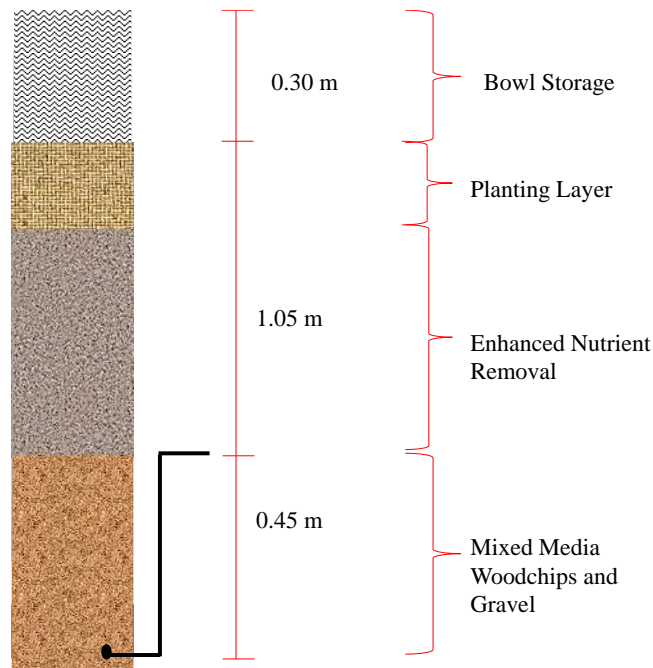
Figure 4-15. Incorporation of a 0.30-m depth bowl to allow for aboveground storage of stormwater during rainfall/runoff events.

The inclusion of above-ground storage elicits an additional conditional statement to quantify stormwater bypass volume. Now, stormwater bypass will only occur if first, the calculated hydraulic loading rates were greater than the restricted v and second, if the accumulated ponding volume was greater than the allowable bowl storage. Thus, bowl depth must sufficient to temporarily retain stormwater but underlying media must ensure intra-event percolation to maintain a total ponding time less than 24 hours (Hunt et al. 2012). Results of Figure 4-16 suggest that a bowl storage volume will increase the nitrate removal performance because the model has a defined above-ground storage compartment. The accumulated stormwater volume in the bowl was defined by a non-

steady state mass balance by calculating the difference stormwater inflow rate, developed

by the Modified Rational Method and stormwater outflow rate, limited by a 4.0-hour

HRT. Results of Figure 4-16 verify that a bowl storage reduces the nitrate export for all

sized storms, as it increases the overall system efficiency. The most notable difference is

for the 7.620-cm storm, when comparing results of Figure 4-10, Figure 4-14, Figure 4-16.

Predicted nitrate export is 11.64 kg-N/ha (for default conditions), 12.2 kg-N/ha (24-hour

restricted ponding), and 8.3 kg-N/ha (0.3-m bowl storage), respectively. Annual nitrate

mass removal efficiency improved to 48%.
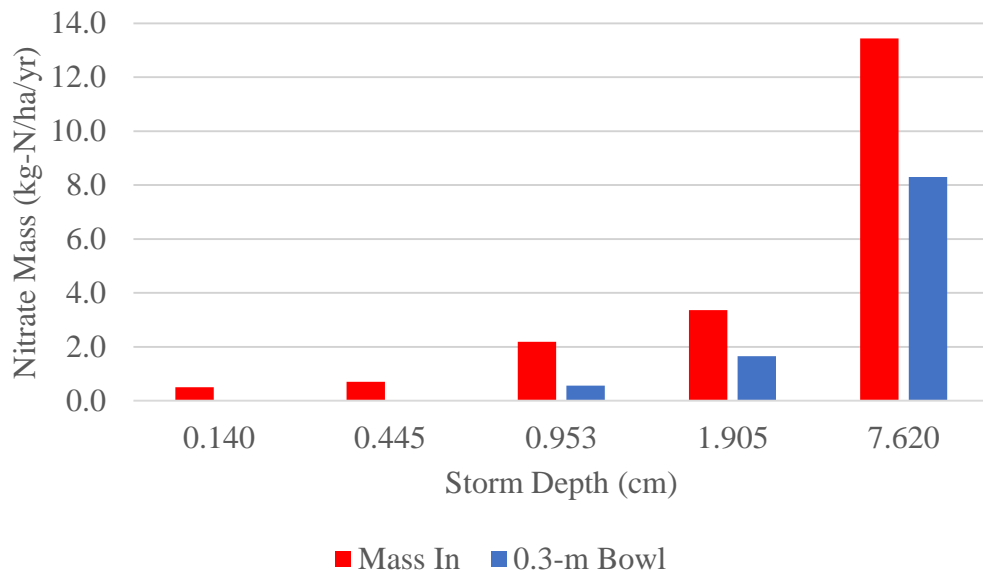
Figure 4-16. Effect of a 0.3-m depth bowl storage on the aboveground storage capacity of the cell when flow is limited to a 4.0 hour HRT. Ponded stormwater is only allowed for 24 hours, afterwards the stormwater is assumed to bypass the system entirely.

This adaption of a 0.3-m bowl demonstrates consistency with prior field scale

observations. Findings of Davis et al. (2012b) suggest that a bioretention cell, or any

infiltration-based SCM for that matter, should increase total storage volume so it is better

equipped to manage increased volume storage and attenuation. The total storage volume

is defined as the bioretention abstraction volume (BAV) or the runoff volume that is completely captured by the bowl and pore storage of the cell; the BAV can be increased via larger bowl storage, increased layer depth(s), available percolation to the surrounding soils, etc. In particular, an increased bowl storage volume will allow for larger above ground storage of water where the rate of infiltration is limited by underlying media characteristics. As Figure 4-16 and previous studies suggest, water quality treatment can be improved with volume attenuation and peak reduction (Hunt et al. 2006, 2012).

<u>System Geometry</u>

It is possible to encourage in-storm denitrification from another design component – system geometry. If the cell geometry is designed to physically resemble a plug-flow reactor, mixing is minimized within the system itself. Current results of predicted nitrate behavior assume the lack of stormwater interaction, and rather movement is only controlled by advection. Therefore, nitrate annual performance models do not account for the possibility of solute bypass, and may over-predict field-scale performance.

As laboratory-scale mesocosm results suggest, dispersion parameters can be indicators of nitrate performance. Therefore, if geometry is adjusted to increase the depth and reduce cross sectional area, less media volume is necessary to achieve the same nitrate performance under the same loading conditions (Lynn et al. 2016). Total bioretention costs are reduced, as smaller, more efficient treatment volumes can be designed, to achieve the same nitrogen removal goals (Lynn et al. 2016). Thus, it is recommended to conduct field-scale tracer studies to best quantify dispersion parameters and incorporate a more complex approach to estimating nitrate effluent profiles. In doing

so, the model can be further developed to reflect the co-existence of advection and dispersion under flow conditions.

4.3.3. Modifying Rate-Limiting Kinetics

The first-order denitrification rate constant specific to the selected woodchip media suggests that contact time on the order of days is necessary for nitrate concentrations to fall below 0.05 mg-N/L. Chapter 3 laboratory results indicated that treated woodchips designed to accelerate the degradation and bioavailability of carbon did not increase the apparent denitrification rate constant.

However, such shortcomings offer insight for future work. Rather than increase simple resources, media amendments should exhibit a diversity of complex carbon. A more diverse microbial community has demonstrated an affinity for multiple carbon sources, some of which were responsible for denitrification (Cherchi et al. 2009). So instead of relying on a single woodchip species, other media amendments could be explored as to promote a greater diversity of denitrifiers. Furthermore, the surface areas and roughness should be maximized, without sacrificing excessive leaching, to allow for biofilm acclimation and maturation (Gharechahi et al. 2012).

One way to modify the current microbial community in the woodchips is to create conditions conducive for both autotrophic and heterotrophic denitrification. Heterotrophic denitrification is specific to an external organic carbon source, e.g.,

woodchips, sawdust, and newspaper (Kim et al. 2003; Peterson et al. 2015); autotrophic

denitrifiers use an inorganic substance, such as sulfur or iron, as the electron donor

(Ashok and Hait 2015; Li et al. 2016). Soares (2002) successfully removed synthetic

nitrate contaminated groundwater at a rate of 0.20 kg-N/m^3-d^1 at a 1 hour retention time

via elemental sulfur for autotrophic denitrification, sodium bicarbonate as a buffering

agent, and an inorganic carbon source for microbes. Another option for an electron donor

and buffering agent are thiosulfate and limestone, respectively (Lampe and Zhang 2012;

Zhou et al. 2011). Findings of Zhao et al. (2012) demonstrated a cooperative effect of the

autotrophic and heterotrophic denitrification processes to treat nitrate-contaminated

drinking water; Li et al. (2016) demonstrated similar behavior of the denitrifier

community using woodchips and elemental sulfur without an added buffering agent in

laboratory-scale batch experiments. Li et al. (2016) proved that combined denitrification

activity was superior over single autotrophic or heterotrophic denitrification.

Additional research is necessary to determine if combined heterotrophic-

autotrophic denitrification (HAD) is feasible in a field-scale bioretention cell and if

increased denitrification kinetics can be observed. Identification of community structure

and population dynamics with respect to known autotrophic and heterotrophic denitrifiers

may be of interest to characterize the synergistic relationship (Li et al. 2016).

Results of Figure 4-17 explore the predicted annual nitrate behavior if the denitrification rate constant is increased. The parameters in Figure 4-10 are the same with the exception of a modified k value of 2.20×10^{-3} min^{-1} and 2.75×10^{-3} min^{-1}, which are 2.0 and 2.5-times the Willow Oak-based rate constant. As the k increases, all storms demonstrate a reduced nitrate export, with the exception of the 0.140-cm storm, which is completely captured by the IWSZ. The difference between the output mass by storm depth is significantly different due to the variance in k ($p > 0.05$). Such a difference is most apparent when comparing the two largest storm depths; the smaller k reports an annual 1.5 kg-N/ha and 10.5 kg-N/ha leaching, while the larger k corresponds to 1.3 kg-N/ha and 10.0 kg-N/ha, respectively. Overall, each system demonstrates an overall nitrate mass removal efficiency of 38% and 42%, whereas, a media with $k = 0.0011$ min^{-1} was only 28% efficient. Undoubtedly, the denitrification rate constant is essential to the efficiency of the system with regards to in-storm denitrification potential. Results of this simulation may motivate future research to consider alternative media to increase the denitrification rate. However, the media selection should not sacrifice system longevity nor excessively leach.
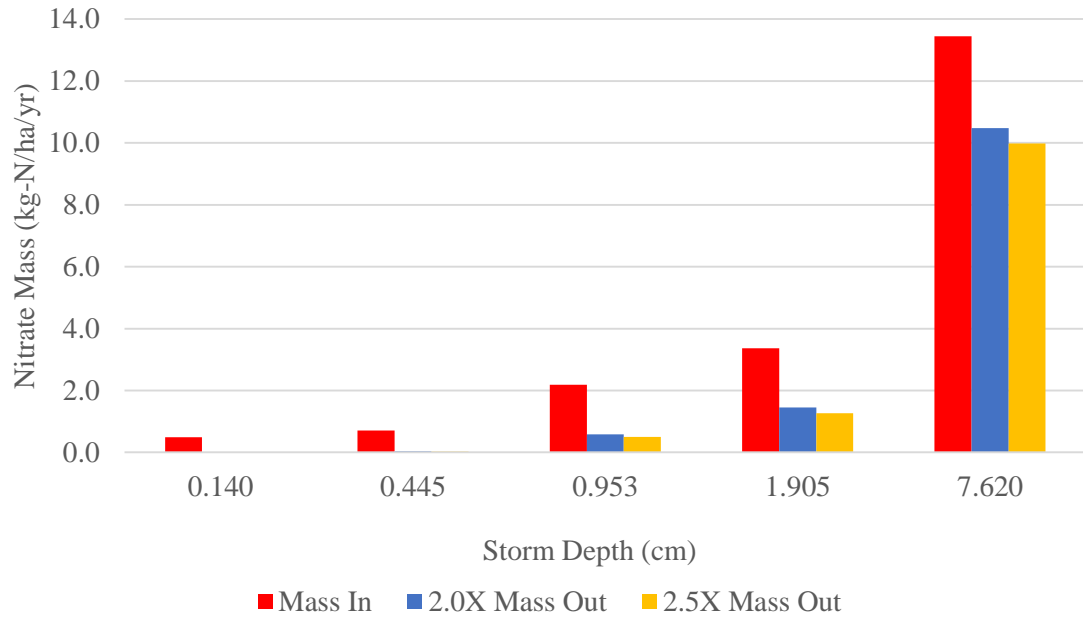
Figure 4-17. Effect of accelerated denitrification rate constant and the annual predicted nitrate removal as categorized by storm depth.

4.4. Case Study: Maximizing Design Components to Increase N-Removal Performance

In order to address the accelerated pollutant loading rate of incoming runoff,

integration of the aforementioned design recommendations are presented and quantified.

Table 4-7 details the four design components and summarizes possible options for field

scale integration.

Table 4-7. Design Guidance for Bioretention to Target Denitrification Removal.

Design Component	Guidance	Supporting Evidence
Inclusion of an IWSZ	Upturned elbow configured drainage pipe to ensure permanently saturated conditions. Supplemented reducing agent must be present in media.	Kim et al. (2003); Lynn et al. (2015, 2016); Peterson et al. (2015)
Increased IWSZ Storage	Raised height of the elbow configured pipe to construct a deeper excavated cell and/or permanently saturate upper media layers as to increasingly resemble a submerged gravel wetland. Create adjacent subsurface storage to increase total storage volume.	Mostly anecdotal evidence but Brown and Hunt (2011) and Lynn et al. (2016) provide some support
Restrict Flow Through IWSZ	Add pretreatment mechanisms as traditionally employed in erosion control. Include bowl storage where the depth and total volume can store water-quality volume and allows for intra-event percolation. Hydraulic conductivity of media layer(s) above IWSZ must restrict incoming as to allow diffusional mass transport and increase the overall contact time. Outlet of the IWSZ can also restrict flow without the sacrifice of infiltration rates of overlying media.	Some anecdotal but Davis et al. (2012b); Hunt et al. (2012a) and Lucas and Greenway (2008, 2011a; b) begin to quantify nitrate removal
Media Amendments	Addition and/or replacement of woodchip-based media to supply as reducing agent. Selected media shall increase the apparent first-order *k* rate constant. Emphasis should be placed on enhancing the denitrifying-specific microbial population without sacrificing media longevity nor leaching and/or production of other pollutants.	Mostly anecdotal evidence Li et al. (2016) demonstrates possibility of heterotrophic-autotrophic denitrification

Model results incorporated multiple adaptive management strategies to improve the nitrate annual performance based on current knowledge. Design focused on increasing temporary storage volume and denitrifying treatment volumes, and enhancing the opportunity for in-storm denitrification by maintaining a minimum 4.0-hour HRT of all stormwater through the IWSZ (Table 4-8). Other parameters are consistent with those presented in Table 4-6, including a rate constant of 0.0011 min^{-1}.

Table 4-8. Multiple bioretention design components to address challenges of climate change, urbanization, and first-order limited kinetics.

Design Components	Purpose
100-cm elbow drainage pipe height	Increase denitrifying storage capacity
Variable cell to catchment footprint– 3%, 5%, 10%, 15%	Incorporate horizontal subsurface storage
30 cm bowl depth	Reduce stormwater bypass Increase total volume storage
Restrict flow through IWSZ to 4.0 hour HRT	Promote in-storm denitrification for all storm events

Results indicate that increasing the cell to catchment footprint improved nitrate removal performance. Findings shown in Figure 4-18 suggest that the difference in nitrate removal performance is most substantial with regards to the 7.620-cm storm depth. As the ratio increases from 3% to 15%, the annual predicted nitrate export reduces from 9.1 kg-N/ha to 1.3 kg-N/ha. The increased ratios correspond to an annual mass removal efficiency of 51%, 64%, 83%, and 94%. Therefore, as a system allocates more storage specific to denitrification, it can more easily adapt to higher pollutant loading rates.
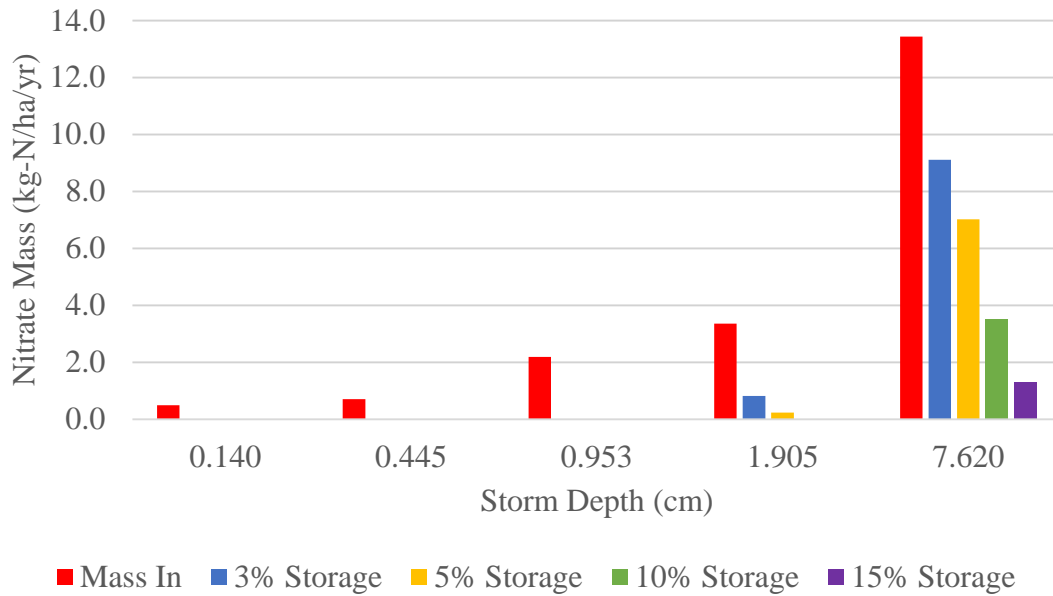
Figure 4-18. Variance of cell to catchment footprint or increased horizontal subsurface storage on annual nitrate removal while incorporating other design components to increase volume attenuation and in-storm denitrification.

It is recommended that designers use both aboveground and subsurface space more efficiency to best meet hydrologic and water quality goals. Bioretention design can only successfully address stringent denitrification and N-management goals through the integration of recommendations as presented in Table 4-8. As denitrification-conducive conditions are established and maintained through an entire storm event, nitrate removal can be substantially improved by increasing the contact time of nitrified stormwater in the system without sacrificing total treatment volume. In that way, bioretention design must focus its efforts on increasing the overall HRT of the stormwater via reduced velocity through the denitrifying zone and increased volume of permanently saturated conditions. In this study, a minimum HRT of 4.0 hours is proposed based on the consideration of batch study, *low flow* events, and PFR-reactor model denitrification rate determinations. If future research is capable of improving denitrification kinetics without

compromising overall water quality, i.e., leachate of other unwanted pollutants, then, the HRT recommendation can be redefined.

This model does not account for nitrate removal via volume reduction and infiltration to native soils. Field studies observed that unlined bioretention cells corresponded to an adjustment in water balance, which was the main contributor to measured nitrogen load reduction (Li and Davis 2014). Additional work may focus on the adaption of an unlined cell as to improve observed nitrate load reduction along with hydrologic improvements. However, if denitrification is ineffective, nitrate can contaminate groundwater (Kaushal et al. 2008).

Chapter 5 Conclusion

5.1. General Conclusions

The results of this study verified the necessity of an internal water storage zone in a bioretention cell to effectively target denitrification and improve total nitrogen removal efficiency. An IWSZ is only as successful as the media components that serve as the electron donor for denitrification, the retention time of the stormwater, and the storage capacity of the denitrifying zone.

The incorporation of Willow Oak woodchips, 4.5% by mass, to the IWSZ media corroborated previous studies to describe first-order denitrification kinetics with a rate constant of 0.0011 min^{-1}. Experimental results suggest that stormwater must be retained for at least 2.6 days in order for nitrate concentrations to fall below 0.05 mg-N/L. An attempt to reduce the necessary retention time for complete denitrification, via adaption of woodchip pretreatment methods to target lignin removal, compromised the longevity and minimal nutrient leaching of the untreated woodchip. The inability to encourage faster denitrification rates further reinforces the linkage between water quality treatment and the microbial processes that govern nitrogen transformation and removal.

When nitrate was applied to the laboratory-designed IWSZ, results indicated that the relationship between macroscale transport processes, e.g., advection and dispersion, and microscale diffusion and biodegradation, was central to the prediction of nitrate performance. Nitrate removal was not affected by a dynamic pollutant loading or preservation of macroscale anoxic and reduced conditions. Storm simulated events were characterized as either *low flow* or *high flow* dependent upon the capability of nitrate transport out of the stormwater and in contact with the biofilm. In-storm nitrate profiles

coupled with ORP measurements allude to a biofilm around the woodchip structure that is responsible for denitrification. In this study, consideration of experimental and theoretical PFR-reactor model predictions led to a 4.0-hour HRT threshold to separate *low flow*, demonstrating in-storm denitrification, and *high flow* events, exhibiting a washout behavior. While this value may be somewhat conservative, it is recommended that 4.0 hour stormwater retention time is necessary for at most 80% nitrate concentration recovery; as the contact time approaches 2.6 days, denitrification kinetics predict complete nitrate removal.

Based on the findings of experimental work in this study, a simple model was developed to characterize annual IWSZ performance. Model results are specific to the Maryland rainfall distribution presented by Kreeb (2003). The model first predicted annual performance using default bioretention design parameters. Additional simulations incorporated challenges posed by rapid urbanization, seasonality effects of varying water temperature and elevated road salt concentrations, and climate change.

Collectively, experimental and modeling results demonstrate the potential of bioretention to increase nitrate removal efficiency by incorporating larger denitrifying treatment volumes and encouraging in-storm denitrification via flow restrictions into and/or through the IWSZ. Bioretention, or any infiltration-based SCM, must allow for a minimum contact time of 4.0 hours in order to significantly improve performance. Specifically, the simple model results of the laboratory-designed 45-cm IWSZ predicted an annual 28% mass removal. Incorporation of a 30-cm bowl depth, increased 100-cm IWSZ depth, and a 15% cell footprint to catchment area ratio, i.e., tripling the IWSZ storage volume from the default parameters in Table 4-1, can improve annual nitrate

removal efficiency to 94%. By efficiently utilizing aboveground and subsurface storage space, bioretention can meet hydrologic and nitrogen related water quality goals. While not included in this model, if denitrification is effective, runoff volume reduction via infiltration may be another opportunity for N removal.

5.2. Future Work

In order to validate the experimental results of this study, field-scale application is recommended. The system should be monitored for at least a decade to verify the predicted longevity of the media and stable degradation rate. Water quality parameters, e.g., nitrate, total N, and ammonium, should be monitored over the life-cycle of the system. Identification and analysis of the microbial community responsible for lignocellulose degradation, denitrification, and competing metabolic activities may help to assess the structure and dynamicity of the system. Biological analysis specific to nitrate transformation processes can correlate the abundance, diversity and efficiency of denitrifiers with observed water quality performance. Collectively, results may offer insight to best improve the denitrification rate by manipulating nutrient availability and content provided by the IWSZ media. Without significantly improving the denitrification rate constant, nitrate removal will continue to be limited by slow first-order kinetics.

Additional modeling efforts may be useful for designers. Quantified annual nitrate removal performance may encourage designers to best utilize above-ground and subsurface space to allocate maximum storage, target denitrification, and maintain a minimum 4.0 hour retention time. More complex modeling can incorporate measured field hydraulic loading rates, modify rainfall distributions to more accurately depict current storm intensities and probability of occurrence, and adapt alternative runoff

calculation methods for comparison. Additionally, field-scale dispersion parameters and variability of the reported rate constant should be included. Research efforts that define that variability of k with respect to the available carbon source and the lignocellulose degradation rate, improves the ability for future modeling to accurately predict nitrate removal performance.

Appendix

Appendix I

A-1   Control Test Raw Data

Pea Gravel Test

Sample ID	Average Time (min)	Volume (L)	Nitrate (mg/L-N)	Mass (mg)
Stormwater Influent	0	0.08	2.736	6.84
Effluent 1	50	0.19	2.976	0.565
Effluent 2	150	0.29	2.848	0.826
Effluent 3	212.5	0.082	2.925	0.24
Effluent 4	362.5	0.295	2.981	0.879
Effluent 5	850	0.295	2.881	0.85
Effluent 6	1530	0.194	2.966	0.575
Effluent 7	2250	0.085	2.927	0.249
Effluent 8	3045	0.989	2.983	2.951
Total		2.5		7.135

Sodium Azide Test

Sample ID	Average Time (min)	Volume (L)	Nitrate (mg/L-N)	Mass (mg-N)
Stormwater Influent	0	0.035	3.162	7.904
Effluent 1	55	0.123	3.405	0.419
Effluent 2	75	0.092	3.101	0.285
Effluent 3	630	1.332	3.162	4.211
Effluent 4	765	0.172	3.101	0.533
Effluent 5	1357.5	0.538	3.192	1.717
Effluent 6	1485	0.036	3.101	0.112
Effluent 7	2910	0.172	2.918	0.502
Total		2.5		7.78

A-2   Establishing Denitrification and Associated Statistics for Determination of Reaction Rate Order and Rate Constant

Run 1 - 3.0 mg-N/L				6.0 mg-N/L			
Elapsed Time	Avg. Time	pH	Nitrate	Time	Avg. Time	pH	Nitrate
0	0	5.43	2.838	0	0	6.17	5.632
100	50	5.2	2.353	100	50	5.2	3.180
200	150	5.68	2.486	200	150	5.61	4.652
225	212.5	5.5	2.616	225	212.5	5.78	4.434
500	362.5	5.39	2.585	500	362.5	5.47	4.353
1200	850	5.61	2.124	1200	850	5.28	3.030
1860	1530	6.93	0.417	1860	1530	6.7	1.135
2640	2250	6.48	0.025	2640	2250	6.77	0.296
3450	3045	6.65	0.025	3450	3045	7.17	0.025

1.0 mg-N/L			
Time	Avg. Time	pH	Nitrate
0	0	5.83	1.004
100	50	5.32	0.796
200	150	5.55	0.747
225	212.5	5.73	0.674
500	362.5	6.72	0.530
1200	850	6.56	0.174
1860	1530	6.65	0.076
2640	2250	7.24	0.102
3450	3045	6.24	0.079
4110	4110	5.6	0.073

Run 2 - 3.0 mg-N/L			
Time	Avg. Time	pH	Nitrate
0	0	5.66	2.935
100	50	5.38	2.233
200	150	5.83	2.397
225	212.5	5.64	2.293
500	362.5	6.61	1.743
1200	850	5.96	0.840
1860	2640	7.02	0.305
2640	4080	6.25	0.165

Assumed Reaction Order	Influent Concentration (mg-N/L)	R^2
Zero	6	0.8675
Zero	3	0.7764
Zero	1	0.6601
First	6	0.9406
First	3	0.9574
First	1	0.7702

K Value	Sum of Squares Values			
	Influent Concentration			
(min^{-1})	(mg-N/L)			Compiled
	6	3	1	
0.0008	2.154	1.272	0.287	3.713
0.0009	1.353	0.988	0.221	2.562
0.001	7.427	0.777	0.171	8.376
0.0011	1.074	0.625	0.133	1.832
0.0012	1.35	0.518	0.103	1.971
0.0015	3.041	0.406	0.052	3.498
0.0017	4.552	0.456	0.037	5.045
0.0018	5.365	0.509	0.034	5.908
0.0019	6.201	0.576	0.034	6.811
0.002	7.054	0.425	0.035	7.514

Statistical Measures			
Influent Concentration	Bias	Average Bias	SSE
1.0	-0.711	-0.071	0.133
3.0	0	-0.155	0.625
6.0	-0.519	-0.065	1.074

A-3   Establishment of Anoxic Conditions: Continuous System ORP Measurements Under No Flow Condition

Time	Elapsed Time (min)	ORP (mV)
8:40 AM	0	80
9:05 AM	25	71.4
9:20 AM	40	62.9
9:35 AM	55	53.9
9:50 AM	70	46
10:05 AM	85	38.3
10:25 AM	100	26.9
10:40 AM	115	18.9
10:55 AM	130	11.1
11:10 AM	145	2.1
11:25 AM	160	-8
11:45 AM	180	-22.2
11:55 AM	190	-33
12:50 PM	245	-84.7
1:15 PM	270	-111.5
1:55 PM	310	-163.8
2:10 PM	325	-178.1
2:25 PM	340	-190.1
2:45 PM	360	-204.1
3:05 PM	380	-218
3:30 PM	405	-229.4

A-4   Batch Study Data: Control Woodchips

Week 1 - TOC (mg-C/L)				
	Run 1	Run 2	Run 3	Average	STDEVS
Influent	1.671	1.713	2.844	2.076	0.666
Sample 1	16.21	17.742	13.959	15.97	1.903
Sample 2		24.32	19.338	21.829	3.523
Sample 3	46.66	32.56	25.64	34.953	10.712
Sample 4	47.52	47.28	49.9	48.233	1.448
Sample 5	17.656	22.62	18.328	19.535	2.693
Sample 6	18.19	19.198	19.7	19.029	0.769
Sample 7	25.04	23.5	18.378	22.306	3.488
Week 2 - TOC (mg-C/L)				
	Run 1	Run 2	Run 3	Average	STDEVS
Influent	2.902	2.592	2.454	2.649	0.229
Sample 1	4.344	2.156	3.788	3.429	1.137
Sample 2	6.694	3.566	4.68	4.98	1.585
Sample 3	10.982	8.202	9.98	9.721	1.408
Sample 4	13.434	8.302	11.802	11.179	2.622
Sample 5	13.57	9.84	13.572	12.327	2.154
Sample 6	20.24	12.78	17.844	16.955	3.809
Sample 7	23.04	13.748	19.142	18.643	4.666
Sample 8	25.7	17.532	25.22	22.817	4.584
Sample 9	32.38	19.218	25.22	25.606	6.589
Week 3 - TOC (mg-C/L)				
	Run 1	Run 2	Run 3	Average	STDEVS
Influent	2.716	2.734	2.514	2.655	0.122
Sample 1	8.408	8.092	7.11	7.87	0.677
Sample 2	9.96	8.612	8.42	8.997	0.839
Sample 3	14.896	12.028	13.488	13.471	1.434
Sample 4	16.206	12.128	14.158	14.164	2.039
Sample 5	18.336	13.678	14.624	15.546	2.462
Sample 6	22.16	17.536	16.462	18.719	3.028
Sample 7	20.088	17.004	14.376	17.156	2.859
Sample 8	25.78	18.82	20.82	21.807	3.583
Sample 9	34.84	20.56	18.518	24.639	8.893

Week 1 - Nitrate (mg-N/L)				
	Run 1	Run 2	Run 3	Average	STDEVS
Influent	3.059	3.17	2.999	3.076	0.087
Sample 1	3.296	3.086	3.351	3.244	0.14
Sample 2	3.212	3.222	2.93	3.121	0.166
Sample 3	2.741	2.493	2.559	2.598	0.128
Sample 4	2.554	2.327		2.441	0.16
Sample 5		1.998	2.38	2.189	0.27
Sample 6	1.24	0.961	1.983	1.395	0.528
Sample 7	0.729	0.403	0.143	0.425	0.294
Week 2 - Nitrate (mg-N/L)				
	Run 1	Run 2	Run 3	Average	STDEVS
Influent	3.198	3.097	3.094	3.13	0.059
Sample 1	3.159	3.172	3.111	3.147	0.032
Sample 2	3.225	3.228	3.081	3.178	0.084
Sample 3	1.281	2.055	1.456	1.597	0.406
Sample 4	0.815	1.42	1.437	1.224	0.354
Sample 5	0.473	1.23	0.768	0.824	0.382
Sample 6	0.11	0.261	0.133	0.168	0.081
Sample 7	0.094	0.172	0.303	0.189	0.106
Sample 8	0.258	0.085	0.358	0.234	0.138
Sample 9	0.158	0.317	0.467	0.314	0.155
Week 3 - Nitrate (mg-N/L)				
	Run 1	Run 2	Run 3	Average	STDEVS
Influent	3.084	3.078	3.016	3.059	0.037
Sample 1	2.457	2.632	2.686	2.592	0.119
Sample 2	1.777	2.234	2.204	2.072	0.256
Sample 3	0.123	0.895	0.712	0.577	0.403
Sample 4	0.169	0.674	0.478	0.44	0.255
Sample 5	0.142	0.604	0.274	0.34	0.238
Sample 6	0.139	0.172	0.142	0.151	0.018
Sample 7	0.137	0.118	0.094	0.116	0.022
Sample 8	0.137	0.115	0.12	0.124	0.011
Sample 9	0.182	0.083	0.357	0.207	0.139

Week 1 - TN (mg-N/L)				
	Run 1	Run 2	Run 3	Average	STDEVS
Influent	3.254	3.252	4.686	3.731	0.827
Sample 1	4.036	3.69	2.966	3.564	0.546
Sample 2		4.458	3.045	3.752	0.999
Sample 3	3.868	3.644	1.954	3.155	1.047
Sample 4	3.736	3.504	3.588	3.609	0.117
Sample 5	2.834	2.7	2.568	2.701	0.133
Sample 6	2.81	2.454	2.264	2.509	0.277
Sample 7	2.844	2.572	2.114	2.51	0.369
Week 2 - TN (mg-N/L)				
	Run 1	Run 2	Run 3	Average	STDEVS
Influent	3.318	3.13	2.798	3.082	0.263
Sample 1	3.122	3.086	2.912	3.04	0.112
Sample 2	3.24	3.042	2.698	2.993	0.274
Sample 3	1.489	2.178	1.604	1.757	0.369
Sample 4	1.368	1.631	1.83	1.61	0.231
Sample 5	0.914	1.578	1.676	1.389	0.414
Sample 6	0.752	0.714	0.69	0.719	0.031
Sample 7	0.635	0.6	1.146	0.794	0.305
Sample 8	1.035	0.595	1.348	0.993	0.378
Sample 9	1.178	1.213	1.025	1.139	0.1
Week 3 - TN (mg-N/L)				
	Run 1	Run 2	Run 3	Average	STDEVS
Influent	3.078	2.638	2.858	2.858	0.22
Sample 1	3.026	2.652	2.78	2.819	0.19
Sample 2	2.552	2.398	2.788	2.579	0.196
Sample 3	0.912	1.511	2.222	1.548	0.656
Sample 4	0.793	1.361	1.65	1.268	0.436
Sample 5	1.28	1.601	1.223	1.368	0.204
Sample 6	0.819	1.446	1.084	1.116	0.315
Sample 7	0.692	0.815	0.449	0.652	0.186
Sample 8	0.842	0.638	0.764	0.748	0.103
Sample 9	0.978	0.503	0.72	0.733	0.238

		Sample #	Ammonia (mg-N/L)
Week 1	Run 1	1	0.212
	Run 2	1	0.556
	Run 3	1	0.196
Week 2	Run 1	2	0.23
	Run 2	1	0.234
	Run 3	1	0.214
Week 3	Run 1	1	0.183
	Run 2	1	0.282
	Run 3	2	0.16

	Week 1, pH				
	Run 1	Run 2	Run 3	Average	STDEVS
Influent	3.94	3.72	4.30	3.99	0.29
Sample 1	4.63	4.34	4.27	4.41	0.19
Sample 2	4.64	4.43	4.28	4.45	0.18
Sample 3	4.73	4.53	4.47	4.58	0.14
Sample 4	4.78	4.65	4.60	4.68	0.09
Sample 5	4.87	4.56	4.53	4.65	0.19
Sample 6	5.01	4.8	4.68	4.83	0.17
Sample 7	4.79	4.65	4.72	4.72	0.07
	Week 2, pH				
	Run 1	Run 2	Run 3	Average	STDEVS
Influent	5.69	5.46	5.30	5.48	0.20
Sample 1	4.75	4.69	4.62	4.69	0.07
Sample 2	4.64	4.52	4.56	4.57	0.06
Sample 3	4.61	4.48	4.38	4.49	0.12
Sample 4	4.69	4.54	4.60	4.61	0.08
Sample 5	4.79	4.58	4.48	4.62	0.16
Sample 6	4.68	4.48	4.41	4.52	0.14
Sample 7	4.65	4.48	4.47	4.53	0.10
Sample 8	5.00	4.78	4.72	4.83	0.15
Sample 9	4.57	4.44	4.43	4.48	0.08
	Week 3, pH				
	Run 1	Run 2	Run 3	Average	STDEVS
Influent	5.19	4.61	4.78	4.86	0.30
Sample 1	4.46	4.30	4.21	4.32	0.13
Sample 2	4.36	4.30	4.21	4.29	0.08
Sample 3	4.50	4.52	4.45	4.49	0.04
Sample 4	4.39	4.33	4.27	4.33	0.06
Sample 5	4.42	4.38	4.34	4.38	0.04
Sample 6	4.42	4.36	4.31	4.36	0.06
Sample 7	4.49	4.51	4.50	4.50	0.01
Sample 8	4.34	4.34	4.31	4.33	0.02
Sample 9	4.48	4.46	4.42	4.45	0.03

A-5   Batch Study Data: Treated Woodchips

	Week 1 - TOC (mg-C/L)				
	Run 1	Run 2	Run 3	Average	STDEVS
Influent	2.086	2.156	1.898	2.047	0.133
Sample 1	6.52	6.434	5.932	6.295	0.318
Sample 2	7.512	9.132	8.7	8.448	0.839
Sample 3	7.752	9.51	7.82	8.361	0.996
Sample 4	11.412	12.35	16.66	13.474	2.799
Sample 5		45.3	34.5	39.9	7.637
Sample 6	49.71	45.99	50.25	48.65	2.319
Sample 7	55.65	66.86	54.12	58.877	6.956
	Week 2 - TOC (mg-C/L)				
	Run 1	Run 2	Run 3	Average	STDEVS
Influent	2.318	1.814	1.666	1.933	0.342
Sample 1	9.95	6.036	11.892	9.293	2.983
Sample 2	9.528	8.992	11.516	10.012	1.33
Sample 3	6.248	6.656	10.246	7.717	2.2
Sample 4	7.922	5.084	13.844	8.95	4.47
Sample 5	5.828	6.62	13.878	8.775	4.437
Sample 6	8.17	9.12	19.852	12.381	6.488
Sample 7	8.33	8.526	18.952	11.936	6.077
Sample 8	9.36	9.136	20.6	13.032	6.555
Sample 9	10.098	10.342	22.64	14.36	7.172
	Week 3 - TOC (mg-C/L)				
	Run 1	Run 2	Run 3	Average	STDEVS
Influent	2.472	1.326	1.304	1.701	0.668
Sample 1	6.916	4.79	4.742	5.483	1.242
Sample 2	4.94	4.034	5.034	4.669	0.552
Sample 3	5.904	3.794	4.094	4.597	1.142
Sample 4	5.656	3.816	4.402	4.625	0.94
Sample 5	5.644	4.248	6.642	5.511	1.203
Sample 6	6.148	5.178	8.316	6.547	1.607
Sample 7	6.544	5.09	6.708	6.114	0.891
Sample 8	5.844	5.504	6.914	6.087	0.736
Sample 9	8.238	5.696	6.692	6.875	1.281

Week 1 – Nitrate (mg-N/L)					
	Run 1	Run 2	Run 3	Average	STDEVS
Influent	2.736	2.785	2.86	2.794	0.062
Sample 1	2.785	2.7	2.639	2.708	0.073
Sample 2	2.532	3.812	2.655	3	0.706
Sample 3	2.868	2.625	2.599	2.697	0.148
Sample 4	2.333	1.807	2.234	2.125	0.28
Sample 5	2.207	2.01	1.906	2.041	0.153
Sample 6	1.216	0.901	0.565	0.894	0.326
Sample 7	0.555	0.349	0.093	0.332	0.232
Week 2 - Nitrate (mg-N/L)					
	Run 1	Run 2	Run 3	Average	STDEVS
Influent	3.008	3.117	3.2	3.108	0.096
Sample 1	2.49	1.52	2.498	2.169	0.562
Sample 2	2.295	2.44	2.172	2.302	0.134
Sample 3	1.2	1.389	0.952	1.18	0.219
Sample 4	0.782	0.941	0.804	0.842	0.086
Sample 5	0.695	1.111	0.67	0.825	0.247
Sample 6	0.23	0.888	0.219	0.446	0.383
Sample 7	0.598	0.695	0.108	0.467	0.315
Sample 8	0.077	0.464	0.094	0.212	0.219
Sample 9	0.208	0.372	0.119	0.233	0.129
Week 3 - Nitrate (mg-N/L)					
	Run 1	Run 2	Run 3	Average	STDEVS
Influent	3.135	3.215		3.175	0.057
Sample 1	2.89	2.589	2.378	2.619	0.257
Sample 2	2.075	2.283	2.289	2.216	0.122
Sample 3	1.833	1.961	1.774	1.856	0.095
Sample 4	1.535	1.961	1.719	1.738	0.213
Sample 5	1.71	1.944	1.699	1.785	0.138
Sample 6	1.34	1.85	1.496	1.562	0.261
Sample 7	1.307	1.858	1.443	1.536	0.287
Sample 8	1.377	1.722	1.449	1.516	0.182
Sample 9	1.477	1.677	1.336	1.497	0.171

Week 1 - TN (mg-N/L)					
	Run 1	Run 2	Run 3	Average	STDEVS
Influent	2.718	2.672	2.686	2.692	0.024
Sample 1	2.974	2.928	2.804	2.902	0.088
Sample 2	2.798	4.042	2.760	3.200	0.729
Sample 3	2.976	2.986	2.658	2.873	0.187
Sample 4	2.598	2.560	2.584	2.581	0.019
Sample 5		3.273	2.302	2.788	0.686
Sample 6	2.277	1.955	1.810	2.014	0.239
Sample 7	2.092	1.928	1.715	1.912	0.189
Week 2 - TN (mg-N/L)					
	Run 1	Run 2	Run 3	Average	STDEVS
Influent	3.144	2.768	2.856	2.922	0.197
Sample 1	2.576	1.225	2.502	2.101	0.76
Sample 2	2.422	2.37	2.404	2.399	0.026
Sample 3	1.433	1.666	1.282	1.46	0.194
Sample 4	1.354	1.002	1.084	1.147	0.184
Sample 5	0.704	1.294	0.964	0.988	0.296
Sample 6	0.663	1.455	1.293	1.137	0.418
Sample 7	0.855	1.292	0.611	0.92	0.345
Sample 8	0.384	0.903	0.614	0.634	0.26
Sample 9	0.571	0.985	0.856	0.804	0.212
Week 3 - TN (mg-N/L)					
	Run 1	Run 2	Run 3	Average	STDEVS
Influent	2.774	2.91	3.01	2.898	0.118
Sample 1	2.556	2.582	2.588	2.575	0.017
Sample 2	2.27	2.474	2.798	2.514	0.266
Sample 3	2.036	2.07	1.855	1.987	0.115
Sample 4	1.685	2.088	2.056	1.943	0.224
Sample 5	1.845	2.068	2.304	2.072	0.229
Sample 6	1.494	2.078	2.372	1.981	0.447
Sample 7	1.613	2.094	2.37	2.026	0.383
Sample 8	1.765	1.767	1.996	1.843	0.133
Sample 9	2.068	1.866	1.924	1.953	0.104

		Sample #	Ammonia (mg-N/L)
Week 1	Run 1	3	0.154
	Run 2	2	0.158
	Run 3	3	0.432
Week 2	Run 1	1	0.167
	Run 2	2	0.123
	Run 3	1	0.1
Week 3	Run 1	1	0.125
	Run 2	1	0.105
	Run 3	2	0.175

		Week 1, pH			
	Run 1	Run 2	Run 3	Average	STDEVS
Influent	5.59	5.18	5.03	5.27	0.29
Sample 1	7.83	7.27	7.06	7.39	0.40
Sample 2	7.79	8.08	8.08	7.98	0.17
Sample 3	7.74	7.30	7.35	7.46	0.24
Sample 4	7.82	7.44	7.40	7.55	0.23
Sample 5	7.61	7.35	7.24	7.40	0.19
Sample 6	7.44	7.12	7.12	7.23	0.18
Sample 7	7.47	7.20	7.13	7.27	0.18
		Week 2, pH			
	Run 1	Run 2	Run 3	Average	STDEVS
Influent	5.67	4.55	4.64	4.95	0.62
Sample 1	5.89	5.80	5.81	5.83	0.05
Sample 2	5.90	5.75	5.70	5.78	0.10
Sample 3	5.78	5.69	5.61	5.69	0.09
Sample 4	5.84	5.68	5.70	5.74	0.09
Sample 5	5.83	5.66	5.68	5.72	0.09
Sample 6	5.81	5.63	5.64	5.69	0.10
Sample 7	5.91	5.77	5.71	5.80	0.10
Sample 8	5.70	5.57	5.54	5.60	0.09
Sample 9	5.59	5.56	5.60	5.58	0.02
		Week 3, pH			
	Run 1	Run 2	Run 3	Average	STDEVS
Influent	5.26	5.17	4.92	5.12	0.18
Sample 1	5.61	5.50	5.57	5.56	0.06
Sample 2	5.46	5.27	5.33	5.35	0.10
Sample 3	5.41	5.24	5.23	5.29	0.10
Sample 4	5.42	5.25	5.21	5.29	0.11
Sample 5	5.42	5.25	5.23	5.30	0.10
Sample 6	5.73	5.42	5.31	5.49	0.22
Sample 7	5.42	5.41	5.59	5.47	0.10
Sample 8	5.43	5.29	5.27	5.33	0.09
Sample 9	5.38	5.34	5.53	5.42	0.10

A-6 Experimental and Predicted Nitrate Concentration in Week 2 and 3 Batches to Quantify SSE

Control, Week 2			Control, Week 3		
k=6.40E-04			k=1.2E-03		
Time	Nitrate	Fitted	Time	Nitrate	Fitted
0	3.13	3	0	3.0594	3
75	3.147	2.859	150	2.5916	2.506
270	3.178	2.524	345	2.0717	1.983
1290	1.597	1.314	1290	0.5767	0.638
1530	1.224	1.127	1515	0.4404	0.487
1710	0.824	1.004	1710	0.3401	0.385
2730	0.168	0.523	2730	0.1509	0.113
3090	0.189	0.415	3120	0.116	0.071
4140	0.234	0.212	4200	0.124	0.019
4380	0.314	0.182	4560	0.2074	0.013
Treated, Week 2			Treated, Week 3		
7.60E-04			2.30E-04		
Time	Nitrate	Fitted	Time	Nitrate	Fitted
0	3.108	3	0	3.175	3
150	2.169	2.677	135	2.619	2.908
345	2.302	2.308	315	2.216	2.79
1290	1.18	1.125	1350	1.856	2.199
1515	0.842	0.949	1560	1.738	2.096
1710	0.825	0.818	1770	1.785	1.997
2730	0.446	0.377	2805	1.562	1.574
3120	0.467	0.28	3210	1.536	1.434
4200	0.212	0.123	4245	1.516	1.13
4560	0.233	0.094	4665	1.497	1.026

where time (minutes); nitrate (mg-N/L); k (min^{-1})

A-7   SEM Imaging of Control and Treated Woodchips Prior to Three-Week Batch Study
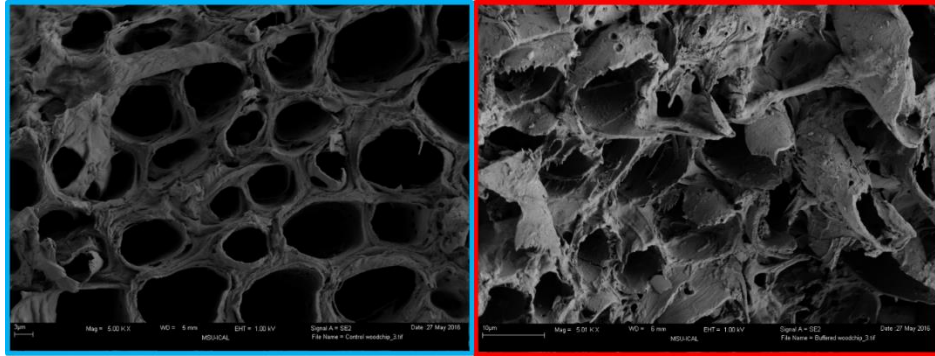
Magnification is 5,000X. Scale is 3µm for the control media (left) and 10µm for the treated media (right).

A-8   SEM Imaging of Control and Treated Woodchips After Three-Week Batch Study
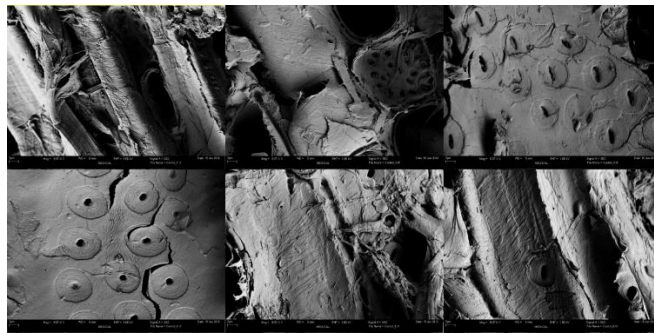
Magnification: 8,000X
Scale: 2µm
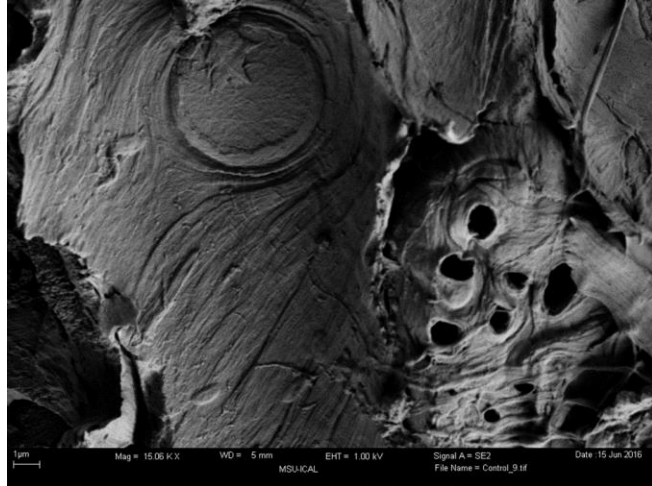
Magnification: 15,000X
Scale: 1µm
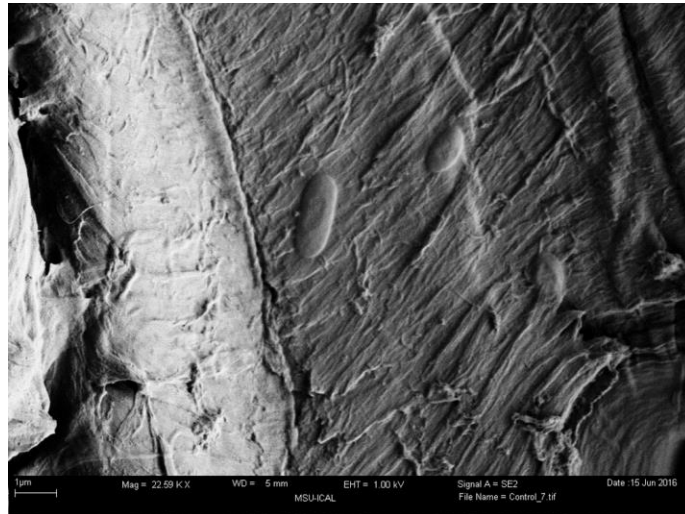
Magnification: 22,000X
Scale: 1µm

Magnification: 23,000X
Scale: 1µm
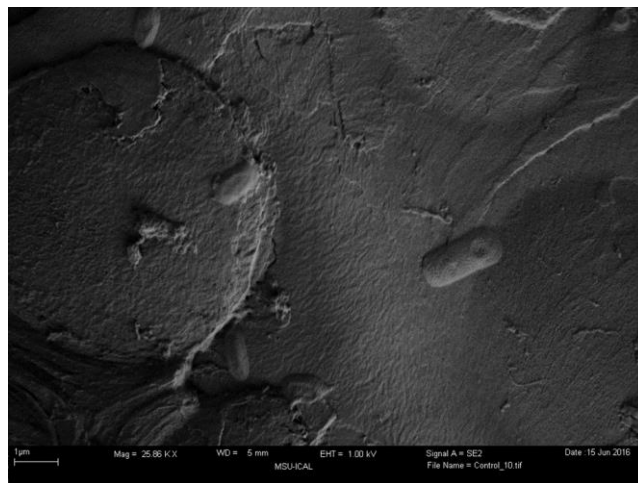
Magnification: 26,000X
Scale: 1µm
Treated Woodchips:
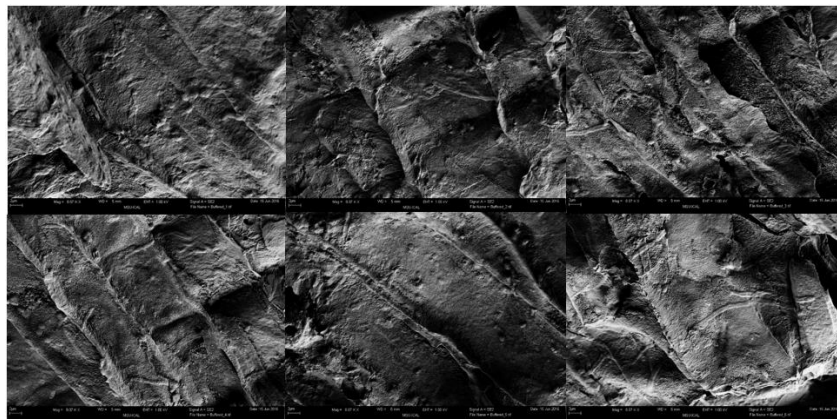
Magnification: 8,000X
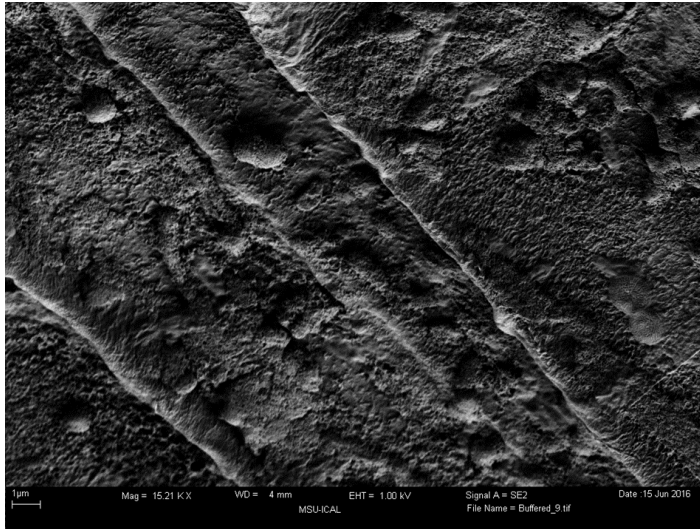
Scale: 2µm

Magnification: 15,000X
Scale: 1µm
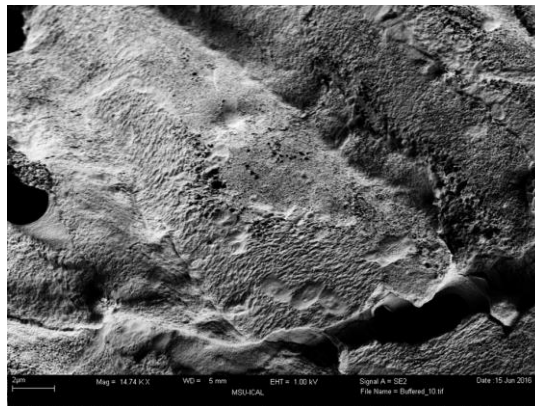
Magnification: 15,000X
Scale: 2µm
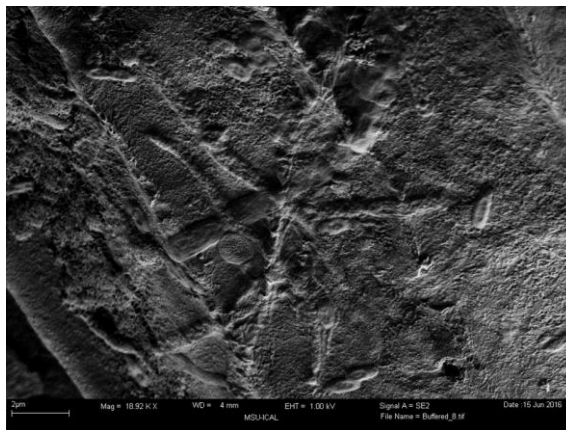
Magnification: 18,000X

Scale: 2μm
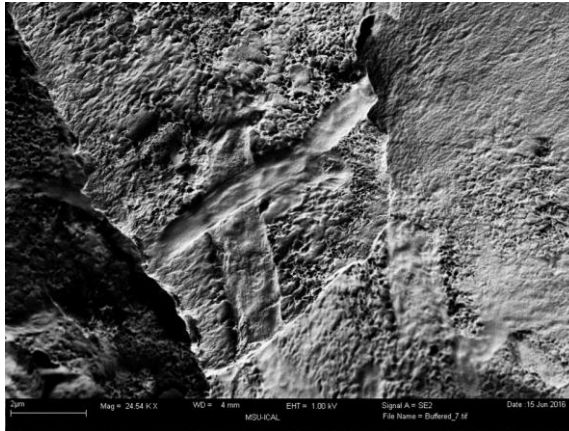
Magnification: 24,000X
Scale: 2μm

A-9   pH Inhibition of Denitrification in Batch Study (Prior to 1N H$_2$SO$_4$ Buffer) for Treated Woodchips

Sample ID		pH	Nitrate (mg-N/L)
Run 1	Influent	5.54	3.056
	Sample 1	8.64	3.028
	Sample 2	9.86	3.061
	Sample 3	9.61	3.398
	Sample 4	9.54	2.852
	Sample 5	9.38	2.940
	Sample 6	9.40	3.415
	Sample 7	9.21	3.028
	Sample 8	9.17	2.927
Run 2	Influent	5.40	2.918
	Sample 1	9.13	
	Sample 2	9.79	3.022
	Sample 3	9.45	2.957
	Sample 4	9.40	2.759
	Sample 5	9.12	2.776
	Sample 6	9.22	2.888
	Sample 7	9.16	2.861
	Sample 8	9.02	2.872

A-10 Tracer Test Data for 3 Specified HRTs to Evaluate Advection-Dispersive Properties of the 45-cm IWSZ System

Figure comparing F-Curves based on normalized EC Measurements is shown below raw data.

HRT (hrs.)	Synthetic Stormwater (µS/cm)	NaCl Spiked (µS/cm)
0.52	136	308
0.91	151	302
1.82	102	243
Average	130	284

HRT=0.52 hr.			HRT=0.91 hr.			HRT=1.82 hr.		
Time (min)	EC (µS/cm)	Normalized	Time (min)	EC (µS/cm)	Normalized	Time (min)	EC (µS/cm)	Normalized
0	136	0	0	151	0.05	0	102	0
10.5	136	0	10	153	0.063	10	103	0.007
20.5	149	0.076	20	152	0.057	32	101	-0.007
30.5	193	0.331	40	147	0.025	48.5	98	-0.028
35.5	220	0.488	50	148	0.031	58	94	-0.057
38.5	231	0.552	60	166	0.145	65.5	92	-0.071
40.5	239	0.599	70	194	0.321	71.5	89	-0.092
45.5	254	0.686	80	216	0.459	79.5	86	-0.113
50.5	266	0.756	90	244	0.635	87.5	87	-0.106
55.5	278	0.826	100	261	0.742	95.5	88	-0.099
60.6	285	0.866	105	264	0.761	103.5	96	-0.043
65.6	293	0.913	110	272	0.811	111.5	101	-0.007
80.6	289	0.89	115	276	0.836	117.5	110	0.057
85.5	297	0.936	120	281	0.868	124	121	0.135
90.5	297	0.936	125	283	0.881	131.5	128	0.184
95.5	301	0.959	130	284	0.887	137.5	133	0.22
100.5	303	0.971	135	288	0.912	145.5	142	0.284
106.5	300	0.953	140	291	0.931	157.5	150	0.34
110.5	303	0.971	145	293	0.943	165.5	162	0.426
116	301	0.959	150	294	0.95	175.5	177	0.532
120.5	294	0.919	155	294	0.95	185.5	178	0.539
125.5	303	0.971	160	296	0.962	195.5	181	0.56
135.5	308	1	165	298	0.975	205.5	184	0.582
145.5	300	0.96	170	300	0.987	215.5	193	0.645
155.5	247	0.692	180	300	0.987	225.5	195	0.66
160.5	214	0.525	190	301	0.994	235.5	200	0.695
165.5	187	0.389	200	302	1	245.5	206	0.738
170.5	169	0.298	210	301	0.994	255.5	211	0.773
175.5	152	0.212	220	301	0.994	267.5	214	0.794
180.5	143	0.167	230	300	0.987	273.5	216	0.809
195.5	142	0.162	240	293	0.943	283.5	219	0.83
200.5	132	0.111	250	265	0.767	293.5	221	0.844
204.5	125	0.076	260	226	0.522	303.5	223	0.858
209.5	121	0.056	265	215	0.453	311.5	228	0.894
214.5	118	0.04	270	202	0.371	321.5	228	0.894
225.5	116	0.03	275	188	0.283	331.5	230	0.908
235.5	113	0.015	280	183	0.252	341.5	234	0.936
245.5	111	0.005	285	174	0.195	351.5	233	0.929
255.5	110	0	290	169	0.164	359.5	239	0.972
			300	161	0.113	367.5	238	0.965
			310	157	0.088	375.5	243	1
			320	154	0.069	385.5	243	1
			330	152	0.057	395.5	240	0.984
			340	150	0.044	405.5	238	0.973
			350	147	0.025	415.5	242	0.995
			360	147	0.025	425.5	238	0.973
			370	144	0.006	435.5	239	0.979
			380	146	0.019	445.5	235	0.957
			390	145	0.013	455.5	230	0.931
						465.5	221	0.883
						475.5	203	0.787
						485.5	193	0.734
						495.5	169	0.606
						505.5	168	0.601
						515.5	146	0.484
						525.5	126	0.378
						535.5	117	0.33
						545.5	106	0.271
						555.5	96	0.218
						565.5	84	0.154
						575.5	81	0.138
						585.5	74	0.101
						595.5	73	0.096
						605.5	68	0.069
						615.5	70	0.08
						625.5	67	0.064
						635.5	64	0.048
						645.5	59	0.021
						655.5	56	0.005
						665.5	55	0
						675.5	55	0

A-11 *Low-Flow Events:* Steady-State Nitrate Effluent Experiments

	4-HRT	6-HRT	8-HRT
Influent N	2.957	3.005	2.887
Average Effluent N	2.59	2.142	1.968
Standard Deviation	0.061	0.155	0.134
Upper N	2.652	2.297	2.102
Lower N	2.529	1.988	1.834

4-HRT		6-HRT		8-HRT	
Time	Nitrate	Time	Nitrate	Time	Nitrate
(min)	(mg-N/L)	(min)	(mg-N/L)	(min)	(mg-N/L)
1	0.152	7	0.088	12	0.083
930	2.529	170	0.025	105	0.104
1035	2.568	1215	2.192	315	0.077
1155	2.529	1335	2.066	1380	1.817
1350	2.576	1515	1.902	1800	1.82
2370	2.721	1620	1.966	2760	1.952
2490	2.674	2655	2.189	2970	2.151
2670	2.582	2925	2.05	3210	1.997
2760	2.618	3060	2.289	4230	2.073
3840	2.526	4095	2.353		
4035	2.598	4215	2.275		
4200	2.571				

4-HRT			6-HRT			8-HRT		
Time (min)	pH	ORP (mV)	Time (min)	pH	ORP (mV)	Time (min)	pH	ORP (mV)
0	4.83	-355	0	3.99	-339.4	0	3.52	-352.5
0	4.93	-355	7	4.52	-340.4	12	3.82	-353.7
1	5.22	-357.1	170	4.98	-171.3	105	4.94	-354.2
930	4.78	228.5	1215	4.9	257.8	315	4.94	161.1
1035	5.07	231.8	1335	5.19	259.4	1380	4.88	139.6
1155	4.93	230.8	1515	5.02	261.6	1620	4.98	127.4
1350	4.85	233.3	1620	5.03	259.3	1800	5.02	119.1
2370	4.83	229.1	2655	5.12	248.1	2760	5.01	120.1
2490	5.14	230.3	2925	5.28	236	2970	4.94	120.4
2670	5.17	230.3	3060	4.93	235.3	3210	4.98	113.3
2760	5.04	230	4095	5.41	216.9	4230	5.06	80.9
3840	4.82	240.2	4215	5.22	217.7			
4035	4.97	239.6						
4200	5.09	243.4						

A-12 Spiked Salt Toxicity – *Low Flow 8.0 Hour HRT*

Sample ID	Elapsed Time (min)	Nitrate (mg-N/L)
Influent 1	0	1.785
Effuent 1	12	0.086
Effluent 2	1157	1.801
Influent 2	1345	1.761
Effluent 3	1412	1.669
Effluent 4	1562	1.798
Effluent 5	2612	1.868
Effluent 6	2777	1.903
Influent 3	2965	1.758
Effluent 7	2972	1.917
Effluent 8	4007	1.876
Effluent 9	4182	1.914

A-13 Baseline Storms: Modeled Nitrate Washout Behavior and Experimental/Statistical Results

**Selected statistical analysis to compare with CMFR non-steady state washout curves

Q = 11 mL/min				
Run #1				
t (min)	Experiment	Theoretical	Error	Error^2
0	0.169	0	-0.1691	0.029
72	0.604	1.3996	0.7952	0.632
144	1.867	2.0679	0.2005	0.04
216	2.472	2.387	-0.0853	0.007
288	2.662	2.5393	-0.1228	0.015
401	2.358	2.6349	0.2765	0.076
Q = 11 mL/min				
Run #2**				
t (min)	Experiment	Theoretical	Error	Error^2
0	0.119	0	-0.1187	0.014
72	0.11	1.3996	1.2892	1.662
144	0.799	2.0679	1.2693	1.611
216	1.894	2.387	0.4934	0.243
288	2.448	2.5393	0.0913	0.008
360	2.559	2.6121	0.0526	0.003

t (min)	Experiment	Theoretical	Error	Error^2
Q = 22 mL/min				
Run #1				
0	0.058	0	-0.0576	0.003
72	0.844	2.1317	1.2875	1.658
144	2.363	2.6578	0.295	0.087
216	2.477	2.7876	0.311	0.097
288	2.425	2.8197	0.395	0.156
360	2.43	2.8276	0.398	0.158
Q = 22 mL/min				
Run #2				
0	0.132	-0.1318	0.017	0.132
72	0.523	1.6091	2.589	0.523
144	2.286	0.3716	0.138	2.286
216	2.44	0.3481	0.121	2.44
288	2.482	0.3381	0.114	2.482
360	2.42	0.4079	0.166	2.42
Q = 22 mL/min				
Run #3**				
0	0.2341	-0.2341	0.055	0.2341
72	0.6695	1.4622	2.138	0.6695
144	2.2284	0.4294	0.184	2.2284
216	2.3525	0.4352	0.189	2.3525
288	2.629	0.1907	0.036	2.629
360	2.6181	0.2095	0.044	2.6181
Q = 22 mL/min				
Run #4				
0	0.099	-0.0991	0.01	0.099
72	0.502	1.6299	2.656	0.502
144	2	0.658	0.433	2
216	2.479	0.3089	0.095	2.479
288	2.468	0.3518	0.124	2.468
360	2.509	0.3183	0.101	2.509

Q = 38.5 mL/min				
Run #1				
t (min)	Experiment	Theoretical	Error	Error^2
0	0.069	0	-0.0686	0.005
72	2.903	2.6346	-0.2689	0.072
144	2.701	2.8762	0.175	0.031
216	2.665	2.8983	0.233	0.054
288	2.576	2.9003	0.3247	0.105
360	2.527	2.9005	0.3735	0.14
Q = 38.5 mL/min				
Run #2**				
t (min)	Experiment	Theoretical	Error	Error^2
0	0.061	-0.0609	0.004	0.061
72	2.765	-0.1306	0.017	2.765
144	2.791	0.0854	0.007	2.791
216	2.811	0.087	0.008	2.811
288	2.955	-0.0543	0.003	2.955
360	2.637	0.2634	0.069	2.637
Q = 38.5 mL/min				
Run #3				
t (min)	Experiment	Theoretical	Error	Error^2
0	0.0435	-0.044	0.002	0.0435
72	2.3388	0.296	0.087	2.3388
144	2.7513	0.125	0.016	2.7513
216	2.7672	0.131	0.017	2.7672
288	2.737	0.163	0.027	2.737
360	2.6853	0.215	0.046	2.6853

A-14 Compiled Maryland-Type Storm Simulated Results

1. Scenario: Complete Storm Capture

Depth (in)	0.175
Rainfall Duration (hrs.)	0.5
Runoff Application (hrs.)	1

Influent				
	Avg. Time	Run 1 Nitrate	Run 2 Nitrate	Q
	(min)	(mg-N/L)	(mg-N/L)	(mL/min)
Increment 1	6	5.287	5.799	7
Increment 2	18	3.679	3.81	14
Increment 3	30	2.604	2.642	20.9
Increment 4	42	1.89	1.933	14
Increment 5	54	1.403	1.58	7

Run 1 Effluent				
Sample ID	Avg. Time	Nitrate	TN	Nitrite
	(min)	(mg-N/L)	(mg-N/L)	(mg-N/L)
Effluent #1	15	0	0.769	0
Effluent #2	22	0	0.6213	0
Effluent #3	29	0	1.336	0
Effluent #4	36	0	0.499	0
Effluent #5	42.5	0		

Run 2 Effluent				
Sample ID	Avg. Time	Nitrate	TN	Nitrite
	(min)	(mg-N/L)	(mg-N/L)	(mg-N/L)
Effluent #1	20	0	0.9885	0
Effluent #2	24	0	1.245	0
Effluent #3	32.5	0	0.9564	0
Effluent #4	41	0	0.8747	0
Effluent #5	52	0		0

2. Scenario: Nitrate Washout

Rainfall Depth (in.)	0.375
Rainfall Duration (hrs.)	0.5
Runoff Application (hrs.)	1

Influent				
	Avg. Time	Run 1 Nitrate	Run 2 Nitrate	Q
	(min)	(mg-N/L)	(mg-N/L)	(mL/min)
Increment 1	6	7.172	5.722	15
Increment 2	18	2.744	3.821	29.9
Increment 3	30	2.476	2.567	44.9
Increment 4	42	2.682	1.986	29.9
Increment 5	54	2.076	1.472	15

Run 1 Effluent					
Sample ID	Avg. Time	Nitrate	TN	Nitrite	Ammonia
	(min)	(mg-N/L)	(mg-N/L)	(mg-N/L)	(mg-N/L)
Effluent #1	28	0.098	1.259	0	0.086
Effluent #2	34	0.105	0.3215	0	
Effluent #3	40.5	0.057	0.3813	0	
Effluent #4	46	0.171	0.4801	0	
Effluent #5	53.5	0.362	1.481	0	
Effluent #6	60.5	0.586	1.046	0	

Run 2 Effluent					
Sample ID	Avg. Time	Nitrate	TN	Nitrite	Ammonia
	(min)	(mg-N/L)	(mg-N/L)	(mg-N/L)	(mg-N/L)
Effluent #1	26	0.12	0.688		
Effluent #2	32.5	0.092	0.743	0	
Effluent #3	40	0.096	0.704		0.191
Effluent #4	46.5	0.161	0.663	0	
Effluent #5	54	0.349	0.846	0	
Effluent #6	59.5	0.598	1.206	0	

Rainfall Depth (in)	0.375
Rainfall Duration (hrs.)	1.25
Runoff Application (hrs.)	2.5

	Influent			
	Avg. Time	Run 1 Nitrate	Run 2 Nitrate	Q
	(min)	(mg-N/L)	(mg-N/L)	(mL/min)
Increment 1	15	5.342	7.268	6
Increment 2	45	3.592	4.462	12
Increment 3	75	2.545	3.162	18
Increment 4	105	1.977	2.279	12
Increment 5	135	1.451	1.785	6

Run 1 Effluent				
Sample ID	Avg. Time	Nitrate	TN	Nitrite
	(min)	(mg-N/L)	(mg-N/L)	(mg-N/L)
Effluent #1	10	0.118	0.6175	0
Effluent #2	36	0.085	0.6415	0
Effluent #3	70	0.092	0.6161	0
Effluent #4	82	0.096	0.8203	
Effluent #5	137	0.089	0.3453	0
Effluent #6	145	0.122	0.4408	0

Run 2 Effluent				
Sample ID	Avg. Time	Nitrate	TN	Nitrite
	(min)	(mg-N/L)	(mg-N/L)	(mg-N/L)
Effluent #1	47	0.14	2.836	0
Effluent #2	61	0.138	4.355	0
Effluent #3	75	0.156	4.081	0
Effluent #4	103	0.127	3.744	0
Effluent #5	129	0.191	3.283	0
Effluent #6	148	0.245	3.137	0.003

Rainfall Depth (in)	0.75
Rainfall Duration (hrs.)	1.75
Runoff Duration (hrs.)	3.5

Influent				
	Avg. Time	Run 1 Nitrate	Run 2 Nitrate	Q
	(min)	(mg-N/L)	(mg-N/L)	(mL/min)
Increment 1	21	5.775	6.122	8.5
Increment 2	63	4.021	4.219	17.1
Increment 3	105	2.811	2.829	25.6
Increment 4	147	2.096	2.193	17.1
Increment 5	189	1.652	1.728	8.5

Run 1 Effluent				
Sample ID	Avg. Time	Nitrate	TN	Nitrite
	(min)	(mg-N/L)	(mg-N/L)	(mg-N/L)
Effluent #1	5	0	0.2393	0
Effluent #2	67	0.134	0.6436	0
Effluent #3	87	0.372	0.9328	
Effluent #4	114.5	2.257	2.07	0
Effluent #5	133	2.998	3.364	0
Effluent #6	152	3.035	3.628	0
Effluent #7	174	3.046	3.196	0
Effluent #8	208	2.966	2.797	0
Run 2 Effluent				
Sample ID	Avg. Time	Nitrate	TN	Nitrite
	(min)	(mg-N/L)	(mg-N/L)	(mg-N/L)
Effluent #1	3	0.1356	0.9319	0
Effluent #2	51	0.1356	0.4684	0
Effluent #3	78	0.1612	0.5543	0
Effluent #4	84.5	0.1697	0.3483	
Effluent #5	119.5	2.3065	2.36	0.005
Effluent #6	147	3.1209	3.126	0
Effluent #7	174	3.1606	3.334	0
Effluent #8	203	3.1152	2.895	0

Rainfall Depth (in)	0.75
Rainfall Duration (hrs.)	2.75
Runoff Application (hrs.)	5.5

Run 1 Effluent				
Sample ID	Avg. Time (min)	Nitrate (mg-N/L)	TN (mg-N/L)	Nitrite (mg-N/L)
Effluent #1	9	0.147	0.2789	0
Effluent #2	86	0.119	0.8523	0
Effluent #3	121	0.181	0.282	0
Effluent #4	134	0.161	0.3329	0
Effluent #5	175	1.787	2.138	0.005
Effluent #6	249	2.729	2.92	0
Effluent #7	296	2.763	3.281	0
Effluent #8	323	2.84	3.457	0
Run 2 Effluent				
Sample ID	Avg. Time (min)	Nitrate (mg-N/L)	TN (mg-N/L)	Nitrite (mg-N/L)
Effluent #1	5	0.1243	0.243	0
Effluent #2	69.5	0.1442	0.514	0
Effluent #3	112.5	0.2123	0.5196	0
Effluent #4	131	0.164	0.3547	0
Effluent #5	183	2.0426	2.043	0
Effluent #6	232	2.8854	2.937	0
Effluent #7	281	3.0585	3.974	
Effluent #8	324	2.8854	2.925	0

A-15 Effect of Macroscale Conditions

Deoxygenated Trial 1			
Time (min)	Internal ORP (mV)	Influent DO (ppm)	Nitrate (mg-N/L)
0	-373.8	2.79	2.85
0	-373.8	2.43	2.821
1	-373.9	0.75	0
19	62.1		
21	85.7	1.53	0
24	109.5		
34	149.1		
36	155.2		
41	164.9	1.52	0.081
62	194.4	1.89	0.515
85	210.1	2.31	1.297
105	225.4	1.66	1.747
125	237.5	1.83	2.088
145	247.1	1.79	2.259
165	254.7	1.77	2.389
185	261.7	1.75	2.514
205	269.2	1.56	2.54
225	279	1.59	2.603
245	287.4	1.67	2.561
267	294.5	2.32	2.587
297	305.2	4.54	2.603
317	313	3.52	2.637
338	322	3.4	2.72
357	327.2	3.01	2.668

Deoxygenated Trial 2			
Time (min)	Internal ORP (mV)	Influent DO (ppm)	Nitrate (mg-N/L)
0	-367	4.33	2.962
0		3.54	2.941
2	-368.3	1	0
9	-369.1		
14	-321.9		
15	-256.9		
17	-73.9	1.37	0
24	100.3		
26	112.7		
42	160.3		
48	167	1.48	0
69	181.8	1.07	0.713
134	204.2	1.16	2.213
185	212.6	1.92	2.507
280	223.2	1.7	2.645
347	232.5	1.62	2.706

Deoxygenated and Reduced Trial 1				
Time (min)	Internal ORP (mV)	Influent ORP (mV)	Influent DO (ppm)	Nitrate (mg-N/L)
0	-394.6	86.5	0.62	3.034
0	-394.6	86.5	0.62	2.997
1	-394.4	89.7	0.6	0.097
15	-135	99	0.59	0.086
37	99.6	105	0.66	0.12
50	69.7	113.5	0.91	0.711
82	71.5	116.9	0.71	1.196
102	69.9	121.7	0.66	1.443
120	69.3	121.9	0.64	1.708
140	68.7	122.4	0.69	1.955
160	67.7	125.3	0.7	2.144
180	66.7	124.2	0.72	2.228
200	65.9	125.2	0.74	2.37
220	65.2	127.4	0.68	2.349
240	64.3	120.3	0.64	2.293

Deoxygenated and Reduced Trial 2				
Time (min)	Internal ORP (mV)	Influent ORP (mV)	Influent DO (ppm)	Nitrate (mg-N/L)
0	-392.3	116.4	0.64	3.058
0	-392.3	116.4	0.64	3.076
2	-392.6	120	0.7	0.074
15	-341.7			
17	-287.5			
20	-237.5			
22	-208.2			
25	-188.1			
30	-126.6	141.3	0.33	0.097
55	-18.7	126.8	0.35	0.245
84	6.4	154.2	0.33	1.311
116	13.6	137.4	0.33	2.012
160	21	146.2	0.43	2.379
190	21.7	151.5	0.49	2.518
216	26.2	153.9	0.51	2.585
240	28.8	155.7	0.52	2.661

Deoxygenated and Reduced Trial 3				
Time (min)	Internal ORP (mV)	Influent ORP (mV)	Influent DO (ppm)	Nitrate (mg-N/L)
0	-397.4	93.6	0.11	2.947
0	-397.4	93.6	0.11	2.973
2	-400	92.1	0.1	0.094
18	-181.5			
20	-147.6			
24	-66.8			
26	-53.3			
32	-10			
33	-7.9	130.4	0.21	0.089
35	6.6			
62	54.7	146.1	0.08	0.255
94	69.1	150	0.3	1.522
122	79.8	152.7	0.29	2.063
160	75.1	151.4	0.24	2.445
192	84.5	155.1	0.32	2.621
233	85.9	156.7	0.04	2.661
300	84.1	144.7	0.21	2.726
360	89	171.7	0.52	2.746

28

Appendix II

Governing Mass Balance Equation:

$$\frac{dM}{dt} = V\frac{dC}{dt} + C\frac{dV}{dt} = Q_0C_0 - QC \pm rV$$

where   V is the system volume

C is the effluent concentration

t is time

Q_0 is the influent flowrate

Q is the effluent flowrate

r is the reaction rate that can either consume or generate C

Scenario 1: Sequencing batch reactor system, so that $Q_0 = 0$ mL/min and $Q = 1.2$ mL/min by a constricted effluent valve

This simplifies to the mass balance equation to

$$V\frac{dC}{dt} = -rV$$

$$\frac{dC}{dt} = -r$$

When r is a zero-order equation, r =-k

When r is a first-order equation, r=-kC

$$\frac{dC}{dt} = -k$$

$$\frac{dC}{dt} = -kC$$

Including the boundary conditions of the integration,

$$\int_{C_0}^{C} dC = -k\int_{0}^{t} dt$$

$$\int_{C_0}^{C} \frac{dC}{kC} = -\int_{0}^{t} dt$$

Integrating and solving to C yields, for zero-order and first-order, respectively:

$$C = C_0 - kt$$

$$C = C_o \exp(-kt)$$

Scenario 2: Batch reactor with a constant volume and the denitrification rate constant

was assumed first-order

$$\frac{dM}{dt} = V\frac{dC}{dt} + C\frac{dV}{dt} = Q_0 C_0 - QC \pm rV$$

where $Q_0 = 0$ mL/min

$Q = 0$ mL/min

$r = -kC$

Including the boundary conditions for integration and solving for C

$$= C_o \exp(-kt)$$

Scenario 3: First-Order Reaction Rate Equation for a Plug Flow Reactor at Steady State (Column 2 Configuration)

The concentration, C, is a function of distance along the flow path, x, and time, t:
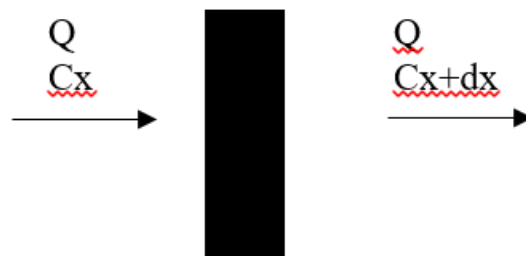
Taking the mass balance on differential axial element with uniform concentration where

dV = differential volume

A = cross sectional area

dx = differential distance

$$dV = Adx$$

$$\frac{dM}{dt} = QCx - (QCx + dx) + dVr_C - dV\frac{\partial Cx}{\partial t}$$

where $dV_{r_C} = Adxr_C$

$$dV\frac{\partial Cx}{\partial t} = Adx\frac{\partial Cx}{\partial t}$$

$$QCx - QCx + dx + dVr_C = dV\frac{\partial Cx}{\partial t}$$

$$Cx + dx = Cx + dCx$$

$$Q(Cx - Cx - dCx) + dVr_C = dV\frac{\partial Cx}{\partial t}$$

Let $\partial\tau = \partial(V/Q)$ where both V and Q are constant

Setting $\frac{\partial Cx}{\partial\tau} = 0$ at steady state conditions

$$\frac{dCx}{d\tau} = r_C$$

Since r is a first-order degradation reaction

$$\frac{dCx}{d\tau} = -kc$$

Applying boundary conditions

$$\int_{C_0}^{C}\frac{dC}{d\tau} = \int_{0}^{\tau}-kd\tau$$

Integration yields

$$C = C_0\exp(-k\tau)$$

Scenario 4: Mass Balance for a Non-Steady State CMFR To Model Nitrate Washout Behavior

Since the system volume is constant and the degradation rate constant is first-order

This simplifies to:

$$V\frac{dC}{dt} = QC_{IN} - QC - kCV$$

$$\frac{dC}{dt} = \frac{QC_{IN}}{V} - \frac{QC}{V} - kC$$

Let $\tau = V/Q$

$$\frac{dC}{dt} = \frac{C_{IN}}{\tau} - \frac{C}{\tau} - kC$$

Separating variables:

- Integrating from C_0 to C, where C_0 is the concentration of nitrate at time 0 and C is the concentration of nitrate at time t
- Integrating from 0 to time t

$$\int_{C_0}^{C} \frac{dC}{\frac{C_{IN}}{\tau} - C\left(\frac{1}{\tau} + k\right)} = \int_0^t dt$$

$$-\frac{1}{\frac{1}{\tau} + k} \ln\left[\frac{\frac{C_{IN}}{\tau} - C\left(\frac{1}{\tau} + k\right)}{\frac{C_{IN}}{\tau} - C_0\left(\frac{1}{\tau} + k\right)}\right] = t$$

Solving for C yields:

$$C = \frac{\frac{C_{IN}}{\tau} - \left[\frac{C_{IN}}{\tau} - C_0\left(\frac{1}{\tau} + k\right)\right]\exp\left[-\frac{t}{\tau} - kt\right]}{\frac{1}{\tau} + k}$$

Appendix III

Translation of Kreeb (2003) Data for Laboratory-Simulated Design Storms

Rainfall Duration	Rainfall Depth (cm)					
	0.0254-0.254	0.255-0.635	0.636-1.27	1.28-2.54	> 2.54	*Sum*
0-2 hr	0.2857	0.0214	0.0167	0.0043	0.0008	0.3289
2-3 hr	0.0164	0.0257	0.0221	0.0089	0.0025	0.0756
3-4 hr	0.0085	0.0223	0.0198	0.0083	0.0038	0.0627
4-7 hr	0.0099	0.0351	0.0475	0.0221	0.0087	0.1233
7-13 hr	0.0058	0.0337	0.0629	0.0528	0.0266	0.1818
13-24 hr	0.0024	0.007	0.0397	0.0611	0.0515	0.1617
>24 hr	0	0.0009	0.0043	0.0172	0.0435	0.0659
Sum	0.3287	0.1461	0.213	0.1747	0.1374	1

Source: Kreeb (2003)

Assumptions:

4. Flowrates were calculated from the Rational Method (McCuen 2005), as defined by

$$Q = CiA$$

The resultant flow pattern follows a triangular hydrograph as to determine runoff volumes.

5. The runoff coefficient, C, is 0.9. This assumes that the catchment area is highly urbanized/impervious (McCuen 2005).

6. The cross-sectional area, i.e., bioretention footprint, represents 5% of the total catchment area (Department of Environmental Resources, P.G. County 2007). It is calculated as follows:

$$A_{bioretention} = \frac{\pi}{4} * 10^2 = 78.54 \ cm^2 = 1.94 \ x \ 10^{-6} ac$$

$$A_{catchment} = 3.88 \ x \ 10^{-5} \ ac$$

7. The intensity, *i*, is defined by the rainfall depth (in.) over the entire storm duration (hours).

a. To determine corresponding intensity when depth is defined as greater
   than 2.54 cm or 1-inch as 3.0 inches

   i. Maryland, on average, receives 40 inches of rainfall per year (US
      Climate Data 2016)

   ii. Maryland, on average, accumulates this total rainfall depth over
       the course of 60 rainfall events

   iii. The depth of all storms is represented as the midpoint of the
        interval range as provided.

   The table is simplified as follows:

Depth (in.)	ΣP(Depth)	Number of Storms	Total Depth (in.)
0.055	0.3287	20	1.08471
0.175	0.1461	9	1.53405
0.375	0.213	13	4.7925
0.75	0.1747	10	7.8615
Unknown	0.1374	8	24.7272
	Sum	60	40
	Unknown Depth (in.)		2.999

8. Following the rational method, the runoff volume, V, is defined as

$$V = depth * A * C$$

where V is in units of ft^3

As with any hydrograph, the area under the hydrograph equals the volume of
runoff.

For each specified depth, a total runoff volume was calculated

Depth (in.)	Runoff Volume (ft^3)
0.055	6.975E-03
0.175	2.219E-02
0.375	4.755E-02
0.750	9.511E-02
3.0	3.792E-01

9. Modified Rational Method assumes that the runoff begins at the start of the storm and increases linearly to the peak value, which occurs at the time of concentration (T_c). Upon which, the runoff rate decreases linearly to zero (Iowa SUDAS 2013). It is assumed that the rainfall duration is equal to T_c so that the hydrograph is symmetrical about the T_c axis and follows a triangular hydrograph. Figure is adopted from Iowa SUDAS (2013).
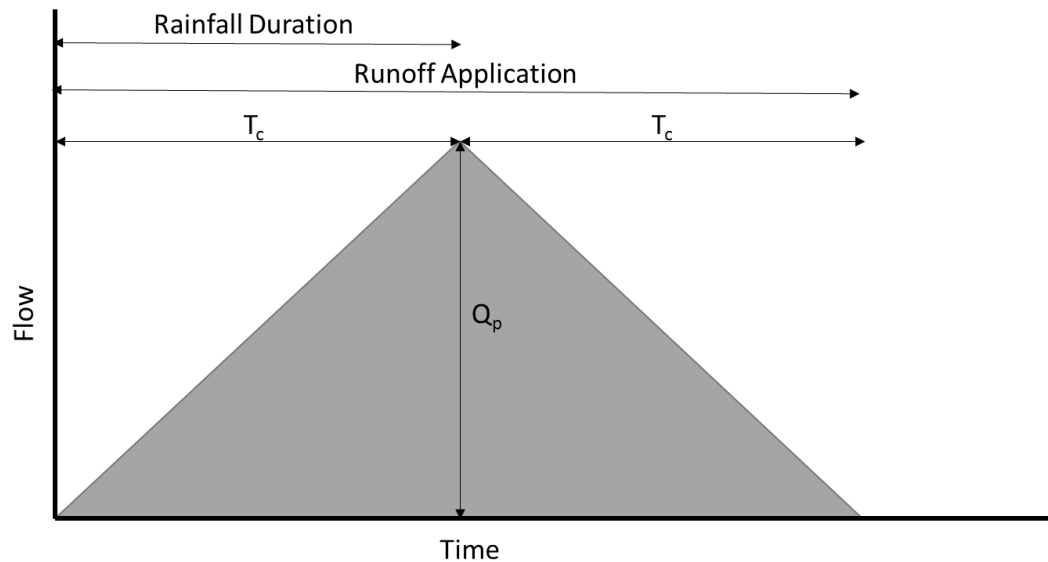
10. Separating the triangular hydrograph into 5 discrete intervals with equal durations, each storm, as defined by depth and runoff duration is compiled with its respective influent flowrates, Q. Q is in units of mL/min.

$$Q_p = \frac{V}{Rainfall\ Duration}$$

Q_p corresponds to the maximum flowrate at *Increment 3.*

Increment 1 and 5: $1/3 * Q_p$

Increment 2 and 4: $2/3 * Q_p$

Runoff Application (hrs.)	Increment 1 & 5	Increment 2 & 4	Increment 3
Rainfall Depth = 0.055 in			
2	1.1	2.19	3.29
5	0.44	0.88	1.32
7	0.31	0.63	0.94
11	0.2	0.4	0.6
20	0.11	0.22	0.33
37	0.06	0.12	0.18
72	0.03	0.06	0.09
Rainfall Depth = 0.175 in.			
2	3.49	6.98	10.47
5	1.4	2.79	4.19
7	1	1.99	2.99
11	0.63	1.27	1.9
20	0.35	0.7	1.05
37	0.19	0.38	0.57
72	0.1	0.19	0.29
Rainfall Depth = 0.375 in			
2	7.48	14.96	22.44
5	2.99	5.98	8.98
7	2.14	4.27	6.41
11	1.36	2.72	4.08
20	0.75	1.5	2.24
37	0.4	0.81	1.21
72	0.21	0.42	0.62
Rainfall Depth = 0.75 in			
2	14.96	29.92	44.89
5	5.98	11.97	17.95
7	4.27	8.55	12.82
11	2.72	5.44	8.16
20	1.5	2.99	4.49
37	0.81	1.62	2.43
72	0.42	0.83	1.25
Rainfall Depth = 3.0 in.			
2	59.65	119.3	178.94
5	23.86	47.72	71.58
7	17.04	34.08	51.13
11	10.85	21.69	32.54
20	5.96	11.93	17.89
37	3.22	6.45	9.67
72	1.66	3.31	4.97

References

Abed, S. E., Ibnsouda, S. K., Latrache, H., and Hamadi, F. (2012). *Scanning Electron Microscopy (SEM) and Environmental SEM: Suitable Tools for Study of Adhesion Stage and Biofilm Formation*. InTech.

Allan, V. J. M., Callow, M. E., Macaskie, L. E., and Paterson-Beedle, M. (2002). "Effect of nutrient limitation on biofilm formation and phosphatase activity of a Citrobacter sp." *Microbiology (Reading, England)*, 148(Pt 1), 277–288.

Allison, S. D., and Vitousek, P. M. (2005). "Responses of extracellular enzymes to simple and complex nutrient inputs." *Soil Biology and Biochemistry*, 37(5), 937–944.

APHA, A. P. H. A. (1992). *Standard Methods of Water and Wastewater*. Water Environment Federation, Washington, D.C.

Ashok, V., and Hait, S. (2015). "Remediation of nitrate-contaminated water by solid-phase denitrification process—a review." *Environmental Science and Pollution Research*, 22(11), 8075–8093.

Bachand, P. A. M., and Horne, A. J. (1999). "Denitrification in constructed free-water surface wetlands: II. Effects of vegetation and temperature." *Ecological Engineering*, 14(1–2), 17–32.

Badran, R. A. (1994). "Cellulolytic activity of some cellulose-decomposing fungi in salinized soils." *Acta Mycologica*, 29(2), 245–251.

Bai, Y., Liu, R., Liang, J., and Qu, J. (2013). "Integrated Metagenomic and Physiochemical Analyses to Evaluate the Potential Role of Microbes in the Sand Filter of a Drinking Water Treatment System." *PLoS ONE*, 8(4).

Bastviken, S. K., Eriksson, P. G., Ekström, A., and Tonderski, K. (2007). "Seasonal Denitrification Potential in Wetland Sediments with Organic Matter from Different Plant Species." *Water, Air, and Soil Pollution*, 183(1–4), 25–35.

Bishop, P. L., Zhang, T. C., and Fu, Y.-C. (1995). "Effects of biofilm structure, microbial distributions and mass transport on biodegradation processes." *Water Science and Technology*, Biological Degradation of Organic Chemical Pollutants in Biofilm SystemsSelected Proceedings of the International Specialized Research Seminar on Biological Degradation of Organic Chemical Pollutants in Biofilm Systems, 31(1), 143–152.

Bremner, J. M., and Yeomans, J. C. (1986). "Effects of nitrification inhibitors on denitrification of nitrate in soil." *Biology and Fertility of Soils*, 2(4), 173–179.

Broszat, M., Nacke, H., Blasi, R., Siebe, C., Huebner, J., Daniel, R., and Grohmann, E. (2014). "Wastewater Irrigation Increases the Abundance of Potentially Harmful Gammaproteobacteria in Soils in Mezquital Valley, Mexico." *Applied and Environmental Microbiology*, 80(17), 5282–5291.

Brown, R. A., and Hunt, W. F. (2011). "Underdrain Configuration to Enhance Bioretention Exfiltration to Reduce Pollutant Loads." *Journal of Environmental Engineering*, 137(11), 1082–1091.

Chaudhary, G., Singh, L. K., and Ghosh, S. (2012). "Alkaline pretreatment methods followed by acid hydrolysis of Saccharum spontaneum for bioethanol production." *Bioresource Technology*, 124, 111–118.

Cherchi, C., Onnis-Hayden, A., El-Shawabkeh, I., and Gu, A. Z. (2009). "Implication of Using Different Carbon Sources for Denitrification in Wastewater Treatments." *Water Environment Research*, 81(8), 788–799.

Chun, J. A., Cooke, R. A., Eheart, J. W., and Cho, J. (2010). "Estimation of flow and transport parameters for woodchip-based bioreactors: II. field-scale bioreactor." *Biosystems Engineering*, 105(1), 95–102.

Chun, J. A., Cooke, R. A., Eheart, J. W., and Kang, M. S. (2009). "Estimation of flow and transport parameters for woodchip-based bioreactors: I. laboratory-scale bioreactor." *Biosystems Engineering*, 104(3), 384–395.

Collins, K. A., Lawrence, T. J., Stander, E. K., Jontos, R. J., Kaushal, S. S., Newcomer, T. A., Grimm, N. B., and Cole Ekberg, M. L. (2010). "Opportunities and challenges for managing nitrogen in urban stormwater: A review and synthesis." *Ecological Engineering*, Managing Denitrification in Human Dominated Landscapes, 36(11), 1507–1519.

Costerton, J. W., Lewandowski, Z., Caldwell, D. E., Korber, D. R., and Lappin-Scott, H. M. (1995). "Microbial Biofilms." *Annual Review of Microbiology*, 49(1), 711–745.

Davis, A. P., Hunt, W. F., Traver, R. G., and Clar, M. (2009). "Bioretention Technology: Overview of Current Practice and Future Needs." *Journal of Environmental Engineering*, 135(3), 109–117.

Davis, A. P., and McCuen, R. H. (2005). *Stormwater Management for Smart Growth*. Springer Science & Business Media.

Davis, A. P., Shokouhian, M., Sharma, H., and Minami, C. (2001). "Laboratory Study of Biological Retention for Urban Stormwater Management." *Water Environment Research*, 73(1), 5–14.

Davis, A. P., Shokouhian, M., Sharma, H., and Minami, C. (2006). "Water Quality Improvement through Bioretention Media: Nitrogen and Phosphorus Removal." *Water Environment Research*, 78(3), 284–293.

Davis, A. P., Stagge, J. H., Jamil, E., and Kim, H. (2012a). "Hydraulic performance of grass swales for managing highway runoff." *Water Research*, Special Issue on Stormwater in urban areas, 46(20), 6775–6786.

Davis, A. P., Traver, R. G., and Hunt, W. F. (2010). "Improving Urban Stormwater Quality: Applying Fundamental Principles." *Journal of Contemporary Water Research & Education*, 146(1), 3–10.

Davis, A. P., Traver, R. G., Hunt, W. F., Lee, R., Brown, R. A., and Olszewski, J. M. (2012b). "Hydrologic Performance of Bioretention Storm-Water Control Measures." *Journal of Hydrologic Engineering*, 17(5), 604–614.

Delay, F., Porel, G., and Chatelier, M. (2013). "A dual flowing continuum approach to model denitrification experiments in porous media colonized by biofilms." *Journal of Contaminant Hydrology*, 150, 12–24.

Delpla, I., Jung, A.-V., Baures, E., Clement, M., and Thomas, O. (2009). "Impacts of climate change on surface water quality in relation to drinking water production." *Environment International*, 35(8), 1225–1233.

Department of Environmental Resources, P.G. County. (2007). "Bioretention Manual." Prince George's County, Maryland.

Desvaux, M. (2006). "Unravelling carbon metabolism in anaerobic cellulolytic bacteria." *Biotechnology Progress*, 22(5), 1229–1238.

Elgood, Z., Robertson, W. D., Schiff, S. L., and Elgood, R. (2010). "Nitrate removal and greenhouse gas production in a stream-bed denitrifying bioreactor." *Ecological Engineering*, 36(11), 1575–1580.

Flint, K. R., and Davis, A. P. (2007). "Pollutant Mass Flushing Characterization of Highway Stormwater Runoff from an Ultra-Urban Area." *Journal of Environmental Engineering*, 133(6), 616–626.

Fogler, H. S. (2011). *Essentials of Chemical Reaction Engineering*. Pearson Education.

Galbe, M., and Zacchi, G. (2002). "A review of the production of ethanol from softwood." *Applied Microbiology and Biotechnology*, 59(6), 618–628.

van Genuchten, M. T., and Wagenet, R. J. (1989). "Two-Site/Two-Region Models for Pesticide Transport and Degradation: Theoretical Development and Analytical Solutions." *Soil Science Society of America Journal*, 53(5), 1303–1310.

Gharechahi, M., Moosavi, H., and Forghani, M. (2012). "Effect of Surface Roughness and Materials Composition." *Journal of Biomaterials and Nanobiotechnology*, 3(4), 541–546.

Glass, C., and Silverstein, J. (1998). "Denitrification kinetics of high nitrate concentration water: pH effect on inhibition and nitrite accumulation." *Water Research*, 32(3), 831–839.

Gruber, N., and Galloway, J. N. (2008). "An Earth-system perspective of the global nitrogen cycle." *Nature*, 451(7176), 293–296.

Han, Y., Lau, S.-L., Kayhanian, M., and Stenstrom, M. K. (2006). "Characteristics of Highway Stormwater Runoff." *Water Environment Research*, 78(12), 2377–2388.

Hatt, B. E., Fletcher, T. D., and Deletic, A. (2009). "Hydrologic and pollutant removal performance of stormwater biofiltration systems at the field scale." *Journal of Hydrology*, 365(3–4), 310–321.

Hawaii State Department of Health. (2015). "Controlling Mosquito Breeding in Rainwater Catchment Systems and 'Dry' Injection Wells."

Herbert, R. B. (2011). "Implications of non-equilibrium transport in heterogeneous reactive barrier systems: Evidence from laboratory denitrification experiments." *Journal of Contaminant Hydrology*, 123(1–2), 30–39.

Hina, K., Bishop, P., Arbestain, M. C., Calvelo-Pereira, R., Maciá-Agulló, J. A., Hindmarsh, J., Hanly, J. A., Macías, F., and Hedley, M. J. (2010). "Producing biochars with enhanced surface activity through alkaline pretreatment of feedstocks." *Soil Research*, 48(7), 606–617.

Hoover, N., Bhandari, A., Soupir, M., and Moorman, T. (2015). "Woodchip Denitrification Bioreactors: Impact of Temperature and Hydraulic Retention Time on Nitrate Removal." *Journal of Environmental Quality*.

Hsieh, C., and Davis, A. P. (2005). "Evaluation and Optimization of Bioretention Media for Treatment of Urban Storm Water Runoff." *Journal of Environmental Engineering*, 131(11), 1521–1531.

Hundecha, Y., and Bárdossy, A. (2004). "Modeling of the effect of land use changes on the runoff generation of a river basin through parameter regionalization of a watershed model." *Journal of Hydrology*, 292(1–4), 281–295.

Hunt, W. F., Davis, A. P., and Traver, R. G. (2012). "Meeting Hydrologic and Water Quality Goals through Targeted Bioretention Design." *Journal of Environmental Engineering*, 138(6), 698–707.

Hunt, W. F., Jarrett, A. R., Smith, J. T., and Sharkey, L. J. (2006). "Evaluating Bioretention Hydrology and Nutrient Removal at Three Field Sites in North Carolina." *Journal of Irrigation and Drainage Engineering*, 132(6), 600–608.

Hunt, W. F., Smith, J. T., Jadlocki, S. J., Hathaway, J. M., and Eubanks, P. R. (2008). "Pollutant Removal and Peak Flow Mitigation by a Bioretention Cell in Urban Charlotte, N.C." *Journal of Environmental Engineering*, 134(5), 403–408.

Iowa SUDAS. (2013). "Design Manual: Chapter 2 - Stormwater; 2B - Urban Hydrology and Runoff."

Isobe, K., and Ohte, N. (2014). "Ecological Perspectives on Microbes Involved in N-Cycling." *Microbes and Environments*, 29(1), 4–16.

Jeong, T.-S., Um, B.-H., Kim, J.-S., and Oh, K.-K. (2010). "Optimizing Dilute-Acid Pretreatment of Rapeseed Straw for Extraction of Hemicellulose." *Applied Biochemistry and Biotechnology*, 161(1–8), 22–33.

Jones, C. M., Stres, B., Rosenquist, M., and Hallin, S. (2008). "Phylogenetic Analysis of Nitrite, Nitric Oxide, and Nitrous Oxide Respiratory Enzymes Reveal a Complex Evolutionary History for Denitrification." *Molecular Biology and Evolution*, 25(9), 1955–1966.

Kadlec, R. H., and Wallace, S. (2008). *Treatment Wetlands, Second Edition*. CRC Press.

Kaushal, S. S., Groffman, P. M., Band, L. E., Shields, C. A., Morgan, R. P., Palmer, M. A., Belt, K. T., Swan, C. M., Findlay, S. E. G., and Fisher, G. T. (2008). "Interaction between urbanization and climate variability amplifies watershed nitrate export in Maryland." *Environmental Science & Technology*, 42(16), 5872–5878.

Kim, H., Seagren, E. A., and Davis, A. P. (2003). "Engineered bioretention for removal of nitrate from stormwater runoff." *Water Environment Research: A Research Publication of the Water Environment Federation*, 75(4), 355–367.

Kreeb, L. B. (2003). "Hydrologic efficiency and design sensitivity of bioretention facilities." Honors Research, University of Maryland, College Park.

Kristensen, J. B., Thygesen, L. G., Felby, C., Jørgensen, H., and Elder, T. (2008). "Cell-wall structural changes in wheat straw pretreated for bioethanol production." *Biotechnology for Biofuels*, 1, 5.

Kumar, M., and Lin, J.-G. (2010). "Co-existence of anammox and denitrification for simultaneous nitrogen and carbon removal—Strategies and issues." *Journal of Hazardous Materials*, 178(1–3), 1–9.

Lampe, D. G., and Zhang, T. C. (2012). "Evaluation of sulfur-based autotrophic denitrification and denitritation." *Bioresource Technology*, 114, 207–216.

Leverenz, H. L., Haunschild, K., Hopes, G., Tchobanoglous, G., and Darby, J. L. (2010). "Anoxic treatment wetlands for denitrification." *Ecological Engineering*, Managing Denitrification in Human Dominated Landscapes, 36(11), 1544–1551.

Li, H., and Davis, A. P. (2009). "Water Quality Improvement through Reductions of Pollutant Loads Using Bioretention." *Journal of Environmental Engineering*, 135(8), 567–576.

Li, L., and Davis, A. P. (2014). "Urban Stormwater Runoff Nitrogen Composition and Fate in Bioretention Systems." *Environmental Science & Technology*, 48(6), 3403–3410.

Li, R., Feng, C., Hu, W., Xi, B., Chen, N., Zhao, B., Liu, Y., Hao, C., and Pu, J. (2016). "Woodchip-sulfur based heterotrophic and autotrophic denitrification (WSHAD) process for nitrate contaminated water remediation." *Water Research*, 89, 171–179.

Lucas, W. C., and Greenway, M. (2008). "Nutrient Retention in Vegetated and Nonvegetated Bioretention Mesocosms." *Journal of Irrigation and Drainage Engineering*, 134(5), 613–623.

Lucas, W., and Greenway, M. (2011a). "Hydraulic Response and Nitrogen Retention in Bioretention Mesocosms with Regulated Outlets: Part I—Hydraulic Response." *Water Environment Research*, 83(8).

Lucas, W., and Greenway, M. (2011b). "Hydraulic Response and Nitrogen Retention in Bioretention Mesocosms with Regulated Outlets: Part I—Hydraulic Response." *Water Environment Research*, 83(8).

Lynn, T., Ergas, S., and Nachabe, M. (2016). "Effect of Hydrodynamic Dispersion in Denitrifying Wood-Chip Stormwater Biofilters." *Journal of Sustainable Water in the Built Environment*, 4016004.

Lynn, T. J., Yeh, D. H., and Ergas, S. J. (2015a). "Performance and Longevity of Denitrifying Wood-Chip Biofilters for Stormwater Treatment: A Microcosm Study." *Environmental Engineering Science*, 32(4), 321–330.

Lynn, T. J., Yeh, D. H., and Ergas, S. J. (2015b). "Performance of Denitrifying Stormwater Biofilters Under Intermittent Conditions." *Environmental Engineering Science*, 32(9), 796–805.

McCuen, R. H. (2005). *Hydrologic Analysis and Design*. Prentice Hall, Inc.

McIlroy, S. J., Starnawska, A., Starnawski, P., Saunders, A. M., Nierychlo, M., Nielsen, P. H., and Nielsen, J. L. (2014). "Identification of active denitrifiers in full-scale nutrient removal wastewater treatment systems." *Environmental Microbiology*, 18(1), 50–64.

Metcalf, and Eddy. (1979). *Wastewater Engineering: Treatment, Disposal, Reuse*. McGraw-Hill, New York.

Morgan-Sagastume, F., Nielsen, J. L., and Nielsen, P. H. (2008). "Substrate-dependent denitrification of abundant probe-defined denitrifying bacteria in activated sludge." *FEMS Microbiology Ecology*, 66(2), 447–461.

Nason, J. A., Bloomquist, D. J., and Sprick, M. S. (2012). "Factors Influencing Dissolved Copper Concentrations in Oregon Highway Storm Water Runoff." *Journal of Environmental Engineering*, 138(7), 734–742.

Natarajan, P., and Davis, A. P. (2015). "Performance of a 'Transitioned' Infiltration BasinPart 1: TSS, Metals, and Chloride Removals." *Water Environment Research*, 87(9), 823–834.

O'Toole, G., Kaplan, H. B., and Kolter, R. (2000). "Biofilm Formation as Microbial Development." *Annual Review of Microbiology*, 54(1), 49–79.

Palmqvist, E., and Hahn-Hägerdal, B. (2000). "Fermentation of lignocellulosic hydrolysates. II: inhibitors and mechanisms of inhibition." *Bioresource Technology*, 74(1), 25–33.

Park, E.-J., Seo, J.-K., Kim, M.-R., Jung, I.-H., Kim, J. yun, and Kim, S.-K. (2001).
  "Salinity acclimation of immobilized freshwater denitrifier." *Aquacultural
  Engineering*, 24(3), 169–180.
Partheeban, C., and Kjaersgaard, J. (2014). "A Review of the factors controlling the
  performance of denitrifying woodchip bioreactors."
Payne, E. G. I., Fletcher, T. D., Cook, P. L. M., Deletic, A., and Hatt, B. E. (2014).
  "Processes and Drivers of Nitrogen Removal in Stormwater Biofiltration."
  Critical Reviews in Environmental Science and Technology, 44(7), 796–846.
Peter, H., Ylla, I., Gudasz, C., Romaní, A. M., Sabater, S., and Tranvik, L. J. (2011).
  "Multifunctionality and Diversity in Bacterial Biofilms." *PLOS ONE*, 6(8),
  e23225.
Peterson, I. J., Igielski, S., and Davis, A. P. (2015). "Enhanced Denitrification in
  Bioretention Using Woodchips as an Organic Carbon Source." *Journal of
  Sustainable Water in the Built Environment*, 1(4), 4015004.
Pitt, R., and Morquecho, R. (2005). *The National Stormwater Quality Database (NSQD,
  version 1.1)*. U.S. EPA Office of Water: Washington, D.C.
Ren, G., Xu, X., Qu, J., Zhu, L., and Wang, T. (2016). "Evaluation of microbial
  population dynamics in the co-composting of cow manure and rice straw using
  high throughput sequencing analysis." *World Journal of Microbiology and
  Biotechnology*, 32(6), 101.
Rietz, D. N., and Haynes, R. J. (2003). "Effects of irrigation-induced salinity and sodicity
  on soil microbial activity." *Soil Biology and Biochemistry*, 35(6), 845–854.
Rivett, M. O., Buss, S. R., Morgan, P., Smith, J. W. N., and Bemment, C. D. (2008).
  "Nitrate attenuation in groundwater: A review of biogeochemical controlling
  processes." *Water Research*, 42(16), 4215–4232.
Robertson, L. A., and Kuenen, J. G. (1990). "Denitrification by Obligate and Facultative
  Autotrophs." *Autotrophic Microbiology and One-Carbon Metabolism*, Advances
  in Autotrophic Microbiology and One-Carbon Metabolism, G. A. Codd, L.
  Dijkhuizen, and F. R. Tabita, eds., Springer Netherlands, 93–115.
Robertson, W. D. (2010). "Nitrate removal rates in woodchip media of varying age."
  Ecological Engineering, Managing Denitrification in Human Dominated
  Landscapes, 36(11), 1581–1587.
Saarenheimo, J., Tiirola, M. A., and Rissanen, A. J. (2015). "Functional gene
  pyrosequencing reveals core proteobacterial denitrifiers in boreal lakes."
  Frontiers in Microbiology, 6.
Schipper, L. A., Robertson, W. D., Gold, A. J., Jaynes, D. B., and Cameron, S. C. (2010).
  "Denitrifying bioreactors—An approach for reducing nitrate loads to receiving
  waters." *Ecological Engineering*, Managing Denitrification in Human Dominated
  Landscapes, 36(11), 1532–1543.
Schmidt, C. A., and Clark, M. W. (2013). "Deciphering and modeling the
  physicochemical drivers of denitrification rates in bioreactors." *Ecological
  Engineering*, 60, 276–288.
Seitzinger, S. P. (1988). "Denitrification in freshwater and coastal marine ecosystems:
  Ecological and geochemical significance." *Limnology and Oceanography*, 33(4),
  702–724.

Selig, M. J., Viamajala, S., Decker, S. R., Tucker, M. P., Himmel, M. E., and Vinzant, T. B. (2007). "Deposition of lignin droplets produced during dilute acid pretreatment of maize stems retards enzymatic hydrolysis of cellulose." *Biotechnology Progress*, 23(6), 1333–1339.

Selig, M. J., Vinzant, T. B., Himmel, M. E., and Decker, S. R. (2009). "The effect of lignin removal by alkaline peroxide pretreatment on the susceptibility of corn stover to purified cellulolytic and xylanolytic enzymes." *Applied Biochemistry and Biotechnology*, 155(1–3), 397–406.

Singh, J., Suhag, M., and Dhaka, A. (2015). "Augmented digestion of lignocellulose by steam explosion, acid and alkaline pretreatment methods: A review." *Carbohydrate Polymers*, 117, 624–631.

Soares, M. I. M. (2002). "Denitrification of groundwater with elemental sulfur." *Water Research*, 36(5), 1392–1395.

Stagge, J. H., Davis, A. P., Jamil, E., and Kim, H. (2012). "Performance of grass swales for improving water quality from highway runoff." *Water Research*, Special Issue on Stormwater in urban areas, 46(20), 6731–6742.

Stephens, D. B. (1995). *Vadose Zone Hydrology*. CRC Press.

Sternberg, C., Christensen, B. B., Johansen, T., Nielsen, A. T., Andersen, J. B., Givskov, M., and Molin, S. (1999). "Distribution of Bacterial Growth Activity in Flow-Chamber Biofilms." *Applied and Environmental Microbiology*, 65(9), 4108–4117.

Stewart, P. S. (2003). "Diffusion in Biofilms." *Journal of Bacteriology*, 185(5), 1485–1491.

Stoodley, P., Dodds, I., Boyle, J. d., and Lappin-Scott, H. m. (1998). "Influence of hydrodynamics and nutrients on biofilm structure." *Journal of Applied Microbiology*, 85(S1), 19S–28S.

Stumm, W., and Morgan, J. J. (1995). *Aquatic Chemistry: Chemical Equilibria and Rates in Natural Waters*. Wiley.

Subramaniam, D., Mather, P., Russell, S., and Rajapakse, J. (2016). "Dynamics of Nitrate-Nitrogen Removal in Experimental Stormwater Biofilters under Intermittent Wetting and Drying." *Journal of Environmental Engineering*, 142(3), 4015090.

Sun, X., and Davis, A. P. (2007). "Heavy metal fates in laboratory bioretention systems." *Chemosphere*, 66(9), 1601–1609.

Tsitko, I., Lusa, M., Lehto, J., Parviainen, L., Ikonen, A. T. K., Lahdenperä, A.-M., and Bomberg, M. (2014). "The Variation of Microbial Communities in a Depth Profile of an Acidic, Nutrient-Poor Boreal Bog in Southwestern Finland." *Open Journal of Ecology*, 4(13), 832–859.

US Climate Data. (2016). "Baltimore Climate Maryland - Temperature, Rainfall and Average." <http://www.usclimatedata.com/climate/maryland/united-states/1872> (Jun. 30, 2016).

Walsh, C. J., Fletcher, T. D., and Burns, M. J. (2012). "Urban Stormwater Runoff: A New Class of Environmental Flow Problem." *PLoS ONE*, 7(9).

Wang, G. S., Lee, J.-W., Zhu, J. Y., and Jeffries, T. W. (2010). "Dilute Acid Pretreatment of Corncob for Efficient Sugar Production." *Applied Biochemistry and Biotechnology*, 163(5), 658–668.

Wang, Z., Keshwani, D. R., Redding, A. P., and Cheng, J. J. (2008). "Alkaline Pretreatment of Coastal Bermudagrass for Bioethanol Production." *Conference Presentations and White Papers: Biological Systems Engineering*.

Warneke, S., Schipper, L. A., Bruesewitz, D. A., McDonald, I., and Cameron, S. (2011a). "Rates, controls and potential adverse effects of nitrate removal in a denitrification bed." *Ecological Engineering*, 37(3), 511–522.

Warneke, S., Schipper, L. A., Matiasek, M. G., Scow, K. M., Cameron, S., Bruesewitz, D. A., and McDonald, I. R. (2011b). "Nitrate removal, communities of denitrifiers and adverse effects in different carbon substrates for use in denitrification beds." *Water Research*, 45(17), 5463–5475.

Wen, Y., Chen, Y., Zheng, N., Yang, D., and Zhou, Q. (2010). "Effects of plant biomass on nitrate removal and transformation of carbon sources in subsurface-flow constructed wetlands." *Bioresource Technology*, 101(19), 7286–7292.

Yuan, B.-C., Li, Z.-Z., Liu, H., Gao, M., and Zhang, Y.-Y. (2007). "Microbial biomass and activity in salt affected soils under arid conditions." *Applied Soil Ecology*, 35(2), 319–328.

Zhao, Y., Zhang, B., Feng, C., Huang, F., Zhang, P., Zhang, Z., Yang, Y., and Sugiura, N. (2012). "Behavior of autotrophic denitrification and heterotrophic denitrification in an intensified biofilm-electrode reactor for nitrate-contaminated drinking water treatment." *Bioresource Technology*, 107, 159–165.

Zhou, W., Sun, Y., Wu, B., Zhang, Y., Huang, M., Miyanaga, T., and Zhang, Z. (2011). "Autotrophic denitrification for nitrate and nitrite removal using sulfur-limestone." *Journal of Environmental Sciences*, 23(11), 1761–1769.